universität wien

MASTERARBEIT

Titel der Masterarbeit

Identification of drug targets for novel antimicrobials within tRNA modifying enzymes

Verfasserin

Melanie Christina Isele, BSc

angestrebter akademischer Grad

Master of Science (MSc)

Wien, 2012

Studienkennzahl lt. Studienblatt:	A 066 834
Studienrichtung lt. Studienblatt:	Masterstudium Molekulare Biologie
Betreuer:	ao. Univ.-Prof. Dr. Gottfried Köhler

Acknowledgments

I would like to thank Prof. Dirk Bumann for giving me the opportunity to make my Master thesis in his laboratory, ao. Univ.-Prof. Dr. Gottfried Köhler for being my supervisor, and Dr. Anna Chirkova for being my co-supervisor.

Thanks a lot to Petra Tienz and Beatrice Müller for all the support, on the technical as well as on the human site.

I would also like to acknowledge the members of the Bumann group, Dr. Alain Mazé, Dr. Julien Limenitakis, Dr. Mauricio Rosas Ballina, Dr. Olga Timoshenko, Dr. Neil Alexander Burton, Dr. David Kentner, Nura Schürmann, and Janine Fabienne Zankl, for welcoming me in the group and supporting me whenever they could.

Additionally I want to thank Dr. Julien Limenitakis, Dr. Anna Chirkova, and Dr. Olga Timoshenko for supporting me in planning the future steps of my career.

Thanks to Michaela Hanisch for the administrative organization.

Further I want to thank my friends in Basel for being always there when I needed them and of course for all the great moments we had together. I hope more of them will follow.

Thanks to Francesco Gallo for being always there for me and for making my life a lot more complete.

I want to thank my parents Dieter and Juliane Isele for supporting me through my whole life and for offering me the opportunity and the financial background to study and make my dreams come true.

Contents

1 Abstract

New antimicrobial drugs are urgently needed, as resistance to known antibiotic agents keeps spreading and outbreaks of multi-drug resistant pathogens become more frequent. Discovery of new drug targets is a central primary activity in drug development. The prokaryotic translation apparatus has been extensively employed as a target source for antimicrobials, due to its structure complexity, high conservation within prokaryotes, and partly low homology to the eukaryotic one.

In this project we have determined the impact of tRNA post-transcriptional modifications on bacterial fitness and virulence. These modifications are involved in translational accuracy control, as they stabilize the tRNAs tertiary structure and partly influence the kinetics of aminoacylation. Further some are implied to prevent misreading or frameshifting during protein synthesis, due to enhancing the kinetics during translation. For our studies we have chosen a variety of universal and specie-specific tRNA modification, which are known or suspected to influence translational accuracy. The modifications are incorporated by single tRNA modifying enzymes (tRMEs) or enzymes arranged into modification biosynthesis pathways. We have evaluated the *in vitro* growth phenotypes of *Salmonella* Typhimurium strains with single and double tRME deletions and their competitive virulence in the mouse model of typhoid fever. Based on these data we have pinpointed tRMEs, which are essential for the virulence of *Salmonella* and have a potential to serve as targets for novel antimicrobial drugs.

2 Zusammenfassung

Neue antimikrobielle Medikamente werden dringen benötigt, da Resistenz gegenüber den verwendeten Antibiotika immer weiter verbreitet ist und Ausbrüche mehrfach medikamentenresistenter Pathogene sich häufen. Die Evaluierung neuer Interaktionsflächen für Arzneimittel ist eine zentrale Aktivität in der Medikamentenentwicklung. Die prokarytische Translationsmaschinerie war aufgrund ihrer strukturellen Komplexität, ihrer hohen Ähnlichkeit unter Prokaryoten und der zum Teil niedrigen Homologie zum eukaryotischen Translationsapparat in der Vergangenheit ein sehr ertragreiches Gebiet für die Entwicklung von Substanzen mit antibakterieller Wirkung.

In dem vorliegenden Projekt haben wir den Einfluss von post-transkriptionalen Modifikationen der tRNA auf die bakterielle Fitness und die Virulenz evaluiert. Diese Modifikationen tragen zur Kodierungsgenauigkeit bei, indem sie die Tertiärstruktur der tRNA stabilisieren und auch zum Teil die Kinetik der Aminoacetylierung beeinflussen. Weiters sind einige für ihren präventiven Einfluss auf translationale Fehler wie fehlerhafte Ablesung der Basenabfolge oder ein Verrutschen des Leserahmens (Frameshift), durch Verbesserung der Kinetik während der Translation, bekannt. Wir haben für unsere Studien verschiedene universelle und auch spezies-spezifische tRNA Modifikationen ausgewählt, für die ein Einfluss auf die translationale Genauigkeit vermutet wird. Die Modifikationen werden von einzelnen tRNA modifizierenden Enzymen (tRMEs) oder auch von Enzymen innerhalb komplexer Enzymabfolgen an die tRNA angebracht. Wir haben die *in vitro* Wachstumscharakteristika von *Salmonella* Typhimurium Stämmen, denen ein oder zwei tRMEs fehlen, und ihrer kompetitiven Fitness im Mausmodel von Typhus analysiert. Basierend auf diesen Daten haben wir tRMEs ausfindig machen können, die essentiell für die Virulenz von *Salmonella* sind und somit Potenzial aufweisen, als Interaktionspunkte für neue antimikrobielle Arzneimittel von Nutzen zu sein.

3 Introduction

3.1 Antimicrobials and their targets

Between 1940 and 1962 more than 10 novel classes of antibiotics became available [1, 2], which mostly derived from antibacterial defense mechanisms of diverse organisms like fungi [3]. Antimicrobials are unfortunately often used inappropriate, quality medicines are lacking, usage of sub-therapeutic doses is not uncommon, and the drugs are used in animal-rearing. Due to the high selection pressure triggered by the antibiotics, bacteria have been developing resistance mechanisms to these drugs. Those include inactivating the antibiotic, reducing membrane permeability to the antibiotic, increasing the efflux of the antibiotic from the cell, overproducing the target enzyme, bypassing the inhibited step, or altering the antibiotic binding site [4]. Moreover, multi-drug resistant bacteria emerged throughout the world [5]. Single-enzyme targets are particularly susceptible to spontaneous resistance [6]. Though compounds which target complex bacterial systems such as the membrane offer a good chance to induce resistance less readily, as synthesis of these structures requires many enzymes and alteration of the target cannot be easily achieved by the bacteria [7]. However, even in those cases a resistance to a new antibiotic compound is observed on average within two years once it is on the market [8]. To bring the public attention to this problem the WHO chose “Antimicrobial resistance: no action today no cure tomorrow” as topic for the World Health Day 2011 [9].

Marketed antibiotics target cell wall biosynthesis, cell membranes, type II topoisomerases, ribosomes, transcription, and folate biosynthesis [10, 11]. For other identified essential gene products no inhibitors were found, although many inhibitor screenings were conducted. In the past decades only two new antibiotic classes were marketed. One of the reasons to that is that production of an analogue imposes lower risk, as similar characteristics (ability to enter the cell in an adequate amount, physicochemical properties, toxicology, chemical safety, tolerability) as of the parent product are expectable [12]. However, the possibilities for analogues which overcome resistance to the parent product became limited. Thus there is an urgent need for industry and academic research to re-enter the search for novel antibiotic classes.

One strategy to develop a new antibiotic class is, first, to define a target and then screen for feasible inhibitors. The target can be a gene product, which is essential for bacterial growth under all conditions or one which is associated with virulence and not shared by bacterial species in general [13]. Targeting products, which are only important for virulence, brings the advantage of a minimized impact on the resident flora, thus side-effects and the probability of resistance emerging are reduced [14]. General problems with target selection arise due to the bacterial diversity and the existence of nonhomologous or duplicate genes [15]. Knowing a validated molecular target allows rational drug design by defining its functionality and structure. Rapid synthesis of a large number of distinct compounds that can then be assayed for antimicrobial activity can be used to explore the structure space and identify lead compounds for optimization; supported by predictions of binding of a lead component to the target executed with X-ray crystallography [16-18].

3.2 *Salmonella* as model pathogen for drug target search

3.2.1 *Salmonella* infections

The genus *Salmonella* includes two species *S. enterica* and *S. bongori*. The later one is found predominantly associated with cold-blooded animals, but can infect humans [19]. *S. bongori* cannot cause a systemic disease, because it lacks SPI-2 [20, 21]. *Salmonella enterica* is a Gram-negative flagellated pathogen of worldwide importance, as it causes 1.3 billion cases of disease in humans annually [22]. There are two major types of diseases caused by *Salmonella enterica* serotypes in humans and higher primates. A systemic disease, typhoid fever, which can be caused by *Salmonella enterica* serotypes Typhi, Paratyphi A, Paratyphi B and Paratyphi C. The disease is endemic in Asia, Africa, and South America, and can be deadly when not treated with antibiotics. Characteristically manifestations of typhoid fever are constipation, fever, infiltration of immunocompetent cells in the intestine, and tissue colonization by the pathogen. Other *Salmonella* serotypes (e.g. Enteritidis and Choleraesuis) have a wider variety of hosts and cause only enterocolitis (inflammation of the colon and small intestine) in humans.

There have been a number of multiple drug-resistant *Salmonella* outbreaks reported. For instance, *Salmonella enterica* serovar Typhimurium NTS emerged in sub-Saharan Africa caused an invasive disease, unusual for serovar Typhimurium, characterized by bacteremia, septic arthritis, and/or meningitis, it [23]. Moreover, multi drug-resistant *S. enterica* Typhi became a challenge for the management of typhoid fever in endemic locations. Resistance has been noticed to all suitable drugs including trimethoprim, ampicillin, quinolones, and cephalosporins with increasing rates [24].

The most common route of infection is through oral uptake within contaminated food or water [25, 26]. During infection in the gut lumen bacteria face the low pH of the stomach and high osmolarity of the small intestine. To cross the intestinal barrier *Salmonella* has developed diverse mechanisms like being taken up by antigen-sampling M cells, being captured in the lumen by CD18-expressing phagocytes that penetrate the epithelial monolayer, forcing non-phagocytic enterocytes to endocytosis, or disrupting tight junctions [26]. Once on the inner side of the barrier, *Salmonella* infects epithelial and dendritic cells. Inside the cells the pathogen first is surrounded by *Salmonella*-containing vacuoles (SCVs). The SCVs move to the perinuclear area, where they grow to *Salmonella*-induced filaments [27]. Contemporaneously, the enclosed bacteria start to replicate, although there are only limited resources available. Typhoid *S. enterica* strains have developed strategies which allow them to infect beside non-mobile epithelial cells also intestinal macrophages manipulating their cellular processes. Infected macrophages transported via the blood stream and the lymphatic system can cause inflammatory processes in the spleen and the liver with further advancement into other organs causing a systemic infection [28].

During infection with non-typhoidal *S. enterica* strains intestinal mucosa is partly destructed, which contributes to inflammatory diarrhea [26]. Nevertheless, once supported with anti-dehydration therapy, healthy adult patients recover from non-typhoidal salmonellosis in a week time. In contrast infants or patients suppressed immune system can develop severe

complications like bacteremia, intestinal perforation, severe toxic encephalopathy and eventually, die [29].

Vaccination is generally considered to be the most effective long term solution for the prevention of infectious diseases, and also the most cost-effective tool. Nowadays two vaccines against typhoid fever, purified Vi polysaccharide and a live attenuated strain, are available with 70 and 50% protective efficacy respectively. Revaccination is often required, protection is only gained against serovars Typhi and Paratyphi C, and the usage of vaccines to prevent *Salmonella* infections is limited [30].

3.2.2 Mouse model of *Salmonella* infections

This section was mainly summarized from [31].

Salmonella can serve as a great model organism being, on one hand, an important human pathogen and, on another hand, a very close relative to extensively studied *E. coli.*

There are *in vitro* models of *Salmonella* infection based on human cell lines available. However, they are prone to focus on one specific aspect of the disease process, ignoring the broader context of interactions during infection. The bacterial response to different cell types and changing conditions during the infection process are overlooked in tissue culture models.

Salmonella serovars causing typhoid fever are restricted to humans. To approximate the conditions during typhoid fever in humans, *S. enterica* serovar Typhimurium infections of inbred, genetically susceptible mice such as the BALB/c strain have been used extensively over several decades. Not all aspects of typhoid fever in humans can be simulated in infection of BALB/c mice with *S.* Typhimurium, as some major aspects (diarrhea, infection of the gall bladder, secondary exposure of the Peyer's Patches leading to perforation of the gut) are not observed. *S. enterica* serovar Typhi and Typhimurium share several major virulence systems as the PhoP/Q regulon, and the *Salmonella* Pathogenicity Islands SPI-1 and SPI-2 [32, 33], but there are also differences in virulence genes known (e.g. SseJ is involved in virulence of *S.* Typhimurium but not in *S.* Typhi), accounting to some extent for the differences between infections caused by the various serovars and their host range [34, 35]. Further genetic differences between the hosts also contribute to host restriction and severity of the resulting disease.

3.3 Role of tRNA modifications in prokaryotic translation

3.3.1 Overview on protein biosynthesis and translational accuracy

Translation is an essential process in every cell, as cellular growth is dependent on synthesis of proteins. During this process mRNA, arising from transcription of the organism's DNA, is translated by the ribosome into an amino acid sequence.

Bacterial 70S ribosomes are build up from two subunits; the 30S subunit contains the decoding site where codon-anticodon interaction takes place, and the 50S subunit contains the active site where peptidyl transfer and peptidyl hydrolysis reactions occur. The ribosome carries three tRNA binding sites – named aminoacyl (A), peptidyl (P), and exit (E) site (Figure 1). During initiation of translation the complex of 30S subunit with initiation factors IF1 and IF3 binds to

the Shine-Dalgarno sequence located on the mRNA upstream of the start codon. This allows fMet-tRNA^{fMet} bound to IF2-GTP to bind also to the complex. Binding of the 50S subunit triggers a release of the initiation factors by GTP hydrolysis at IF2. The fMet-tRNA^{fMet} is then located in the P site of the newly assembled ribosome [36]. During elongation a ternary complex comprised of aminoacyl-tRNA, elongation factor EF-Tu and GTP binds to the codon on the mRNA in the A site of the ribosome. There the peptidyl-transferase reaction with the peptidyl-tRNA located in the ribosomes P site takes place, after the peptidyl-transfer the peptidyl-tRNA and the deacetylated tRNA are translocated to the P and E site, respectively, catalyzed by GTP hydrolysis by EF-G. Elongation is terminated by RFs when a stop codon enters the A site, causing hydrolysis of the peptidyl-tRNA and release the polypeptide chain [37].

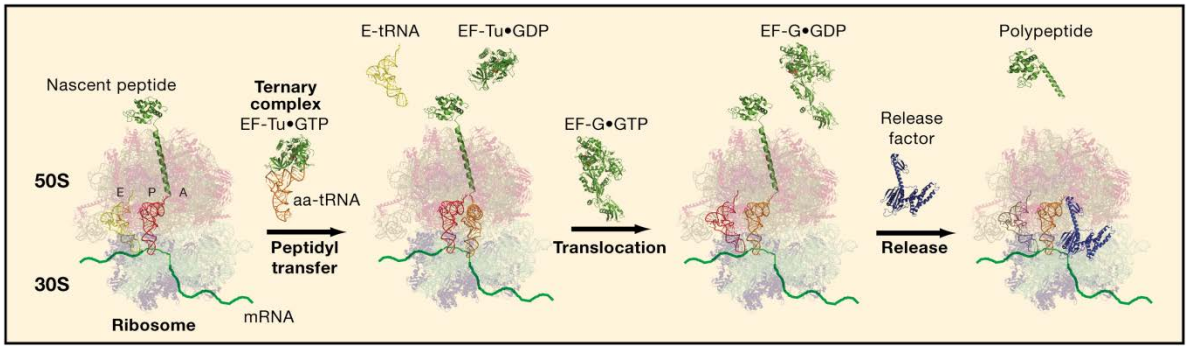

Figure 1: During elongation a ternary complex composed of EF-Tu, aminoacyl-tRNA, and GTP is bound by the A site and reacts with the peptidyl-tRNA in the P site, elongating the nascent peptide by one amino acid. The peptidyl-tRNA and the deacylated tRNA are then translocated by EF-G through GTP hydrolysis into the P and E site. Termination of protein synthesis occurs when a stop codon enters the A site. They are recognized by RFs, which trigger a hydrolytic reaction resulting in release of the growing polypeptide chain from the tRNA [37].

In general every base triplet (codon) on the mRNA encodes for an amino acid, and/or start (AUG) and stop of translation (UAA, UAG, UGA)(Figure 2)[38]. In family codon boxes the first two nucleotides of the codon are important for decoding, as all four nucleotides on the third position encode for the same amino acid (Ser, CUN-Leu, Pro, Arg, Thr, Val, Ala, and Gly). In mixed codon boxes the third nucleotide has a decoding function, but in most cases both purines and both pyrimidines encode for the same amino acid, respectively (Phe/Leu, Tyr/Stop, His/Gln, Lys/Asn, Arg/Ser, and Glu/Asp).

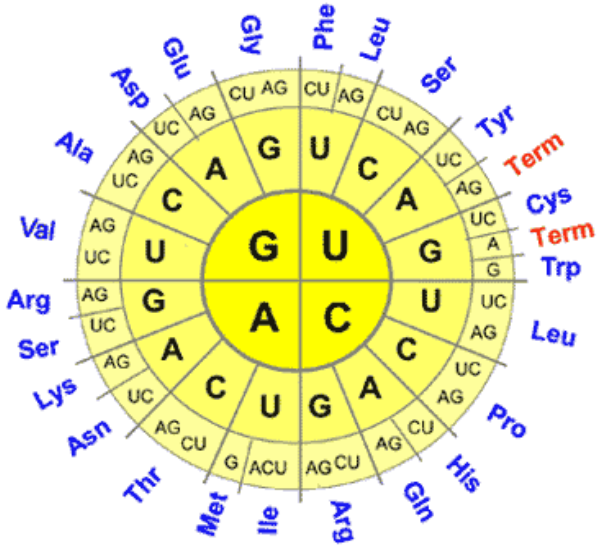

Figure 2: Classical codon code. A triplet is read from inside to outside. For example UCC stands for serine, the start codon is AUG and stop codons which terminate translation are UAA, UAG, and UGA.

A cognate interaction depicts per definition that the codon and the anticodon are capable to form three Watson-Crick pairings. The minihelix formed by cognate codon and anticodon during elongation is stabilized by eight or nine hydrogen bonds between 16S rRNA and the backbones of codon and anticodon, depending on the nature of the nucleotides (purine or pyrimidine). This interaction causes a conformational change of the small ribosomal subunit, triggering GTP hydrolysis, and release of EF-Tu with GDP. The conformational change acts as proofreading mechanism to guarantee the usage of the right tRNA, hence the incorporation of the right amino acid in the growing peptide chain, as the energy of GTP hydrolysis is necessary for the peptidyl-transfer [39].

Near-cognate anticodons (with a single mismatch in formation of the second or third base pair with the codon) form only with two bases of the codon perfect Watson-Crick pairs [40, 41]. This interactions can also offer enough energy for the conformational change in the small ribosomal subunit [39]. The rules for wobbling are shown in Table 1. Theoretically wobbling can result in incorporation of the wrong amino acid in the growing peptide chain, especially in mixed coding boxes where the codons differ only in the 3rd nucleotides (e.g. Lys and Asn).

First base of anticodon	anticodon	Third base of codon
A → I	ACG	U, C, A
G		C, U
C→ k^2C	CAT	A
C	other than CAT	G
U → xo^5U	UGC, UGA, UAC	A, U, G, C
other modified or unmodified U	other than UGC, UGA, UAC	A, G

Table 1: Wobble pairing rules used at the third base of codons for E. coli [42].

In good growth conditions translational errors occurs every 1 x 10^3 – 1 x 10^4 amino acid incorporated, in nutrition-limited conditions the error rate is shown to be higher [43]. The occurring error types are read through, premature termination, miscoding, and frameshifting. Translation mistakes which cause formation of a nonfunctional protein can be very cost intense and stressing for the cell, as resources and energy are lost and ribosomes are occupied. Furthermore erroneous proteins show problems to fold, and by that occupy chaperones trying to fold them correctly. If the chaperones are unsuccessful, the erroneous proteins have to be degraded by proteases [44]. In the worst case the wrong translated proteins can build up toxic aggregates, and might even kill the cell [45]. Frameshifts, the most severe translational errors, occur with a frequency of approximately 3 x 10^{-5} per codon [43]. The severity is due to production of completely useless proteins and lost recognition of the original stop codon. The genetic code acquired many out-of-frame stop codons, presumably to lower the costs of frameshifts [46]. Further evolution seems to trigger the development of highly frameshift-resistant codon combinations and also boosts increased usage of less frameshift-prone codons, especially in highly expressed genes [42].

Frameshifts can also be programmed; they are ubiquitous mechanisms to raise the variation of functions from proteins while keeping the additional information on genomic level minimal, or frameshifts are used as time switches between genes for structural and enzymatic products, or as regulatory elements. The *prfB* gene encoding for the termination factor RF2 of *E. coli* for example is regulated by a frameshift mechanism. Translation of the full protein requires a +1 frameshift on position 26 of the mRNA to bypass an in-frame UGA stop codon, which is usually read by RF2. Frameshift is caused on the sequence AGG GGG UAU CUU UGA C when RF2 concentrations are low causing slow recognition of the weak UGA stop codon, because weak binding of the $tRNA^{Leu}$ at the P site to the mRNA by a G:U wobble base pair, perfect realignment in the new frame of $tRNA^{Asp}$ and a Shine-Dalgarno-like sequence precede the UGA stop codon, which slows the ribosome down [47].

3.3.2 tRNA modifications and mistranslation

All tRNAs are modified post-transcriptionally by a high diversity of tRNA modifying enzymes (tRMEs). tRMEs are classified into two groups; group I enzymes do not require the L-shape of tRNA, whereas group II enzymes recognize the three-dimensional structure of the tRNA (Figure 3). The group I enzymes are further divided into subgroup Ia, which modifies exposed nucleotides located mainly in the anticodon loop, and subgroup Ib, which targets residues buried inside the tRNA three-dimensional structure [48, 49].

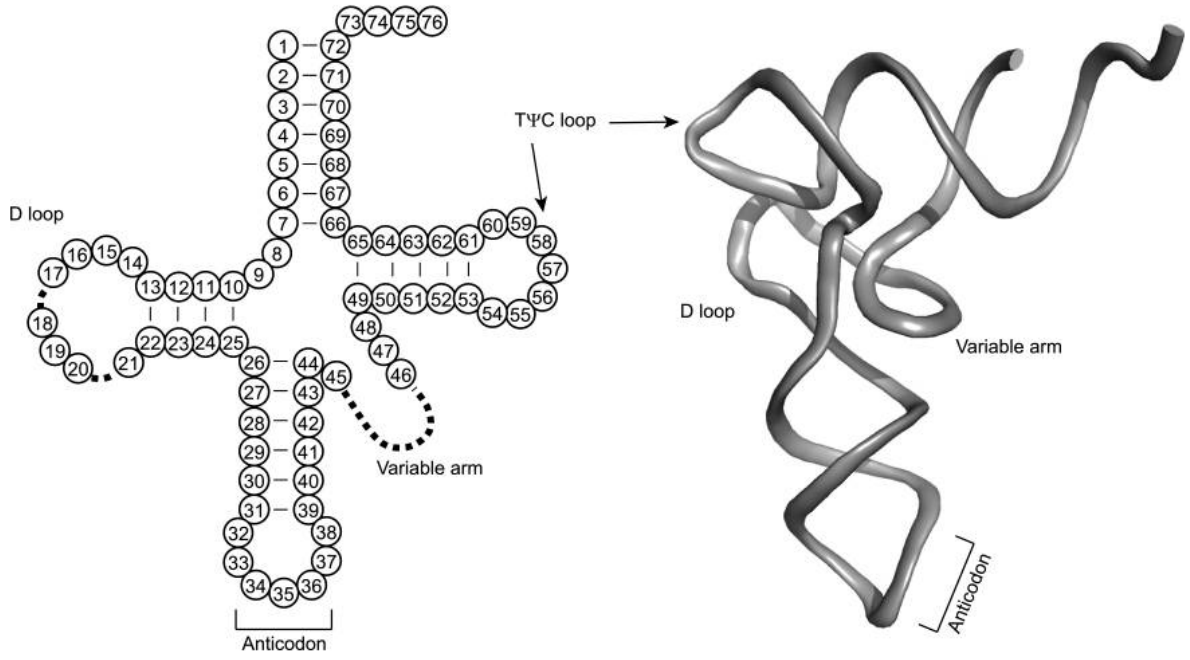

Figure 3: Secondary (left) and tertiary (right) structure of yeast tRNA^{Phe}, the major structure elements and the universal nucleotide positions are labeled [41].

Studies on the evolution of the genetic code showed that at an early point of evolution ancient organisms used a smaller amino acid repertoire and no mixed codon boxes occurred, meaning all amino acids where encoded by the first two positions of the base triplet and the base at the wobble position had no encoding function. As a result of rising complexity of the amino acid repertoire used, it was necessary to split the codon boxes in a 2/2 or 3/1 manner. To maintain translational accuracy tRNA modifications arose and the tRNA repertoire was optimized to the cell's needs [50].

Nowadays over 100 modifications with very diverse effects on the behavior of the tRNA are known (Figure 4). tRNA modifications located all over the tRNA stabilize its structure by initializing additional interactions and can further influence the kinetics of aminoacylation in a supporting or inhibiting manner, thus influence misreading [51, 52].

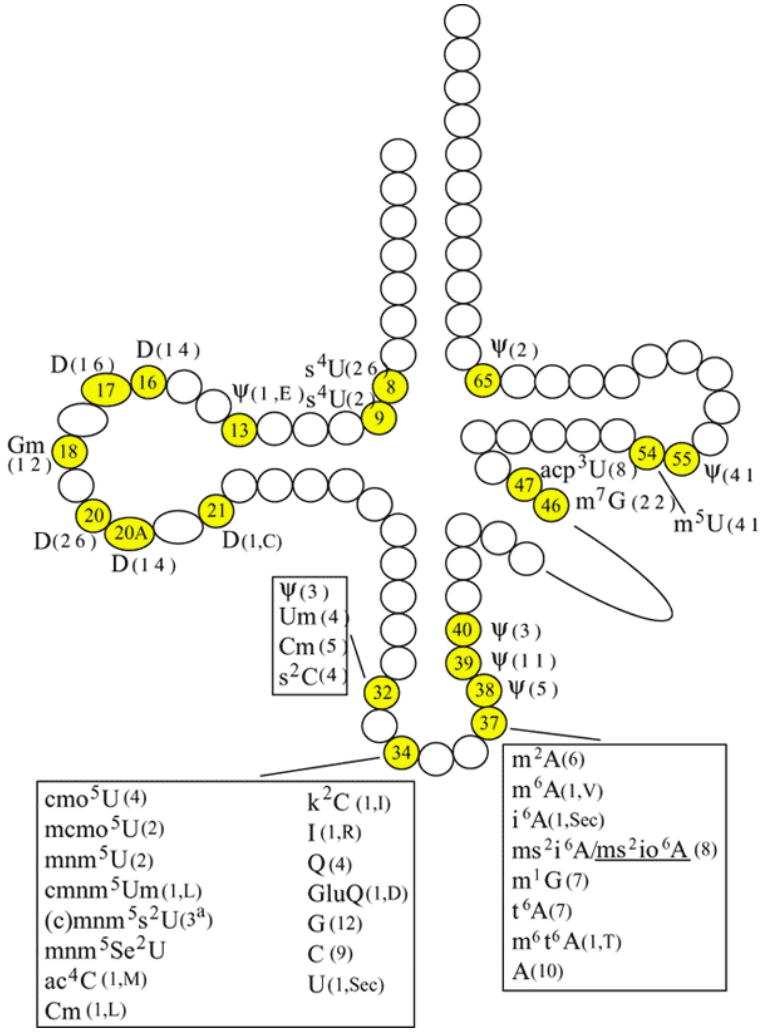

Figure 4: Locations of modified nucleosides on the tRNA. Positions where modified nucleotides can occur are marked yellow. Within parentheses numbers indicate the count of tRNA species carrying the modified nucleoside and the amino acid specificity occurring through this modification is shown (one-letter code; Sec denotes selenocysteine). $ms^{2i}o^{6}A$ (underlined) is only found in tRNA of S. Typhimurium [60].

Modifications on positions 34 and 37 of the anticodon specify the interactions of tRNA and mRNA on the ribosome during protein synthesis and support the ribosome in the maintenance of decoding accuracy to avoid translational errors like misreading or frameshifting (Figure 5) [53-55].

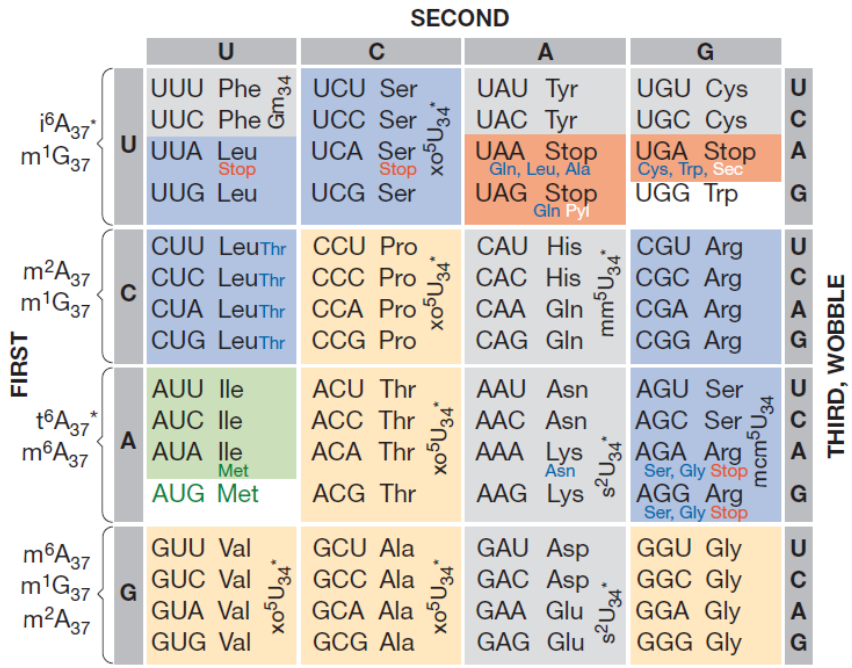

Figure 5: The 64 codons of the genetic code associated with the most important tRNA modifications for decoding and/or translocation. Twofold degenerate amino acid codes are highlighted in grey and fourfold degenerate codes are highlighted in tan. Amino acids with six codons are highlighted in blue. The threefold degenerate codons of Ile are highlighted in green, whereas the single codons of Met and Trp are highlighted in white. The three stop codons are highlighted in orange. Non-canonical codon use by some organisms and mitochondria is shown by using a small font for the amino acids (blue) or translational stop codons (red) [39].

No tRNA modified at positions 35 and 36 was found in *E. coli*. Table 2 shows the general pattern of modifications at position 34, and Table 3 the general pattern of modifications at position 37 (summarized from [50, 60] and Modomics database, 13/10/12 (*E. coli*)).

Modification	Characteristic
xcmo⁵U	family codon boxes
xmn⁵xUx	mixed codon boxes, purine-reading tRNAs
unmodified A	not found
Q or GluQ	mixed codon boxes, pyrimidine-reading tRNAs

*Table 2: Pattern of modifications at position 34 on the tRNA. * - $tRNA^{Sec}_{UCA}$ U34 is unmodified in S. Typhimurium.*

Modification	Characteristic
ms²i(o)⁶A	codons starting with U*
t⁶A	codons starting with A**
m¹G	codons starting with C (Leu, Pro and Arg***)
unmodified G	not found, always m¹G
most unmodified A	followed by C36****

*Table 3: Pattern of modifications at position 37 on the tRNA. * - except $tRNA^{Ser}_{GGA}$ ** - except initiator $tRNA^{Met}_{CAU}$, *** - except $tRNA^{Arg}_{ICG}$ with m^2A, **** - strong C36:G(I) base pair*

tRNA harboring an anticodon $A_{34}NN$ never coexists with another tRNA harboring an anticodon $G_{34}NN$ for the same amino acid (Figure 6). $tRNA_{GNN}$ or $tRNA_{INN}$ read U(III) and C(III) codons by wobbling in bacteria. tRNAs with ANN anticodons could cause cross-box miscoding of purine-ending codons, therefore they are avoided [56]. Further uridine 5-oxyacetic acids (cmo^5U) are used in some family codon boxes (Val, Pro and Ala; less frequently Leu, Ser and Thr) at position 34 to read all 4 codons. For the family codon box Arg two tRNAs are found in bacteria, $tRNA_{ICG}$ and $tRNA_{CCG}$. Modifications are important to distinguish the mixed decoding boxes. For Ile $tRNA_{GAU}$ and surprisingly $tRNA_{CAU}$ are used, which is modified on position 34 to lysidine. This modification allows exclusively decoding of the Ile codon AUA. The $tRNA^{Met}$ on the other hand is modified with ac^4 on position 34, which causes straightening of the base pair interaction between C and G. To distinguish Cys, Trp, and the stop codons only the less frameshift-prone bases C(III) (Trp) and G(III) (Cys) are used, but no modifications within the decoding region are found. To avoid wobbling between Tyr, Gln and the stop codon, Tyr is encoded by $tRNA_{QUA}$ (Q inhibits in this case wobbling) and Gln is encoded by $tRNA_{cmnm5s2UUG}$ and $tRNA_{CUG}$, both with a 2-methyladenosine at position 37 (summarized from [50] and Modomics database, 13/10/12 (*E. coli*)).

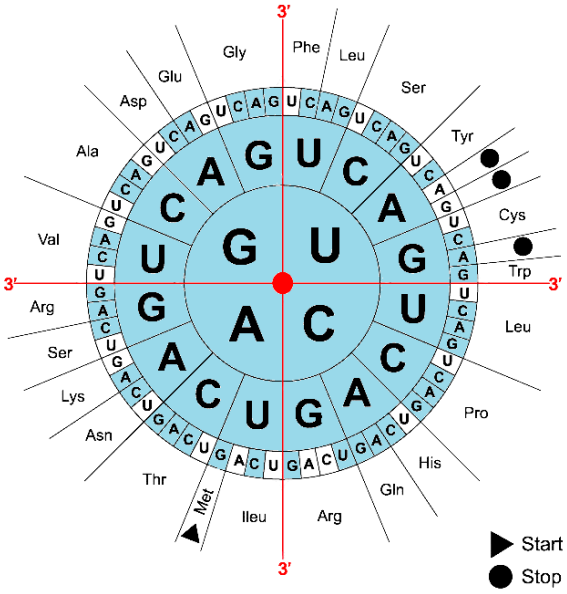

Figure 6: Adapted codon sun. All codons for which associated tRNAs in E. coli are known are colored in blue. The white codons are read via wobbling. tRNAs with A on position 36 avoided to be used, as they are prone to wobble [56].

Many tRNA modifications are of central importance for translational accuracy and inhibition of frameshifts; because they refine the interactions between codon and anti-codon, support the ribosome to maintain its position on the mRNA, and thereby to keep the right reading frame for the translated protein. Since decades, the influence of tRNA modifications on the frequency of frameshifting are studied i.a. by Björk and his co-workers. They study *E. coli* and *S.* Typhimurium

mutants lacking genes for diverse tRNA modifying enzymes and investigate their effect on frameshifting with distinct codon combinations. They use plasmids to report the frameshifts, and also to show if the frameshifts occur when the codon is bound to the A or P site of the ribosome. The systems are based on known programmed frameshift causing sequences (e.g. of HIV-1) or especially designed sequences, and the *lacZ* gene for visualization or a stop codon following the frameshift region in a defined reading frame. They show that lacking tRNA modifications can cause a higher frameshifting rate, mostly in +1 direction and hardly in -1 direction. Their results are shortly summarized in Table 4 [57-59].

		Increased −1 fs		Increased +1 fs	
Modification tested	**Codon tested**	**P site**	**A site**	**P site**	**A site**
Q34	UAU	ND	No	No	Yes
Q34	AAC	ND	No	ND	ND
s^2- of mnm^5s^2U34	AAA	No	ND	Yes	Yes
mnm^5- of mnm^5s^2U34	AAA	No[b]	ND	Yes	Yes
ms^2io^6- of ms^2io^6A37	UUU	No	ND	Yes	No
ms^2- of ms^2io^6A37	UUU	No	ND	Yes	No
o^6- of ms^2io^6A37	UUU	No	ND	Yes	ND
ms^2io^6- of ms^2io^6A37	UUA	ND	No	ND	ND
ms^2- of ms^2io^6A37	UUA	ND	No	ND	ND
o^6- of ms^2io^6A37	UUA	ND	No	ND	ND
ms^2io^6- of ms^2io^6A37	UAU	ND	No	Yes	Yes
Y-base	UUU	No	ND	ND	ND
m^1G37	UUA	ND	No	ND	ND
Ψ39	UUU	No	ND	No	ND
Ψ39	UUA	ND	No	ND	ND
Ψ39	AAA	No	ND	ND	ND
Ψ39	AAC	ND	No	ND	ND
Ψ55	UUU	No	ND	No	ND
Ψ55	UUA	ND	No	ND	ND
Ψ55	AAA	No	ND	ND	No
Ψ55	AAC	ND	No	ND	ND

Table 4: Influence of the lack of diverse tRNA modifications to the probability to frameshift +1 or -1 at distinct codons. ND stands for not determined [57-59].

Their hypothesis how frameshifts occur is as follows: hypomodified tRNAs are less affine to their codons than near-cognate tRNAs, which then bind to the codons and cause shifts; the hypomodified tRNAs enter proportionally slowly the A site entailing a translational pause, which can cause the tRNAs in the P site to shift the frame (A site effects). Or the hypomodified cognate tRNA is bound too leaky to the codon in the P site and thereby cannot maintain the position of the ribosome on the mRNA while the A site is empty (P site effect). tRNAs showing A site effects also show P site effect, in two cases strong P site effects were observed but no A site effects for the same modification ($tRNA^{Phe}$ deficient in ms^2io^6A37 and $tRNA^{Gln}$ deficient in mnm^5s^2U34)(Figure 7).

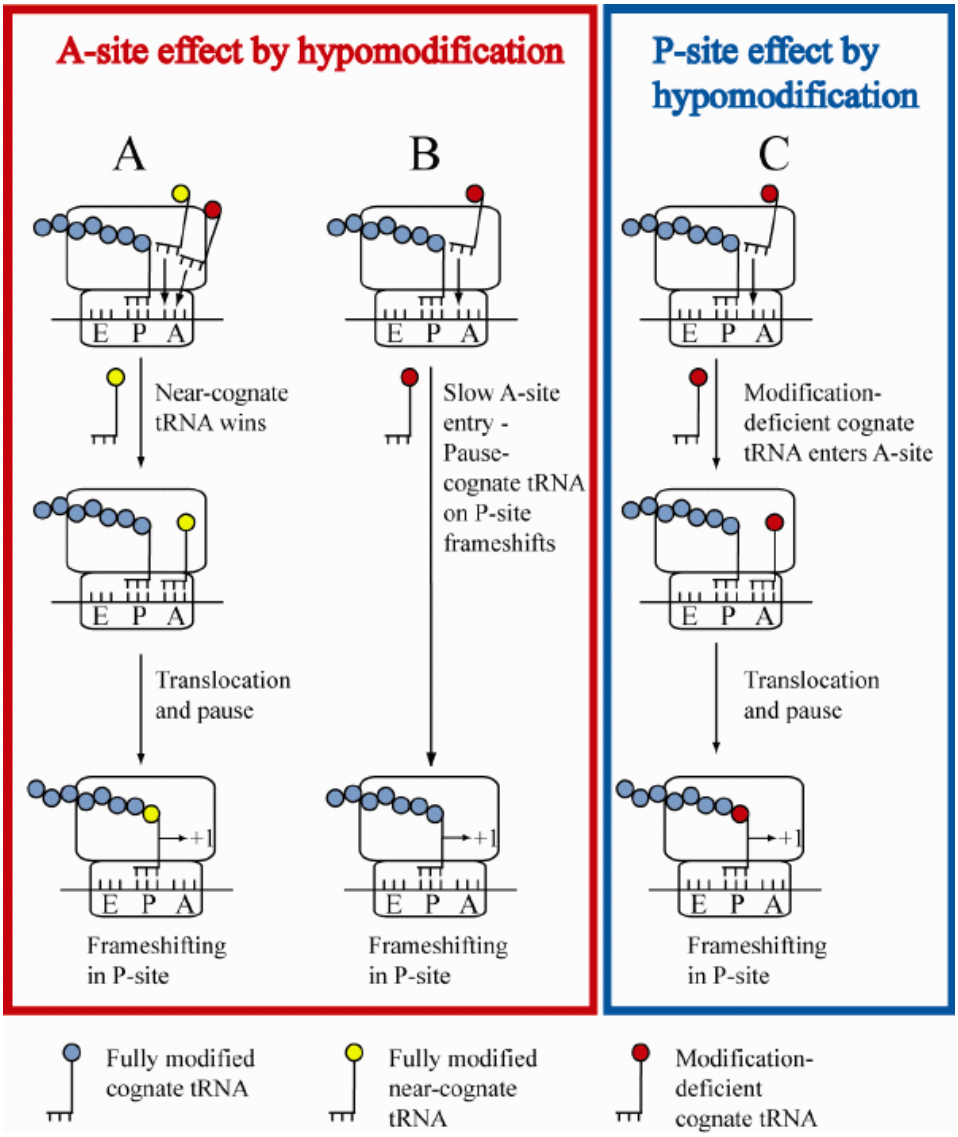

Figure 7: Illustration of the frameshift model. Case A: a near-cognate tRNA wins the competition to bind to the codon in the ribosomes A site and shifts +1 or -1 in the P site after translocation. Case B: the hypomodified tRNA binds slowly to the anticodon, causing a translational pause; this can cause a shift, when the tRNA in the P site is not capable to stabilize the position on the mRNA long enough. Case C: the hypomodified tRNA is accepted in the A site and causes a shift when it is residing in the P site [60].

Beside the situation on the A and P site of the ribosome, also the tRNA within the E site has an influence on frameshifting, as shown for the programmed +1 frameshift during translation of termination factor RF2. In this sequence 3' of the position causing the frameshift, a SD-like sequence is located, which binds to the anti-SD sequence of the ribosomal rRNA. In a minimal *in vitro* system the SD-like sequence is shown to cause premature release of the E site's tRNA and thereby causing a high-level frameshifting. Without the SD-like sequence the +1 frameshifting event at this sequence was not monitored [47].

Additionally to the data shown in Table 4, the following findings about tRNA modifications and frameshifts are published: lacking Gm18 modifications increase frameshifting by 60% at the CUU-UAU/C sites (A site effect) and by 40% at the UAU-UAG site (P site effect) [61]; contradictory studies if lacking xm^{5}U-type or Q modifications cause frameshifts [41, 62-64].

Studies of the importance of tRNA modifications for bacterial virulence are published for *S. flexneri* [65, 66], *E.coli* [61, 67], *P. syringae* [68], *P. aeruginosa* [69] , and *A. tumefaciens* [70].

3.3.3 Biosynthesis of tRNA modifications

In frame of this project a selection of tRNA modifications was studied (Figure 8). Pathways which are already elucidate to some extent, for which already some effects on frameshifting were monitored, and which modify nucleotides within the anticodon stem-loop were preferred. Further the enzymes should not be described as being essential.

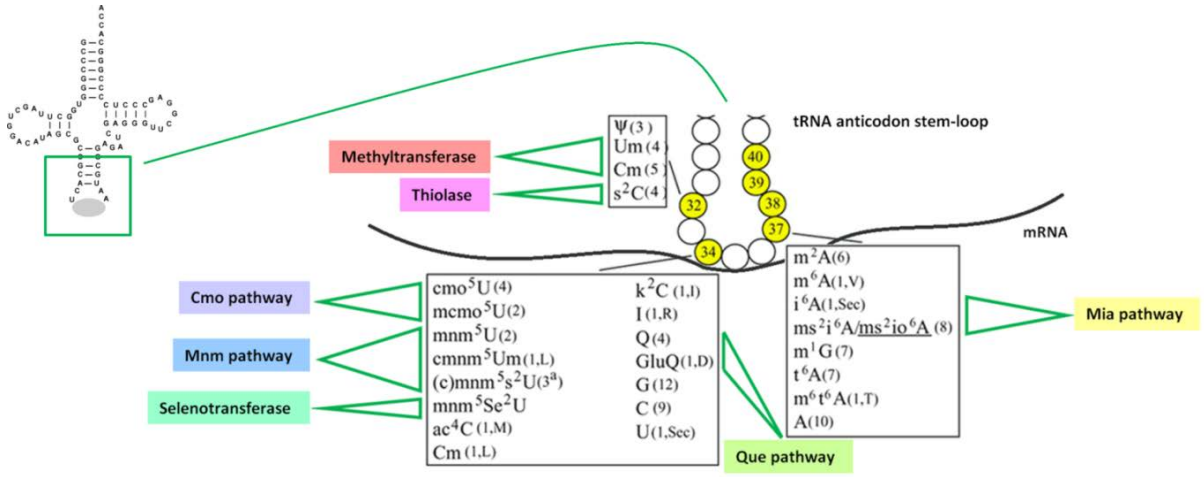

Figure 8: Illustration of the tRNA anticodon stem-loop, showing all in 2005 known modifications of positions 32, 34, and 37. The pathways and single enzymes studied in frame of this project are indicated (modified from [60]).

3.3.3.1 Queuosine pathway (position 34)

The base queuine is ubiquitously present in prokaryotes and eukaryotes, but can only be produced by prokaryotes [62].

In order to introduce queuosine modifications onto a tRNA a series of enzymatic reactions is need to convert GTP into queuosine precursor preQ$_1$ (Figure 9) [71]. Tgt exchanges guanine for preQ$_1$, thus is the first real tRME in the pathway. Exclusively for tRNA$_{Asp}$ enzyme YadB further modifies queuosine by attaching a glutamic acid residue [72].

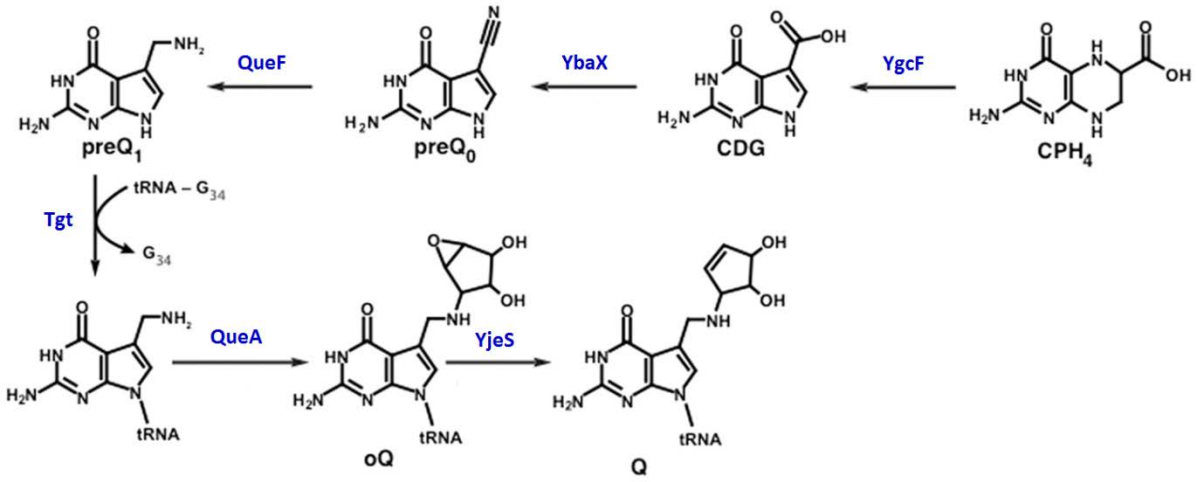

Figure 9: Synthesis of queuine in E. coli K-12. GTP is converted to 7-amino-7-deazaguanine (preQ1), catalyzed by a several enzymes (GTP cyclohydrolase I (GCH I), 6-carboxy-5,6,7,8-tetrahydropterin (CPH4) synthase, 7-carboxy-7-deazaguanine (CDG) synthase (in Salmonella YgcF), preQ0 synthase (in Salmonella YbaX), and preQ0 reductase (in Salmonella QueF)). preQ1 is then incorporated instead of guanine at position 34 on the tRNA by tRNA:guanine transglycosylase (Tgt) and elaborated to epoxyqueuosine (oQ) by oQ synthase (in Salmonella QueA). Epoxyqueuosine is further reduced by the B12-dependent oQ reductase (in Salmonella YjeS) to queuosine (modified from [71]).

The Q modifications are present in the first anticodon positions of the tRNAs in mixed coding boxes, encoding NAC codons (Tyr, His, Asp, and Asn)(Table 5, Figure 10).

	Position			
codon	I	II	III	triplet
anticodon	3 36	2 35	1 34	triplet tRNA

Table 5: Visualization of the used nomenclature for the positions on the codon triplet and the associated positions within the anticodon and on the tRNA, respectively.

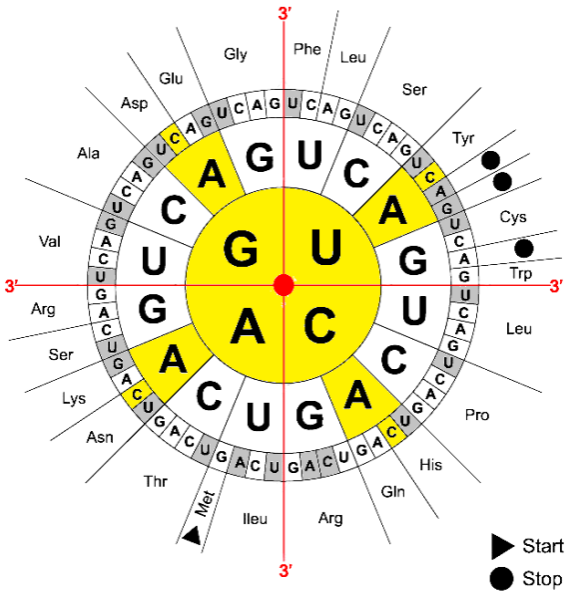

Figure 10: Codon sun colored for the que pathway. Yellow highlighted codons indicate the existence of associated tRNAs carrying the Q modification at position 34 in E. coli (according to Modomics database, 15/10/12). For the codons that are filled grey at position III no associated tRNA in E. coli ate known, instead they are read via wobbling.

In *E. coli* a *Δtgt* mutant showed no growth rate reduction *in vitro*, although its survival in stationary phase was reduced [73]. In *Shigella* the ortholog of Tgt is essential for virulence [66]. No literature indications for the growth rate nor the virulence of *Salmonella Δtgt* mutants have been found.

The findings about the influence of Q modifications on translational accuracy are ambiguous. $tRNA^{His}_{Q34UG}$ prefers the codon CAU in contrast to normal $tRNA^{His}_{G34UG}$, which has a clear preference for the histidine codon CAC [74]. Furthermore $tRNA^{Tyr}_{Q34UA}$ prevents stop codon read through, whereas $tRNA^{Tyr}_{G34UA}$ allows it [75]. Q34 does not influence the decoding efficiency of $tRNA^{His}$ [76]. The binding efficiency of *E. coli* $tRNA^{Tyr}$ to the ribosome is reduced 2-fold without change in the codon choice [77]. Further $tRNA^{Asp}_{QUC}$ forms a stable complex with the two codons GAC and GAU, whereas $tRNA^{Asp}_{GUC}$ binds only the GAC codon [78]. This leads to the suggestion that the influence of Q34 varies with the tRNA species. The functions of the glutamyl residue of $tRNA^{Asp}_{QUC}$ are not understood yet, but *E. coli ΔyadB* mutant has no obvious growth reduction [79].

Queuosine modifications are antideterminants for the aminoacyl-synthetases GlnRS and LysRS, which need to distinguish between purines and pyrimidines on position 34 of tRNAs reading the mixed coding boxes CAN and UUN, respectively [51, 52, 80, 81].

3.3.3.2 Mnm pathway (xmn^{5}xU34)

The mnm pathway envelopes a thiolase and several methylases that introduce modifications at positions C2 (Figure 11) and position O5 of uridine on position 34, respectively.

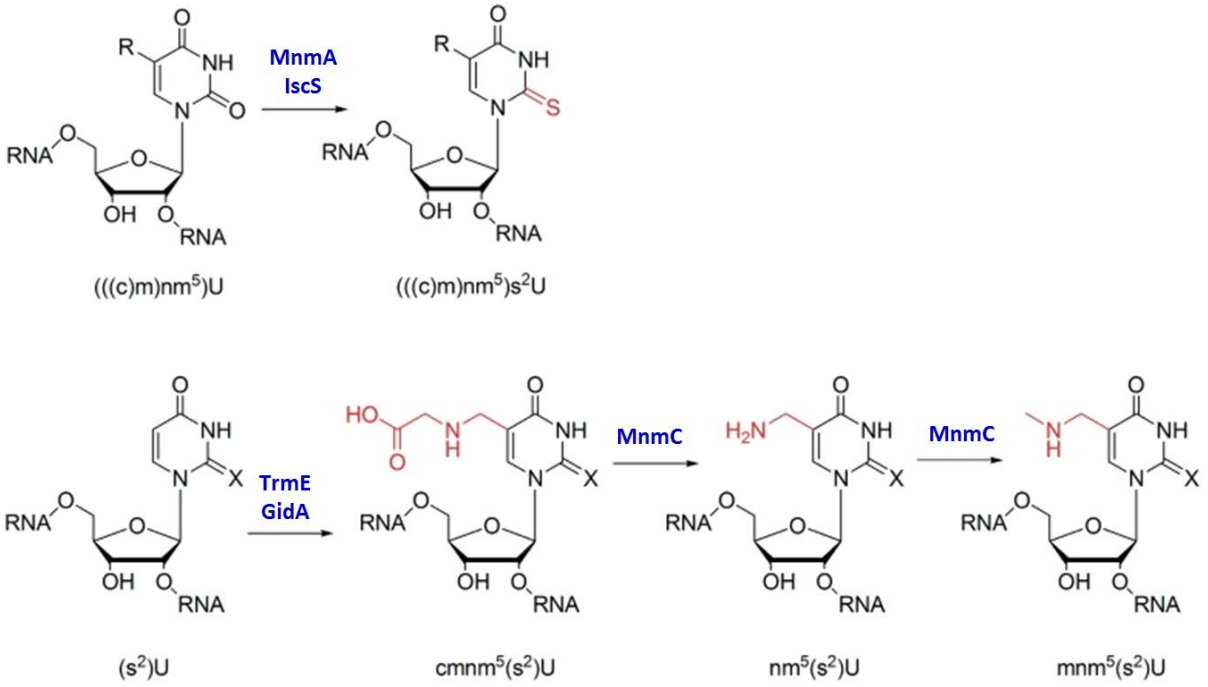

Figure 11: Reaction and enzymes incorporating the s^2 and mnm^5 modifications to U on position 34 in Salmonella showed schematically. Scheme modified from [82].

In *E. coli* MnmA performs thiolation at C^2 of U34 in tRNA molecule. This modification occurs in tRNAs interacting with NAA codons to stabilize weak A:U pairs ($tRNA^{Lys}_{mnm5s2UUU}$, $tRNA^{Glu}_{mnm5s2UUC}$, and $tRNA^{Gln}_{(c)mnm5s2UUG}$).

Modifications of the nm^{5}U-type are realized by the following enzymatic steps: MnmE and MnmG (also called GidA) form a heterotetrameric complex (MnmEG), which is capable to catalyze the GTP- and FAD-dependent reactions necessary to produce 5-aminomethyluridine (nm^{5}U) and 5-carboxymethylaminomethyluridine (cmnm^{5}U) out of ammonium and glycine, respectively. The modifications are found in $tRNA^{Lys}_{mnm5s2UUU}$, $tRNA^{Glu}_{mnm5s2UUC}$, $tRNA^{Gln}_{(c)mnm5s2UUG}$, $tRNA^{Arg}_{mnm5UCU}$, $tRNA^{Leu}_{cmnm5UmAA}$, and $tRNA^{Gly}_{mnm2UUG}$ (Figure 12). In some of the tRNAs ($tRNA^{Lys}_{mnm5s2UUU}$, $tRNA^{Glu}_{mnm5s2UUC}$, $tRNA^{Gln}_{mnm5s2UUG}$, $tRNA^{Arg}_{mnm5UCU}$, and $tRNA^{Gly}_{mnm2UUG}$) MnmC deacetylates the cmnm^5 group previously added by MnmEG in a FAD-dependent manner to nm^5 and furthermore methylates the group SAM-dependent to mnm^5. MnmC consists of two catalytic sites (MnmC1 and MnmC2), which work independently from each other. MnmC1 catalyzes the FAD-dependent reaction and MnmC2 the SAM-dependent one [83].

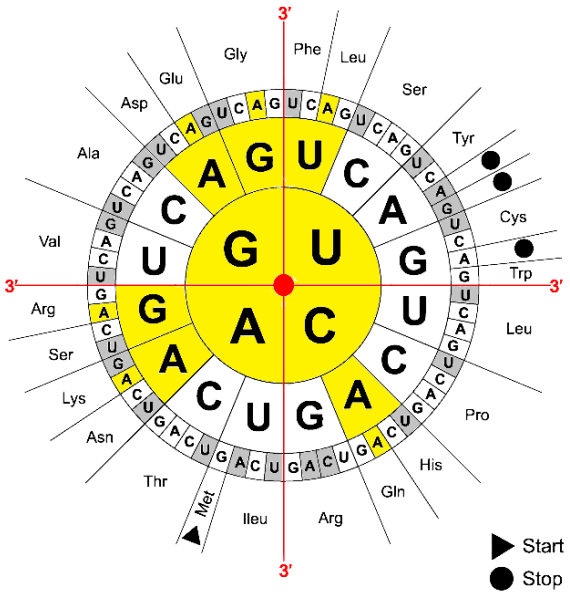

Figure 12: Codon sun colored for the mnm pathway. Yellow highlighted codons indicate the existence of associated tRNAs carrying the xnm^{5}U34 modification in E. coli (according to Modomics database, 15/10/12). For the codons that are filled grey at position III no associated tRNA in E. coli ate known, instead they are read via wobbling.

It is not clear to which extent incorporation of xnm^5 and s^2 are connected to each other (Figure 10). So far no tRNA$_{s2UUN}$ has been detected, but *E. coli* MnmA successfully incorporates the thiol group to tRNA$^{Glu}_{UUC}$ lacking the xnm^5 modification *in vitro* [84].

Nucleotides with an xnm^{5}U34 modification read codons with A(III) in a classical manner and also G(III) codons with high effectivity via a bifurcated hydrogen bond between O_2 of mnm^{5}U34 and N1 and N2 of G(III). Addition of a thiol group, resulting in mnm^{5}s^{2}U34, enhances reading of A(III) and has a neutralizing effect onto the wobble capacity toward G(III), due to weakening of the bifurcated hydrogen bond from mnm^{5}U34 to G(III). Further the thiol group causes stronger base stacking with U35 for binding to both A and G bases [56]. Both modifications restrict the wobble capacity to U(III) (Figure 13).

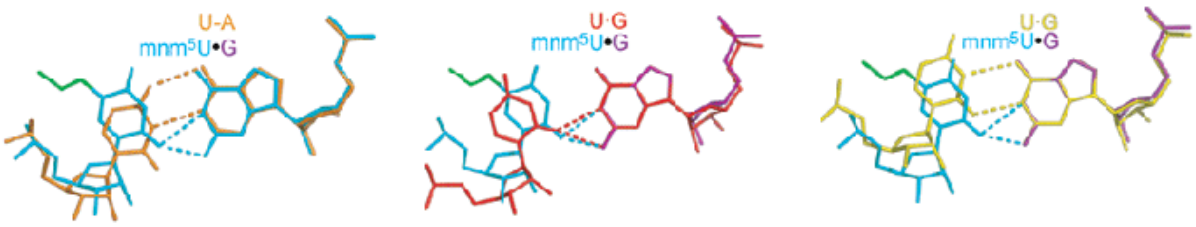

Figure 13: Structural data to mnm^{5}U34:N base pairs. From left to right: mnm^{5}U34:G3 (cyan and green) and U34:A3 (orange). The U34:A3 base pair represents the classic Watson-Crick geometry. mnm^{5}U34:G3 (cyan

and green) and U5:G4 (magenta). Both U:G base pairs use bifurcated hydrogen bonds. mnm^{5}U34:G3 (cyan and green) and G36:U1. The G36:U1 base pair is a classic G:U wobble, but is flipped to align with the mnm^{5}U34:G3 base pair. Hydrogen bonds are indicated via dashed lines [56].

The 2-thio group of the xnm^{5}s^2 modification, but not the xnm^5 side chain alone, is an important identity element for aminoacylation of tRNA$^{Lys}_{mnm5s2UUU}$, tRNA$^{Glu}_{mnm5s2UUC}$, and tRNA$^{Gln}_{(c)mnm5s2UUG}$ [51, 52, 80, 81].

Detailed analysis of a *Salmonella* Typhimurium *ΔgidA* mutant showed that lack of this gene causes defects in invasion of intestinal epithelial cells, bacterial motility, intracellular survival, and induction of cytotoxicity in host cells. The mutant showed a filamentous morphology compared to the normal rod-shaped phenotype of the wild-type. In *in vivo* experiments a significant reduction of inflammatory cytokine and chemokine induction and less histopathological lesions were observed. The LD_{50} dropped down 1000 fold compared to the wild-type. Deletion of *gidA* caused a significant alteration of the expression of several bacterial factors associated with pathogenesis as indicated by global transcriptional and proteomic profiling. According to these results, GidA accomplishes an essential role in virulence [85].

In addition to the gaps in understanding of the biosynthesis pathway architecture, it is also not completely clear how xnm^{5}U34 modifications function. For instance, there is no explanation delivered yet why tRNA$^{Gly}_{mnm5UUG}$ carries a restrictive mnm^5 modification, although it is reading a family codon box.

3.3.3.3 Cmo pathway (xmo^{5}U34)

Incorporation of the (x)mo^5 modification is not fully understood yet. It is known that chorismic acid and methionine are necessary for synthesis of the modification, and that the enzymes CmoA and CmoB are involved in *E. coli* (in *Salmonella* YecO and YecP)(Figure 14)[86].

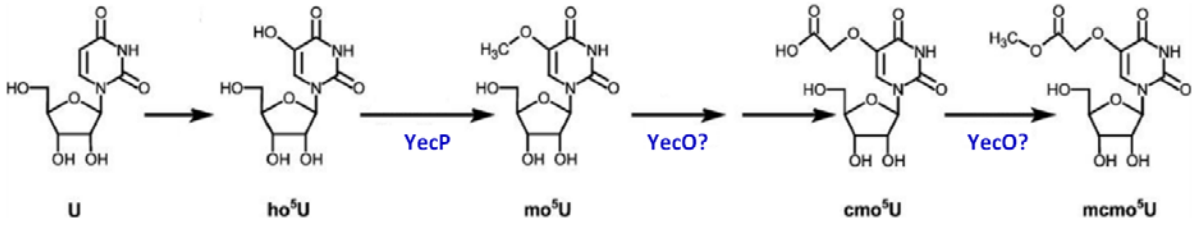

Figure 14: Proposed scheme of the cmo pathway, incorporating the (m)cmo^5 modification onto U at position 34. The pathway is to our knowledge not completely known yet, but YecP and YecO are proven to catalyze reactions of the pathway. mcmo^{5}U34 is not occurring in neither E. coli nor Salmonella (Modomics database, 17/10/12). Scheme modified from [86].

The xmo^{5}U34 modifications are present in all 6 family codon boxes (Ser, Leu, Pro, Thr, Val, Ala) in which tRNAs with U34 have the potential to read all 4 codons due to wobble (Figure 15)[87]. Interestingly in the other family codon boxes (Arg and Gly) tRNA$_{UNN}$ does not exist in bacteria [50].

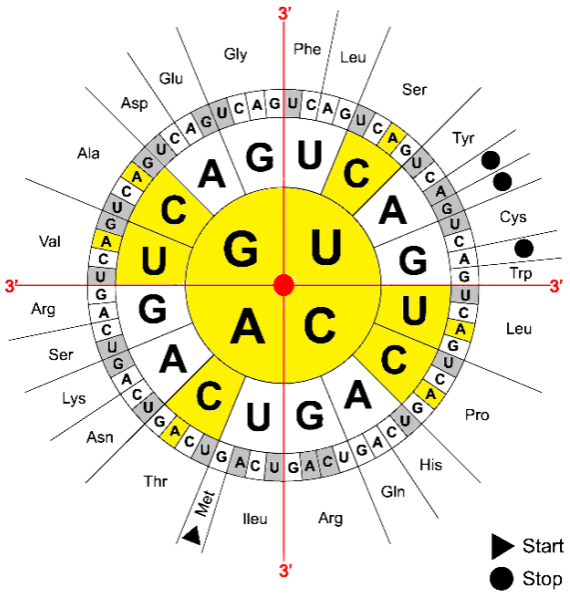

Figure 15: Codon sun colored for the cmo pathway. Yellow highlighted codons indicate the existence of associated tRNAs carrying the cmo⁵U34 modification in E. coli (according to Modomics database, 15/10/12). $tRNA^{Leu}_{UAG}$ is described in literature to carry the modification [87], but not on the database. For the codons that are filled grey at position III no associated tRNA in E. coli ate known, instead they are read via wobbling.

Studies about the impact of cmo⁵U34 done *in vivo* or *in vitro* with different tRNAs present conflicting findings [86, 89-94]. Recently a trial to generate *S.* Typhimurium mutants encoding only for the U34 tRNA of the family codon boxes of Thr, Val, Ala and Pro ($tRNA^{Thr}_{cmo5UGU}$, $tRNA^{Val}_{cmo5UAC}$, $tRNA^{Ala}_{cmo5UGC}$ and $tRNA^{Pro}_{cmo5UGG}$) showed for Thr that the cmo⁵U tRNA cannot read the C(III) codon; for Val, Ala, and Pro that the modified tRNA can read all codons of each family codon box, but except of $tRNA^{Pro}_{cmo5UG}$ NNC at an extremely reduced rate. Further the tRNA deletions were combined with a *cmoB* deletion, these mutants had reduced wobbling to G(III) codons [87]. Based on these data and on a structural analysis [95] the authors suggest that the function of cmo⁵U34 is dual: the ether oxygen (or the hydroxyl of ho⁵U) stabilizes the anticodon loop via an intra-molecular hydrogen bond to the 2' OH of U33 in a conformation where the wobble uridine is prone to form a base pair in Watson-Crick manner, leading to sufficient stabilization to allow pairing with U(III) and C(III). The rest of the modification (-CH_3 in mo⁵U or -CH_3COOH in cmo⁵U) stabilizes the enol form of the wobble nucleoside and thereby allows a U34:G(III) base pair. Further cmo⁵U34:U base pairs are stabilized by interactions with the rRNA.

3.3.3.4 Mia pathway (ms²io⁶A37)

In *Salmonella* the enzymes of the mia pathway MiaA, MiaB and MiaE incorporate a ms²io⁶ modification onto A at position 37 (*Figure 16*)[96].

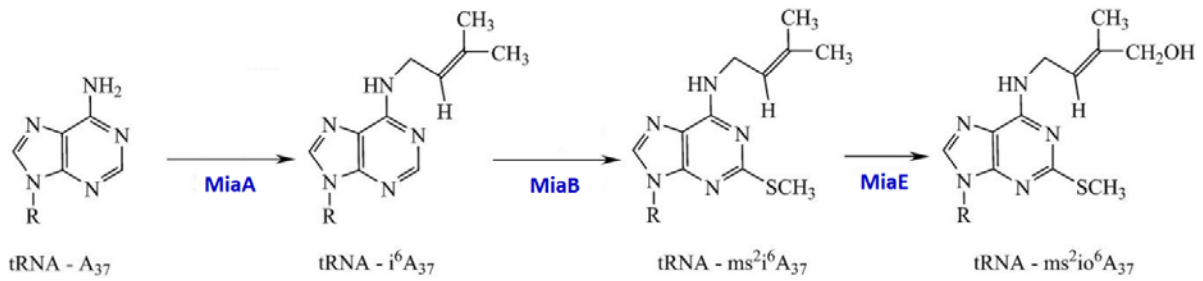

Figure 16: The mia pathway, incorporating the ms²i⁶(o) modification onto A at position 37. The enzyme MiaE and the associated modification ms²i⁶o were only observed in Salmonella. Scheme modified from [96].

In all tRNAs starting with U ms²io⁶A37 (*S.* Typhimurium) and ms²i⁶A37 (*E. coli*) are present (exceptions $tRNA^{Ser}_{GGA}$ (A37) and initiator $tRNA^{Sec}_{UCA}$ (i⁶A37)) (Figure 17). The mutations stabilizes weak A(36):U(I) base pairs (U(36):A(I) base pairs are stabilized by t⁶A37) and are increasing the strength of the interactions nearly to a quadruplet interaction straight in the A and P site of the ribosome (Figure 18)[97].

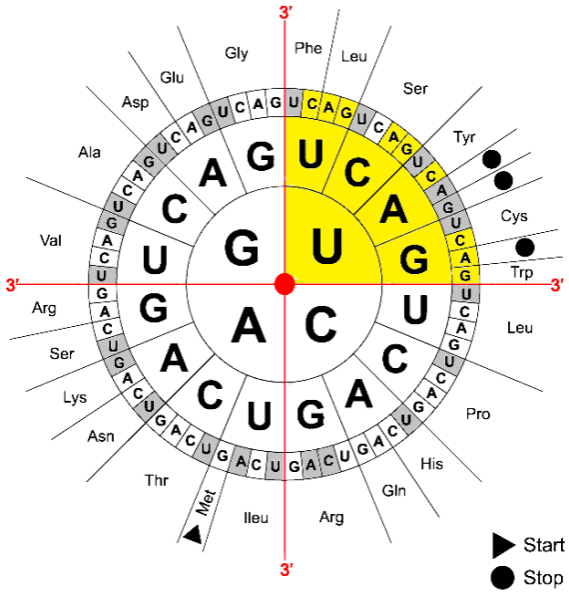

Figure 17: Codon sun colored for the mia pathway. Yellow highlighted codons indicate the existence of associated tRNAs carrying the ms²i⁶A37 modification in E. coli (according to Modomics database, 15/10/12). For the codons that are filled grey at position III no associated tRNA in E. coli ate known, instead they are read via wobbling.

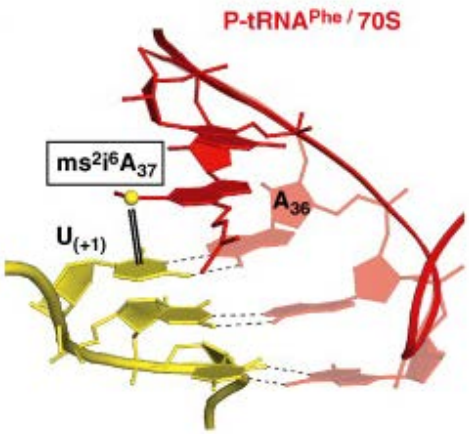

Figure 18: Interactions of of the ms²i⁶A37 modified tRNA^{Phe} and the codon UUU at the P site of the ribosome. Cross-strand stacking of the 2-methylthio group of ms²i⁶A37 with the first base of the codon is indicated [98].

Mutants lacking *miaA* have 20–50% media-dependent growth rate reductions compared to the wild-type [99, 100]. Mutants lacking *miaB* show no difference in the growth rate to the wild-type, but are more sensitive toward several amino acid analogs and metabolizes some carbon sources differently from the wild-type, the same is true for *miaA* deletion mutants [101]. Deletion of *miaE* has no effect on the growth rate in normal conditions; but the gene seems to contribute to the metabolism of *Salmonella* in an unknown way, as *miaE* lacking mutants are unable to grow aerobically on succinate, fumarate or malate, although *miaA* mutants can [102, 103].

Lack of the ms²i⁶ modification reduces the codon reading efficiency of tRNAs *in vitro* [104, 105]. Further the efficiency of suppressor tRNAs is dramatically reduced [99, 106, 107]. The isopentenyl imposes the major effect on the efficiency of the modified tRNA, since mutations in *miaB* suffer a minor effect than mutations in *miaA* [101].

3.3.3.5 Single tRMEs

3.3.3.5.1 Selenotransferase YbbB (mnm⁵se²U34)

YbbB exchanges the sulfur of the mnm⁵s²U34 modification for selenium in the following tRNAs: tRNA$^{Lys}_{mnm5s2UUU}$, tRNA$^{Glu}_{mnm5s2UUC}$, and tRNA$^{Gln}_{cmnm5s2UUG}$ (Figure 19)[108]. Compared with mnm⁵s²U34, mnm⁵se²U34 equalizes the reading of the A- and G-ending codons due to increased wobble interactions with G [109].

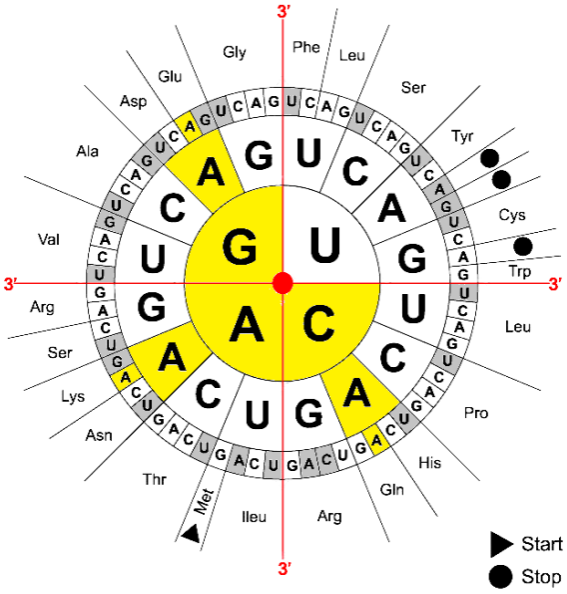

Figure 19: Codon sun colored for the enzyme YbbB. Yellow highlighted codons indicate the existence of associated tRNAs carrying the mnm^{5}se^{2}U34 modification in E. coli (according to [108]). For the codons that are filled grey at position III no associated tRNA in E. coli ate known, instead they are read via wobbling.

Further YbbB catalyzes geranylation (exchange of s^2 with $C_{10}H_{17}$) of the same tRNAs, although these two reactions are likely to proceed through distinct pathways, because the activities of enzyme required to incorporate the modifications are very different from each other. The impact of geranylation onto translation is not understood yet, but it is likely that such a large hydrophobic modification has a broad impact. The actual state of knowledge is that the modification equalizes the preference for A- and G-ending codons [110], similar to exchange of s^2 with se^2.

3.3.3.5.2 Methyltransferase YibK (cmnm^{5}Um34 and Cm34)

YibK modifies the wobble nucleotides in $tRNA^{Leu}_{CmAA}$ and $tRNA^{Leu}_{cmnm5UmAA}$. The enzyme requires a pyrimidine nucleoside at position 34, it has a clear preference for an adenosine at position 35 and it can methylate position 34 only when ms^{2}i^{6}A is priory added at position 37. The methyl modulation carries out a role in fine-tuning of the codon–anticodon recognition process and thereby enhances cognate codon–anticodon recognition. Further *yibK* deletion mutants show no difference in growth compared to the wild-type in rich medium at either 37°C or 42°C [111].

3.3.3.5.3 Thiolase YdaO (s^{2}C32)

YdaO incorporates a thiol group onto C at position 32. All tRNAs having a s^{2}C in position 32 also have an A in position 38, allowing a S2(s^{2}C32):N6(A38) bifurcated hydrogen bond ($tRNA^{Arg}_{CCG}$, $tRNA^{Arg}_{ACG}$, $tRNA^{Arg}_{UCU}$, and $tRNA^{Ser}_{GCU}$). Without the thiol group the structure of the anticodon stem-loop theoretically changes and the tRNA is predicted to have a disadvantage in competing with non-cognate tRNAs [112]. Surprisingly a *ydaO* lacking mutant does not suffer a growth rate reduction *in vitro* [113].

3.3.3.5.4 Methyltransferase YfhQ (Um32 and Cm32)

The methyltransferase YfhQ was recently identified as enzyme catalyzing methylation of uridine and cytosine at position 32 in $tRNA^{Gln}_{CUG}$ and $tRNA^{Ser}_{UGA}$, respectively. The biochemical aspects of the enzyme were recently described [114]. To your knowledge no information about the function of these methylations is available.

3.3.3.5.5 Methyltransferase SpoU (Gm18)

SpoU attaches a methyl group to G at position 18. The Gm18 modification is involved in stabilizing the L shaped structure of tRNA, by interacting with Ψ55 via a hydrogen bond (Figure 20)[115, 116]. Mutants lacking Gm18 modifications grow with a reduced rate in comparison to the wild-type, especially at high temperatures.

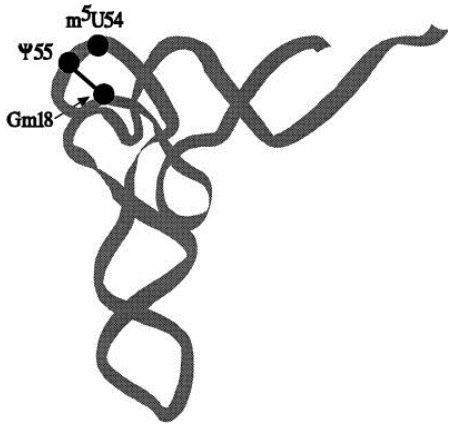

Figure 20: Scheme of the tRNA tertiary structure, showing the hydrogen bond between Ψ55 and Gm18 [61].

4 Aim of the project

During infection *Salmonella* are under continuous pressure of the immune system and starve due to limited resources within macrophages, which slower bacterial growth down and lower translational accuracy. Potential drugs which lower translation accuracy e.g. by inhibiting a tRME's function can cause a life-threatening error catastrophe for the pathogen and thereby have potential to be very useful targets for new antimicrobials.

The project aim was to evaluate tRNA modifying enzymes as potential drug targets for novel antimicrobials. As a starting point we have chosen *Salmonella* serovar Typhimurium to create a comprehensive set of gene deletion mutants, lacking enzymes that introduce modifications in the tRNAs anticodon step loop. According to our hypothesis participation of such undermodified tRNAs in translation should impose bacterial fitness cost due to elevated frameshifting and misreading, and therefore reduce virulence of *Salmonella*. The main approach included systematic analysis of tRMEs' gene deletion influence on bacterial growth in culture as well as during infection in the mouse model of typhoid fever. In order to prove the link between the effects imposed by tRME gene deletions and protein synthesis accuracy, a part of the project has been devoted to development of a reporter tool for protein synthesis accuracy evaluation in a living pathogen.

5 Research design and results

5.1 Creation of *Salmonella* strains lacking tRNA modifying enzymes

First a deletion mutant library of chosen tRMEs was created, in order to analyze the effect of lacking tRME on translational accuracy and consequently bacterial fitness. The enzymes modify nucleotides within the anticodon stem-loop of tRNAs (except of SpoU) or contribute to the synthesis of precursor products (YgcF, YbaX, QueF)(Table 6). Beside the single deletion mutants, also five double mutants were created (YdaO YfhQ, YdaO YecO, YecP YecO, MiaE MnmC, and QueA QueA_p).

Enzyme name	Function	Pathway	Modified position
Ybb	selenotransferase	-	U34
YibK	methyltransferase	-	cmnm5U34 and C34
YdaO	thiolase	-	C32
YfhQ	methyltransferase	-	U32 and C32
SpoU	methyltransferase	-	G18
YecO	methyltransferase	Cmo pathway	U34
YecP	methyltransferase	Cmo pathway	U34
MiaA	dimethylallyltransferase	Mia pathway	A37
MiaB	methylthiotransferase	Mia pathway	A37
MiaE	hydroxylase	Mia pathway	A37
TrmE	GTPase	Mnm pathway	U34
GidA	other	Mnm pathway	U34
MnmC	methyltransferase	Mnm pathway	U34
MnmA	thiolase	Mnm pathway	U34
YgcF	other (non tRME)	Que pathway	Q34
YbaX	other (non tRME)	Que pathway	Q34
QueF	other (non tRME)	Que pathway	Q34
Tgt	transglycosylase	Que pathway	Q34
QueA	isomerase	Que pathway	Q34
QueA_p	isomerase	Que pathway	Q34
YjeS	oxidoreductase	Que pathway	Q34
YadB	other	Que pathway	Q34

Table 6: List of all enzymes characterized within this project, their functions, their pathways, and the type and the position on the tRNA of the modified nucleotide. For more detailed information see chapter 3.3.3.

The above-mentioned genes located on the *Salmonella* chromosome were substituted for a kanamycin cassette (see the Appendices D, F) using λ Red recombination (Figure 21).

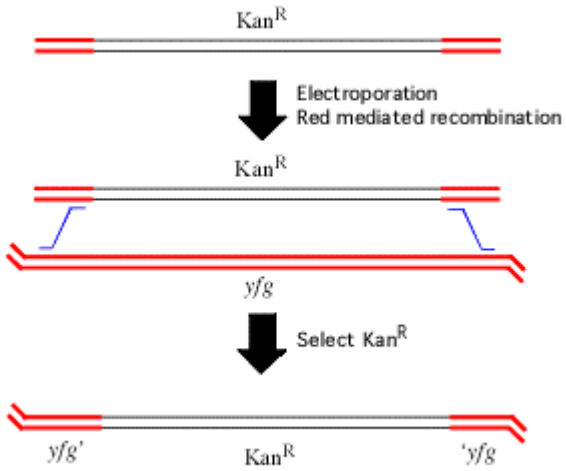

Figure 21: Chromosomal gene deletion using λ Red recombination. The viral recombination system, encoded on the plasmid pKD46, allows the exchange of DNA sequences via recombination.

As electroporation of DNA fragments is in general inefficient, the PCR product has been electroporated into a strain created in the lab that lacks genes (*ΔgalK, ΔhisG, Δres, Δ4495,* and *ΔhsdR*), which are critical for protection from foreign DNA, and further already contains pKD46. During electroporation nonspecific secondary mutations can be introduced. Such mutations can mask the phenotype of gene deletions of interest. In order to guarantee that the observed phenotypes arise due to the tested gene deletion, and not to any additional unknown mutations within the strain, the region containing the deleted gene has been transduced into the wild-type *Salmonella* strain SL1344 using p22 phages.

p22 phages bind to the O-antigen residues comprising the LPS on the outer membrane of *Salmonella*, and translocate their DNA into the host cytoplasm [117]. Phage DNA replication results in long concatemers, which are packaged into phage heads by a "headful" mechanism: packaging is initiated at a specific sequence on the DNA called *pac* site, starting from the *pac* site the nuclease moves down the concatemer, cutting every 48 kb [117]. The *Salmonella* chromosome includes sequences that are homologous to the p22 *pac* site, thus the p22 nuclease can also cut one of these chromosomal sites and packages 48 Kb fragments of chromosomal DNA into the new phages. The arising transducing particles can still inject their DNA in a new host, but they are free of phage DNA. The bacterial DNA in the new host can then recombine into the chromosome by homologous recombination [118]. All strains tested further (with the exception of *Δtgt* and *ΔmnmA*) have been created via phage-transduction.

In order to create double gene deletion strains the Kan resistance cassette has been removed from the initial gene deletion strain as the same antibiotic resistance cassette is used as marker for the second gene deletion. To do so, the site-directed recombination system FLP-FRT of *Saccharomyces cerevisiae* encoded on the plasmid pCP20 is used (Figure 22). To allow usage of this system, all antibiotic cassettes used within this project encode FRT sites on both ends (Appendix D).

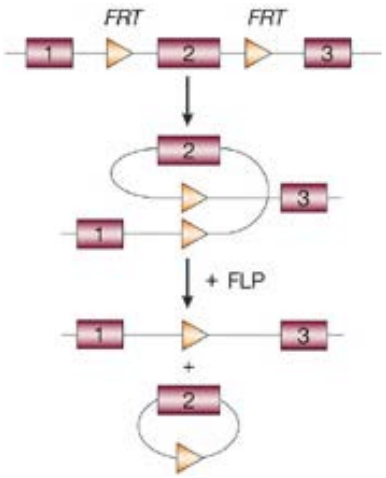

Figure 22: Site-directed recombination system FLP-FRT. FLP (flippase recombination enzyme) binds to the 5'-site of the FRT site and cleaves and ligates its substrates again. The site-specific recombination causes deletion of sequences which are flanked by two FRT sites in the same orientation, leaving behind a scar of one FRT site with no polar effect on downstream genes [119, 120].

The tRME gene deletion strains created by the phage transduction into the wild type background have been further used for the growth rate determination, if necessary with the plasmid pCSα Amp introduced. Further the regions of the deleted genes were transduced into fluorescence-labeled *Salmonella* strains for the growth rates determination during mouse infection (see Table 7, section 6.3. and Appendix E). The genes of the fluorescence proteins are under control of the virulence promoters *sifB* and *virK*. These promoters are exclusively expressed during infection or similar conditions (low pH, low concentration of Mg, and nutrient deficiency), and their usage for fluorescence protein expression does not influence the strains virulence [121].

Strain name	Fluorescence protein 1 (promoter *sifB*)	Fluorescence protein 2 (promoter *virK*)
SBM319	GFP	mCH
SBM321	YFP	mCH
SBM322	CFP	mCH
SRU02	GFPweak	-
SDFR3	GFP	-
SRU05	CFP	-
SNB10	mCH	-

Table 7: List of all wild-type strains capable to express fluorescence proteins used within this project, and the expressed fluorescence proteins with their promoters.

To guarantee that the observed phenotypes arise due to the tested gene deletion, and not to any additional unknown mutations within the strain, the genes need to be restored at their initial positions, and the phenotype of the arising strain is characterized. To restore the gene, phage transduction is used. To create a selection marker for successful phage transduction, *Salmonella* Typhimurium mutants are created from the wild-type with λ Red recombination, which carry the chloramphenicol resistance cassette as near as possible to the target gene in a non-coding region (preferably in a small region where two genes one in plus and the other one in minus direction

end). The resistance cassette and the surrounding DNA are then transduced with p22 phages into the strain, which carries the deletion to be restored. As p22 phages are capable to load about 48 kb it can be roughly estimated that 50% of the phages carrying the resistance cassette also carry the wild-type target gene, when the target gene and the resistance cassette are approximately 5000 bp apart from each other.

A detailed list of all mutants containing also clear information about the respective designer of every strain is attached in Appendix E.

5.2 *In vitro* phenotypes of *Salmonella* lacking tRNA modifying enzymes

5.2.1 *In vitro* growth rates

There is a handful of different tools available to measure bacterial growth rate, and all have their pros and contras (Table 8). We have employed classical methods, like OD_{600} measurements and CFU counting as well as bioluminescence measurements. The latter is based on concurrent to bacterial growth monitoring of luminescent light emission catalyzed by bacterial luciferase.

	spectrometry (OD)	CFU counting	spectrometry (luminescence)	growth competition
measured characteristic	optical density,600 nm	amount of living bacteria	luminescence intensity, 460 nm	amount of fluorescent cells
only living cells	N	Y	Y	Y
cell size influenced	Y	Y	N	N/Y*
automatization possible	Y	N**	Y	N
growth in competition possible	N	N	N	Y
error-prone	Y	Y	N***	N***
time-consuming	Y	Y	N	Y
applicable in rich medium	Y	Y	Y	N
applicable in defined medium	Y	Y	Y****	Y

Table 8: Comparison of the different strategies for bacterial growth rate measurement based on the experimental data obtained during the project implementation. - depends on the quality of gating strategy; ** - usage of image-analysis software is possible, *** - manual visual check is required; **** - the medium should contain single major carbon source, its concentration should be optimized.*

Due to the observation that the cell size of some *ΔtRME* mutants is altered (ranging from filamentous to small, see section 5.2.2), the creditableness of growth rate measurement methods based on optical density or cell count is questionable. To bypass this problem the protein production rate was chosen as criteria for bacterial growth.

Luminescence is proportional to production of bacterial luciferase which is in turn reflects average protein production rate in the cell. Protein production rate is considered correlating well with the bacterial growth. Substrates of the luciferase are long chain fatty aldehydes, molecular

oxygen and reduced flavin mononucleotide ($FMNH_2$), a NAD(P)H-dependent electron carrier of the cells electron transport chain (fully reduced). To replenish the long chain fatty aldehydes a multienzyme complex of a transferase, synthetase, and reductase is needed further [122, 123].

ΔtRME strains have been transformed with the pCSλ plasmid (see Appendix C) encoding the luciferase multi-enzyme complex under a constitutive promoter. Salmonella cells were grown and monitored on the luminescence levels in 96-well plate format in the plate readers Synergy 2 Multi-Mode Microplate Reader and Synergy H4 Hybrid Multi-Mode Microplate Reader (both BioTek), which support medium through put analysis with multiple replicates.

A series of control experiments has been done to evaluate the reliability and reproducibility of the luciferase assay for growth rate measurements.

First of all, a control experiment has been done to evaluate if the luciferase production itself has an influence on *Salmonella* growth rate and the quality of the luciferase data in comparison to typical OD_{600} measurements was evaluated. The growth rates of the strains wild-type, wild-type + pCSλ Amp, *ΔtrmE*, and *ΔtrmE* + pCSλ Amp (randomly chosen *ΔtRME)* were measured with the OD_{600} method, and in parallel the two strains with the plasmid were also measured with the luciferase assay. Both strains expressing the plasmid show a growth rate reduction of 10%, as the luciferase diverts a lot of energy (Figure 23). But the growth rate ratio of the mutant strain to the wild-type strain measured using OD_{600} stays the same (0.79 without plasmid, 0.80 with plasmid, single replica).

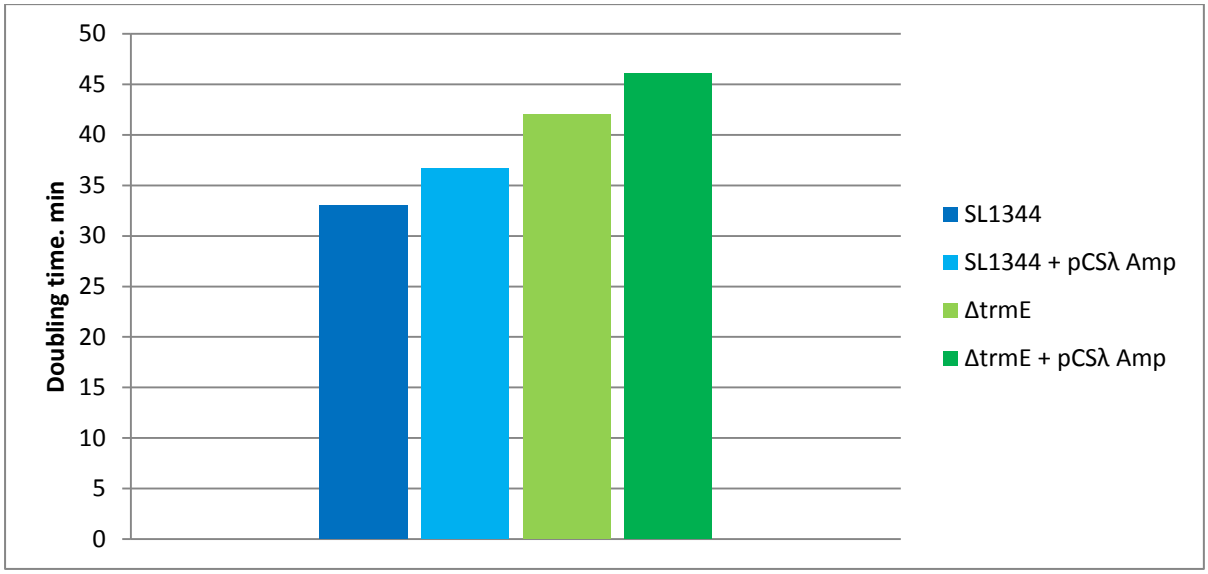

Figure 23: Influence of the luciferase plasmid pCSλ Amp on the Salmonella growth rate. Doubling times of wild-type (SL1344), wild-type with the luciferase plasmid (SL1344 + pCSλ Amp), ΔtrmE, and ΔtrmE with the luciferase plasmid (ΔtrmE + pCSλ Amp) grown in LB low salt and measured at OD_{600}. The data have been obtained in a single experiment.

The growth rate ratio evaluated using the luciferase assay of *ΔtrmE* + pCSλ Amp is 0.92 (7 replicas) (Figure 24). This difference most likely arises because the OD_{600} measurements were only conduced with single replicas.

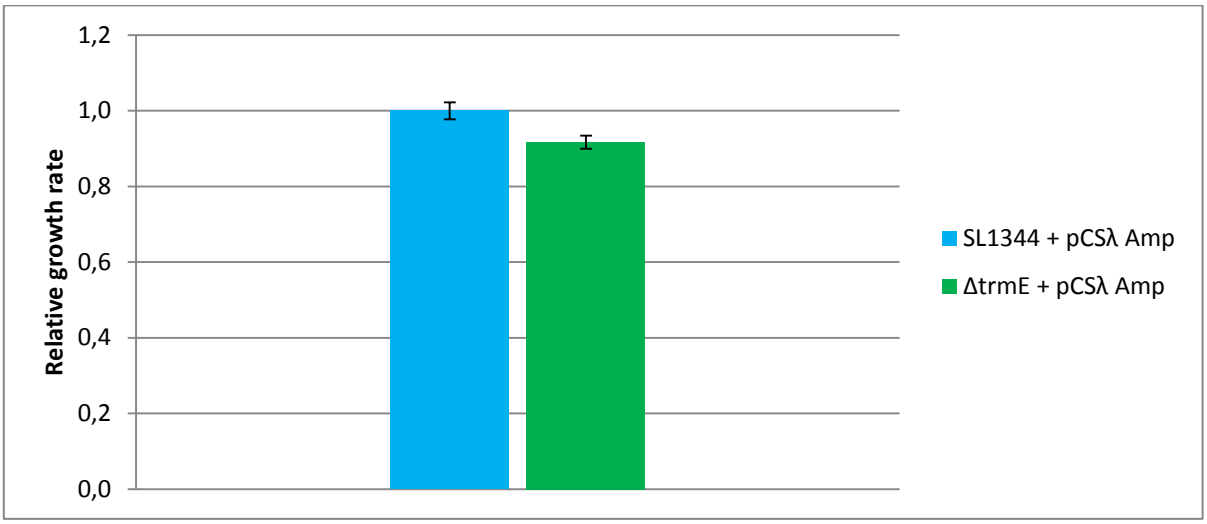

Figure 24: The growth rate of ΔtrmE normalized to the wild-type (both with the luciferase plasmid pCSλ Amp), measured with the luciferase assay. Strains were grown in LB low salt. The data have been obtained in 7 replicas.

Within this project two media were used: the rich LB low salt medium and the defined minimal medium MES-ch. The composition of MES-ch medium has been established to resemble the environment of *Salmonella* during infection in the typhoid fever model and also induces expression of the virulence genes (unpublished data in the lab). If an exchange from LB low salt to MES-ch is conduced, the culture is washed four times with sterile water. To evaluate if the medium of the over-night culture or washing has any influence on the growth rate measured in a day-culture, the effects were monitored with OD_{600} measurements. The used strains (wild-type with and without pCSλ Amp) were grown in both media over-night, the LB low salt cultures were washed, with each over-night culture a LB low salt and a MES-ch day-culture was inoculated, and the growth rates were evaluated using OD_{600} measurements (Figure 25).

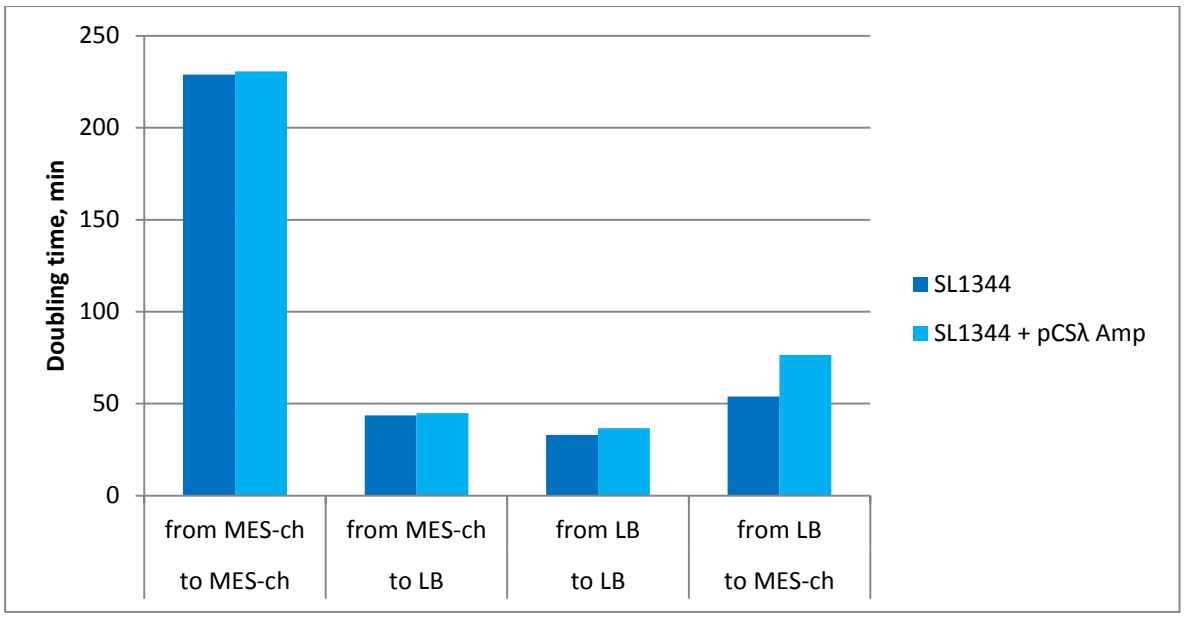

Figure 25: Evaluation of the effects of exchange of growth media and washing. The doubling times of the wild-type with and without pCSλ Amp are shown. Over-night cultures grown in MES-ch and LB low salt (washed) were used for inoculation of MES-ch or LB low salt day-cultures. All cultures arising from MES-ch over-night cultures show a longer doubling time than the respective cultures arising from LB low salt over-night cultures. These data base on single replicas.

The MES-ch cultures which were inoculated with MES-ch over-night cultures grew 3-4.2 fold slower that the MES-ch cultures which were inoculated with washed LB low salt over-night cultures. Also the LB low salt day-cultures inoculated with MES-ch over-night cultures grew 1.2-1.3 fold slower than the LB low salt day-cultures inoculated with LB low salt over-night cultures. This indicates that the bacteria are severely starving in MES-ch. It cannot be excluded that the bacteria run with the time out of necessary nutrients, which are not provided in the minimal medium, and the observed growth in MES-ch depends on nutrient accumulations acquired during growth in LB low salt. To allow performance of the growth rate measurements in MES-ch, it was decided to inoculate always MES-ch day-cultures with washed LB low salt over-night cultures.

The luciferase assay with LB low salt was conducted for all available deletion strains (Figure 26).

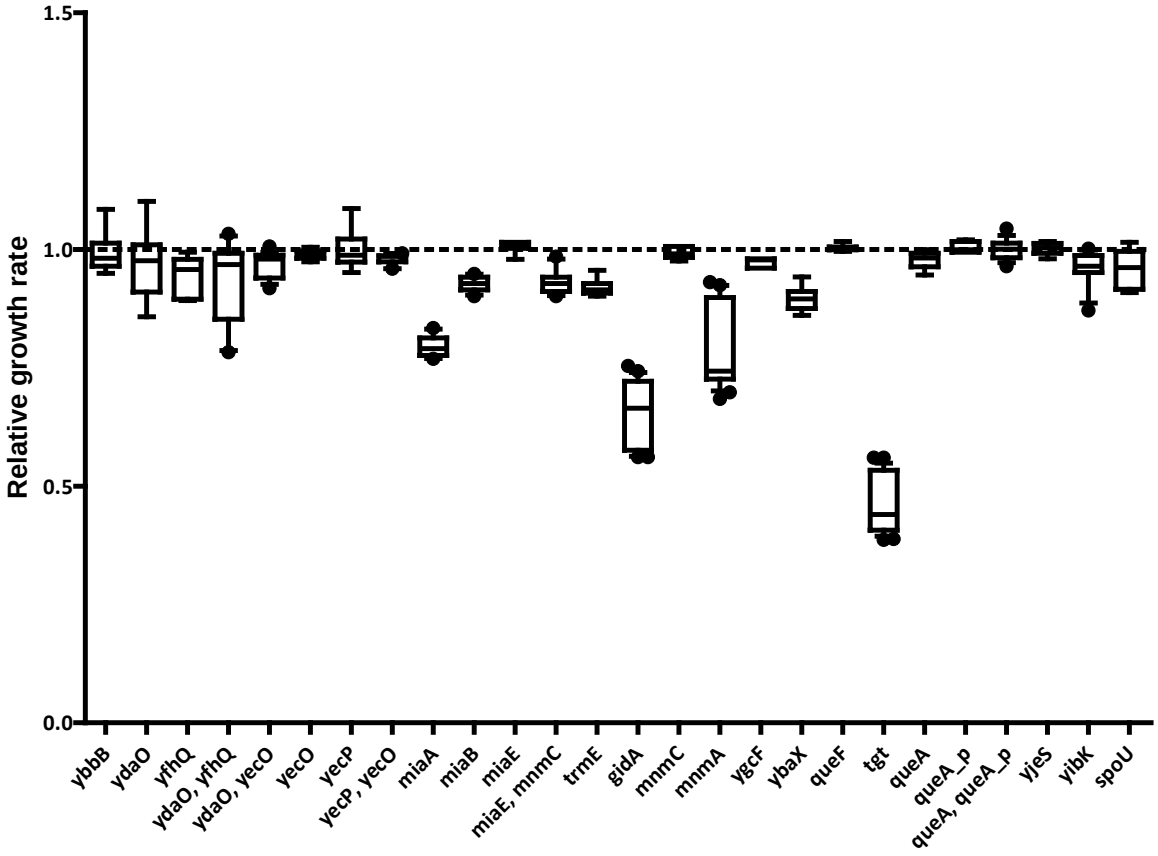

Figure 26: Summary of the relative growth rates for ΔtRMEs grown in LB low salt. The wild-type growth rate is taken as 1. The data are based on the luciferase assay. For every mutant at least 6 replicas were measured in at least two independent experiments.

For the *ΔmnmA* mutant a conspicuously long lag phase of approximately 7 hours was observed, followed by an exponential growth with a rate near to the wild-type (Figure 27).

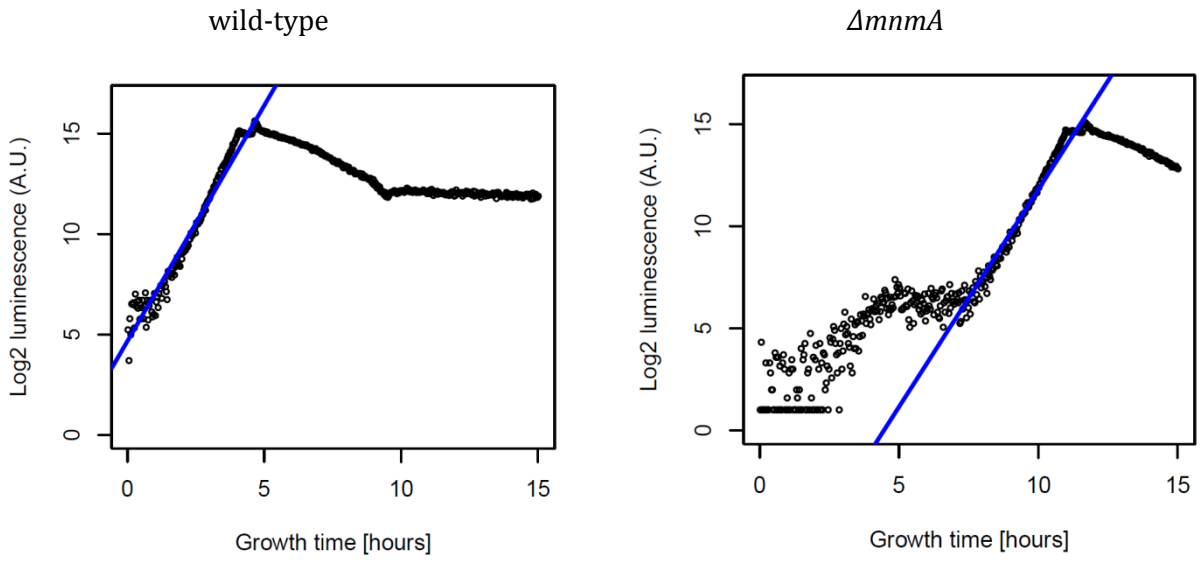

Figure 27: Comparison of the growth curves of wild-type and ΔmnmA strain grown in LB low salt, observed with the luciferase assay. Black points stand for single measurements. The regression line (blue) is shown in blue.

There are many different possibilities to explain this observation. The *ΔmnmA* mutant might show an extremely long lag phase, because it is more starving in stationary phase than the wild-type; by that the ribosomes could be partly degraded and lose their functionality. Or the mutant is more struggling with the switch between the low oxygen conditions during the stationary growth phase in the dense over-night culture in closed falcon tubes and the aerobic conditions in the new inoculated culture.

Most of the growth rate data were obtained with the luciferase assay due to its higher efficiency and reproducibility in the LB medium. However, in order to make a cross-method data comparison and luciferase measurements the OD_{600} and CFU data were plotted against the luciferase assay data, respectively (Figure 28 and 29). The OD_{600} data shows the same trends as the luciferase data (less than 10% difference in the observed growth rates). The outliner *ΔmnmA* (27%) showed in the luciferase assay a long lag phase, which is discussed above. The presence of this lag phase could not be observed with the OD_{600} measurements due to the timeframe in which the monitoring was conducted. Further outliners are *ΔgidA* (14%) and *ΔtrmE* (13%). The CFU data differ significantly from the luciferase data. This effect might be due to the observed aberrations of the cells size, but can also arise from the technically challenging multiple dilution step before plating out, which needs to be conducted very accurate.

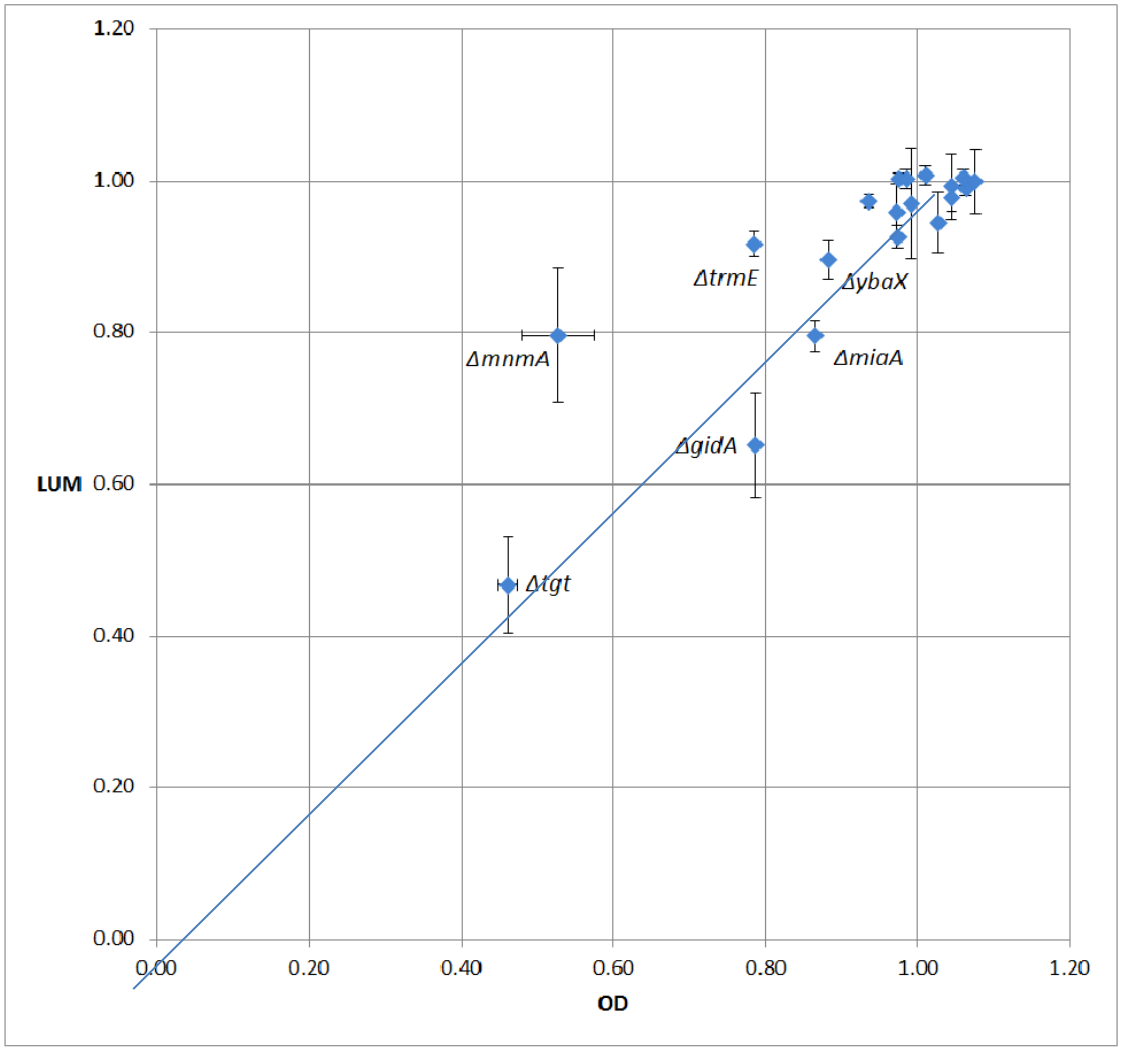

Figure 28: Comparison of the relative growth rates gained with OD_{600} and luciferase assay measurements, respectively, conduced with LB low salt cultures. All growth rates are normalized to the wild-type within the experiment. The deletion strains with the most severe phenotypes are labeled. The blue line indicates the median.

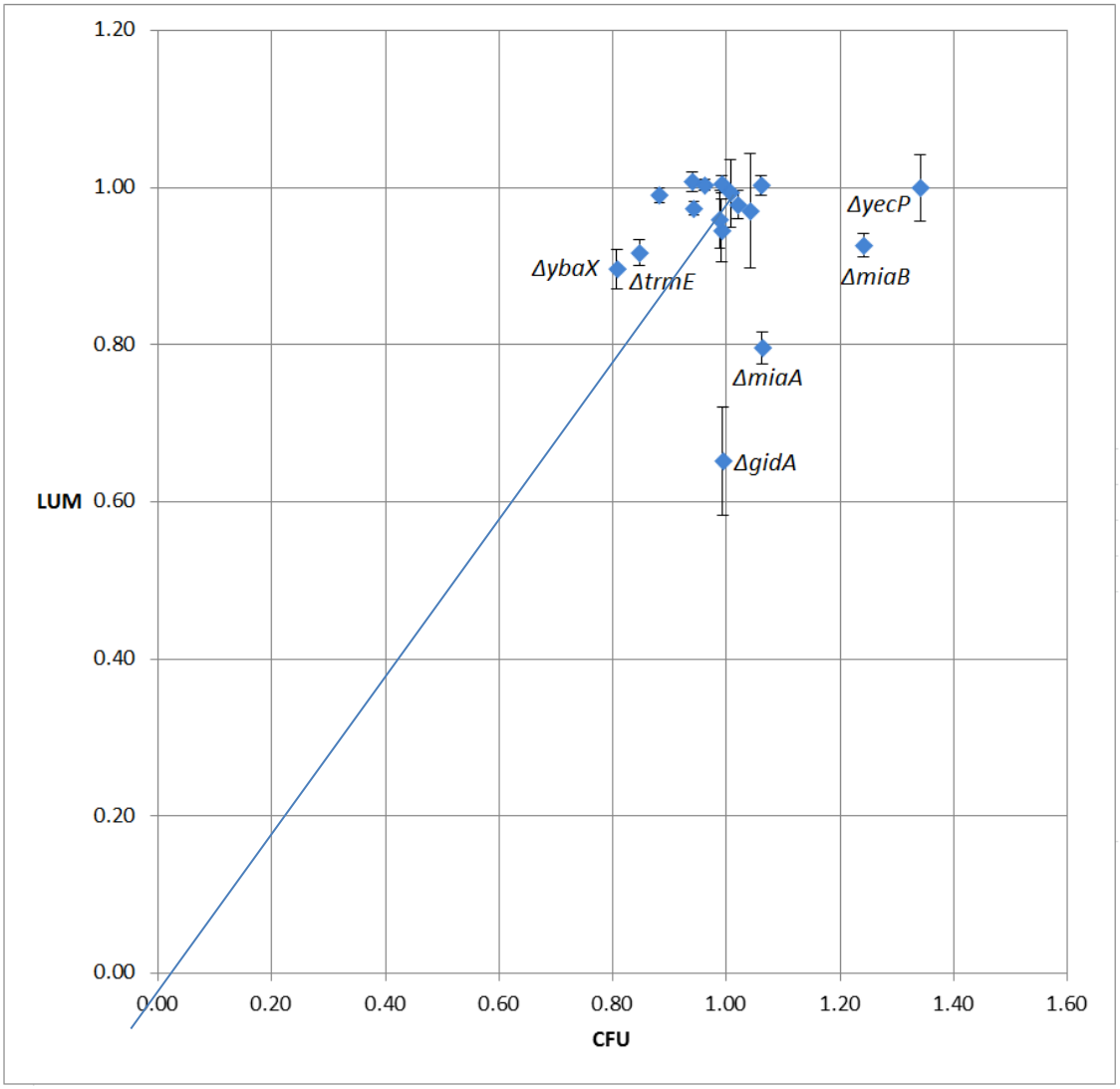

Figure 29: Comparison of the relative growth rates gained with CFU and luciferase assay measurements, respectively, conducted with LB low salt cultures. All growth rates are normalized to the wild-type within the experiment. The deletion strains with the most severe phenotypes are labeled. The blue line indicates the median.

The effect of tRME deletion on the bacterial growth in minimal medium is in general much more meaningful, as it is should more resemble the conditions during infection than the LB medium. The growth rate data obtained from the MES-ch minimal medium in the luciferase assay demonstrate low reproducibility. The reason why the luminescence production varied was most likely due to the low carbon source concentration in the MES-ch in comparison to the LB low salt starting culture medium. To solve this issue the 5-fold concentration of nutrients was used (MES-ch 5x). Unfortunately, the luminescence development of strains grown in MES-ch 5x was still not consistent (Figure 30). Due to that the data has to be considered as not significant. It has been shown later in the lab that reproducible data can be obtained with 20-fold carbon source concentration.

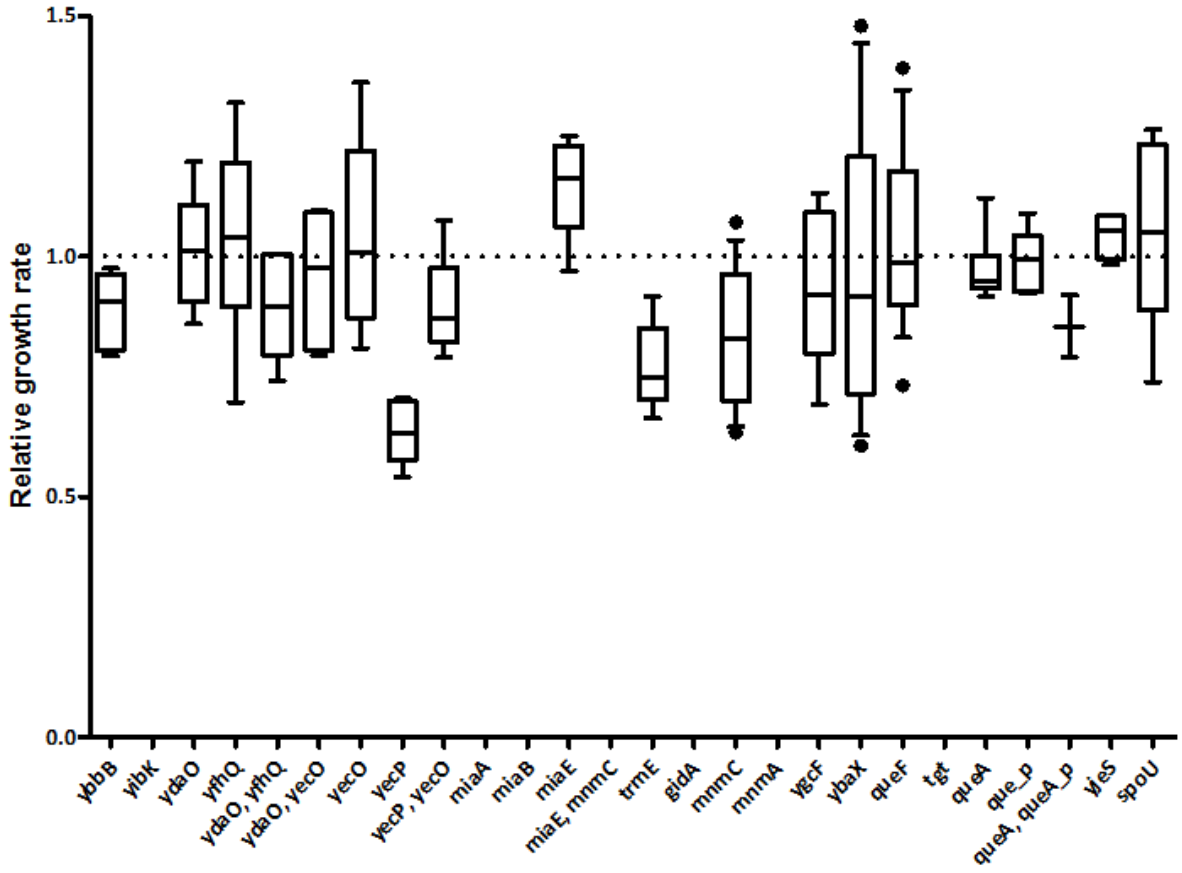

Figure 30: Summary of the relative growth rates for ΔtRMEs grown in MES-ch 5x. The wild-type growth rate is taken as 1. The data are based on the luciferase assay. The measurements were stopped due to inaccurate results.

An alternative method has been applied to estimate the relative growth rates of *ΔtRME* strains in a growth competition setting. Up to three fluorescence-labeled *ΔtRME* strains were grown with a fluorescent wild-type strain in the same culture. The change in relative cell number of the individual strains was followed on by flow-cytometry measurements. The main advantage of this method is that the data on virulence were obtained in the same manner.

The used strains express mCH, YFP, GFP, GFPweak and/or CFP under control of the promoters of the genes *sifB* and *virK* (see Table 7 page 34).

The fluorescence proteins differ in their excitation and emission spectra (Figure 31). This allows distinguishing of up to four different bacterial strains using three lasers and various band-pass and low-pass filters. The most suitable filter to detect CFP allows light around 470 nm to pass, for GFP around 502 nm, for YFP around 525 nm, and for mCH around 595 nm, respectively. As GFP and YFP are excited at the same wavelength and the emission-spectra are overlapping, they can only be separated due to their intensities.

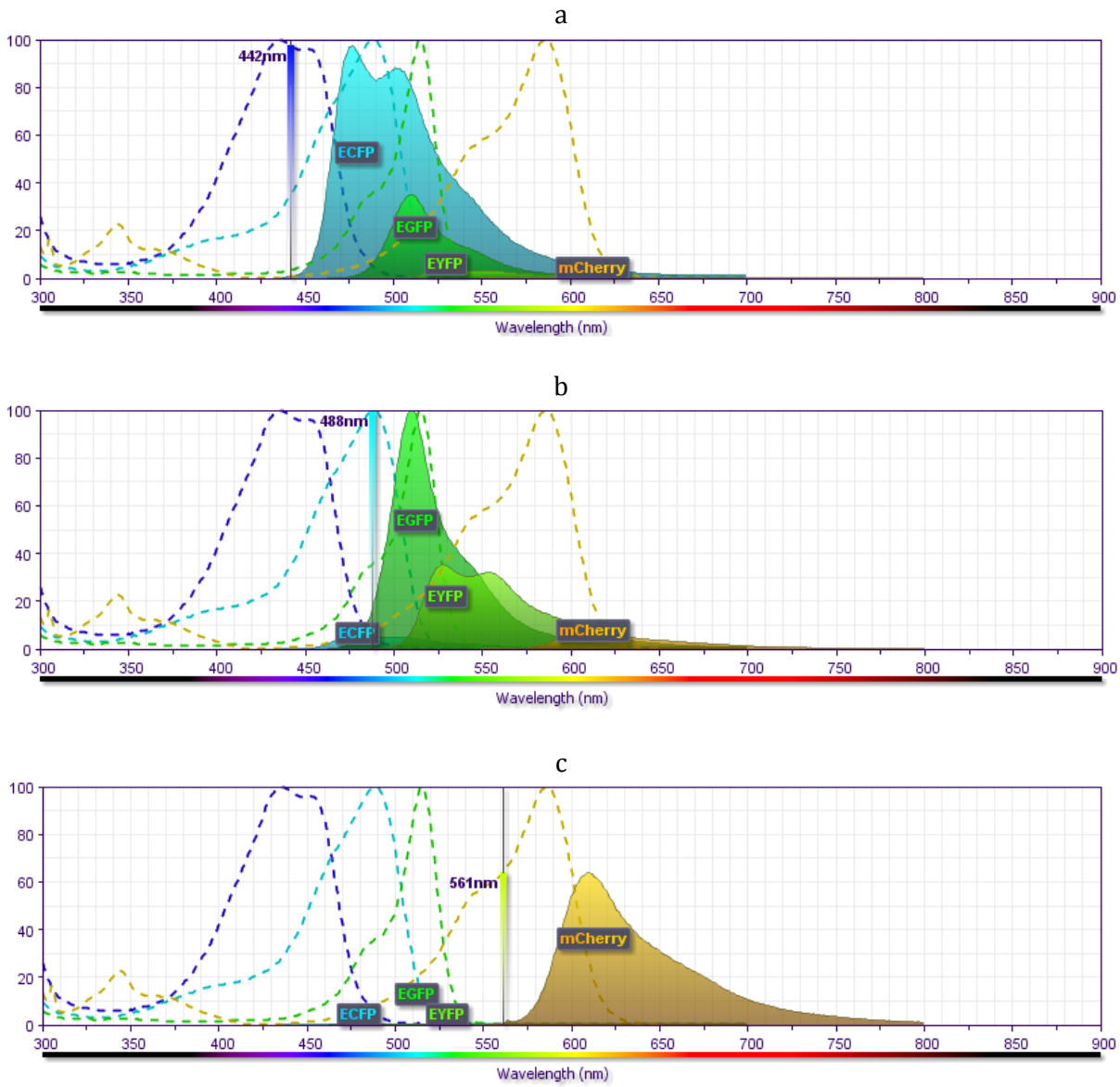

Figure 31: a: Spectra of CFP, GFP, YFP, and mCH due to excitation with a laser at 442 nm (the laser used in this project produces light at a wavelength of 445 nm). CFP is excited intensely and also GFP a bit b: Spectra of CFP, GFP, YFP, and mCH due to excitation with a laser at 488 nm. GFP is excited intensely, and YFP moderately. c: Spectra of CFP, GFP, YFP, and mCH due to excitation with a laser at 561 nm, only mCH is excited. The dashed lines indicate the excitation spectra; the solid lines the emission spectra, when the fluorescence proteins are exited with light at the wavelength shown. The pictures were taken from BD Fluorescence Spectrum Viewer.

The presence, amount, and intensity of a fluorescence protein within a sample was evaluated with FlowJo 10 software. A population expressing CFP can be distinguished from the other populations using the channel Ex445_BP470_15-H and a second arbitrarily channel (Figure 32). To completely dissolve more complex samples like when GFP and YFP are present, two channels are needed. GFP or YFP can be distinguished from the background and each other when the channels Ex488_LP525_BP542_27-H and Ex488_LP502_BP512_25-H are plotted against each

other, because GFP is more intense in the Ex488_LP502_BP512_25-H channel than YFP (Figure 33). Many of the used strains express additionally to CFP, GFP, or YFP also mCH. In the channels Ex488_LP502_BP512_25-H and Ex561_LP595_BP616_23-H the GFP and mCH expressing population gives an intense signal in both channels, the YFP and mCH a relatively moderate in the Ex488_LP502_BP512_25-H channel, and the CFP and mCH or mCH only expressing populations give only a signal in the Ex561_LP595_BP616_23-H channel (Figure 34).

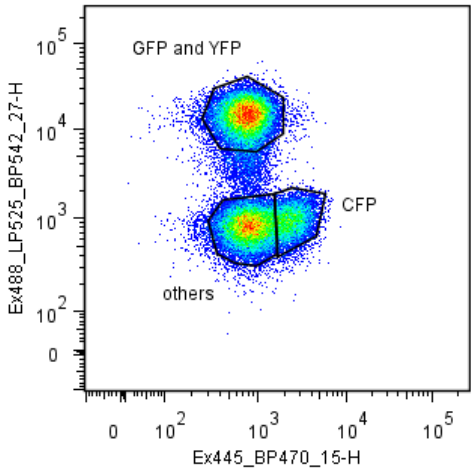

Figure 32: A sample containing the strains SBM319, SBM321, SBM322, and SNB10, which express GFP and mCH, YFP and mCH, CFP and mCH, or only mCH, respectively, plotted in the channels Ex488_LP525_BP542_27-H and Ex445_BP470_15-H. The population shifted slightly right (channel Ex445_BP470_15-H) consists of the CFP producing cells (unfortunately the signal in this sample is quite weak), the population which is more intense in the channel Ex488_LP525_BP542_27-H is formed by the YFP and GFP cells. In the lower left corner the mCH only expressing cells and the uninduced ones are located.

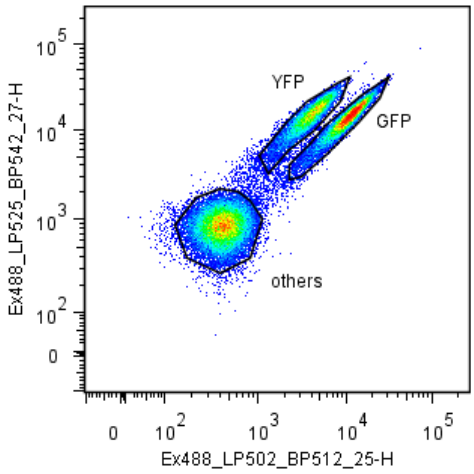

Figure 33: A sample containing the strains SBM319, SBM321, SBM322, and SNB10, which express GFP and mCH, YFP and mCH, CFP and mCH, or only mCH, respectively, plotted in the channels Ex488_LP525_BP542_27-H and Ex488_LP502_BP512_25-H. The population left-hand expresses YFP, the one right-hand GFP. In the lower left corner the CFP and mCH or mCH only expressing cells and the uninduced ones are located.

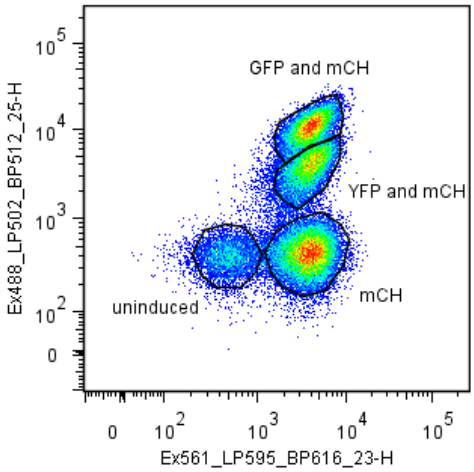

Figure 34: A sample containing the strains SBM319, SBM321, SBM322, and SNB10, which express GFP and mCH, YFP and mCH, CFP and mCH, or only mCH, respectively, plotted in the channels Ex488_LP502_BP512_25-H and Ex561_LP595_BP616_23-H. The signals in the channel Ex561_LP595_BP616_23-H arise from the diverse mCH producing populations. The most intense population in the channel Ex488_LP502_BP512_25-H produces GFP and mCH, the middle one YFP and mCH, and the lower one CFP and mCH or only mCH. The population in the lower left corner is due to uninduced cells within the sample.

In order to estimate the influence of individual fluorescent proteins expression on the bacterial growth rate, a control experiment has been done where wild-type *Salmonella* strains expressing individual fluorescent proteins has been grown in the competition setting.

The competitional growth assay showed several problems. Although the virulence promoters should be activated in the over-night cultures, most cells show only weak fluorescence (Figure 35 a). The intensity of all fluorescence protein signals in the sample grows during the competition growth and the relative count of uninduced cells shrinks (Figure 35). Further the general presence of uninduced cells makes the accuracy of the assay questionable, as they cannot be dedicated to a strain and might manipulate the ratio of fluorescent populations in an unratable manner when expression of fluorescent proteins is suddenly induced. The increase of florescence intensity shows for the mCH signal an additional delay and in some experiments the mCH signal disappeared again (Figure 36). It is known that mCH maturation time is longer than for the other used fluorescent proteins, and that for the folding O_2 is required, which is a limiting factor in liquid cultures after some time [124]. As the culture is growing exponentially it might be, that the mCH signal loses its relative presence compared to the other fluorescence proteins, because mCH cannot be folded in oxygen-limited conditions. This issue can be solved by addition of Chloramphenicol to the aliquot to stop bacterial growth and addition of O_2 via dilution and shacking to allow folding of mCH within an hour [125]. Or mCh is degraded for an unknown reason.

a: 0 min

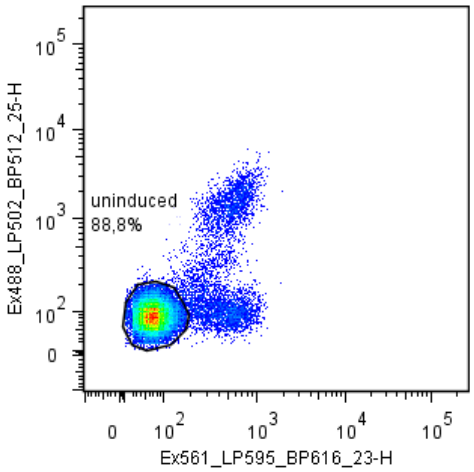

b: 30 min

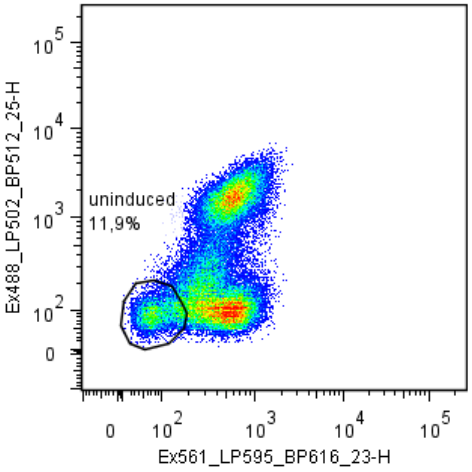

c: 60 min

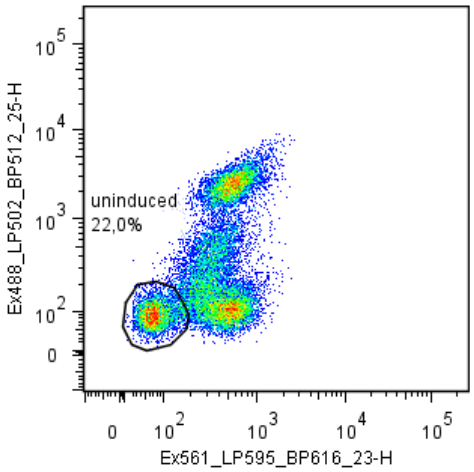

d: 90 min

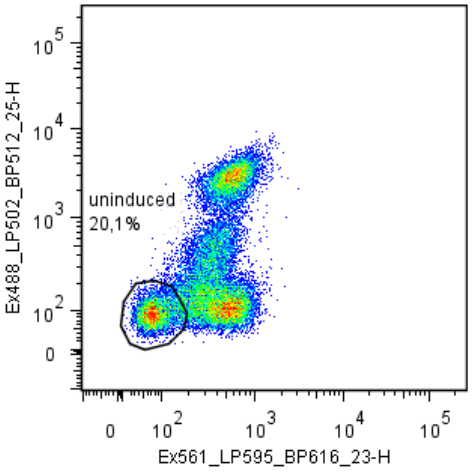

e: 120 min

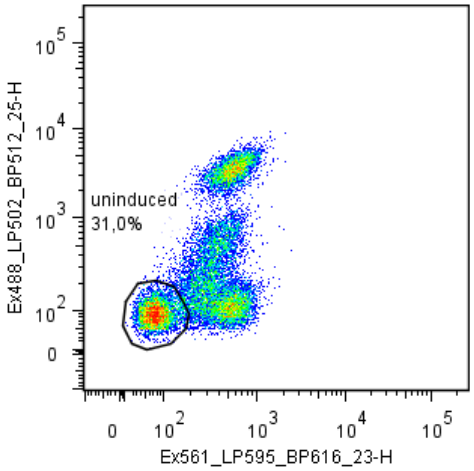

f: 150 min

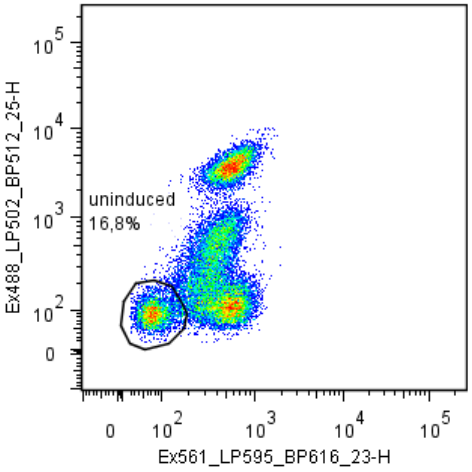

g: 180 min

h: 210 min

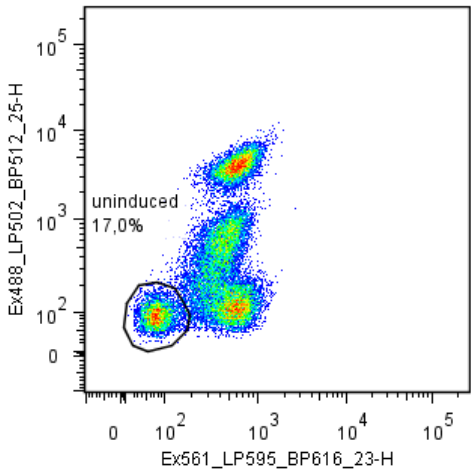

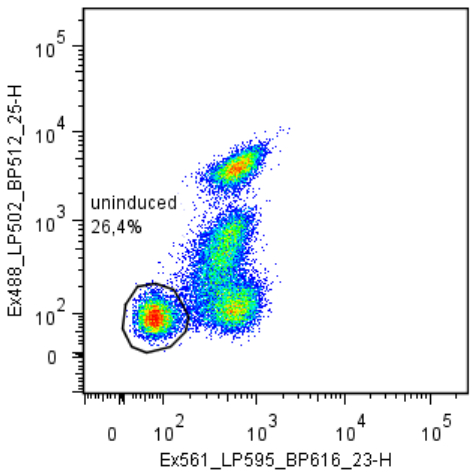

i: 240 min

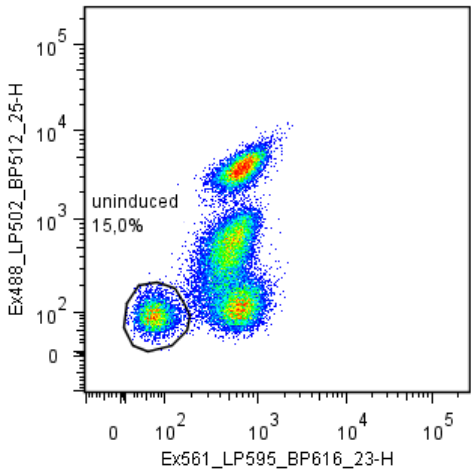

j: 300 min

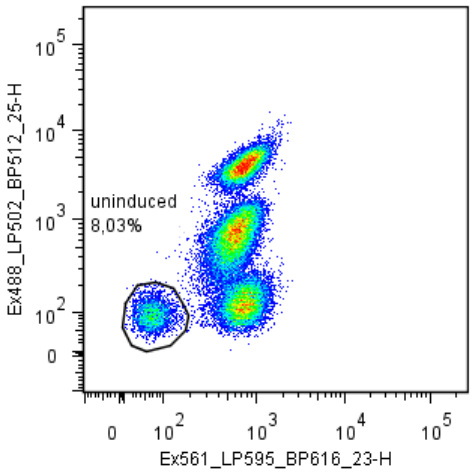

k: 360 min

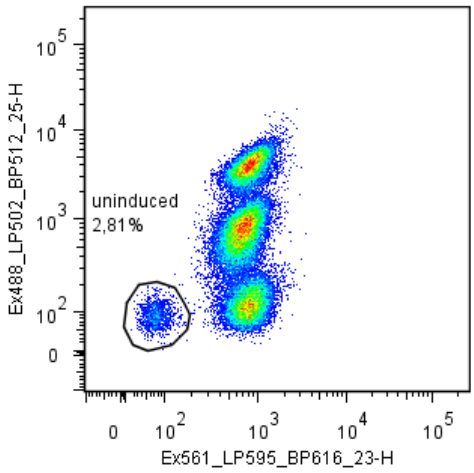

l: 420 min

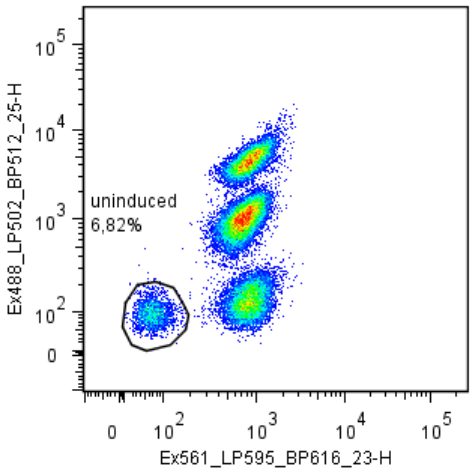

Figure 35: Time course of an even mixture of SBM319 (expressing GFP and mCH), SBM321 (expressing YFP and mCH), and SBM322 (expressing CFP and mCH). The sample was measured every 30 min in the first four hours of growth (a-i), then every hour until the seventh hour of growth was reached (i-l). The channels used for visualization are Ex488_LP502_BP512_25-H Ex561_LP595_BP616_23-H. The population in the lower left corner corresponds to uninduced cells within the sample (black circle), of which the percentage decreases over time. The populations in the middle correspond to the GFP mCH double positive SBM319, the YFP mCH double positive SBM321, and the CFP mCH double positive SBM322, respectively (top down).

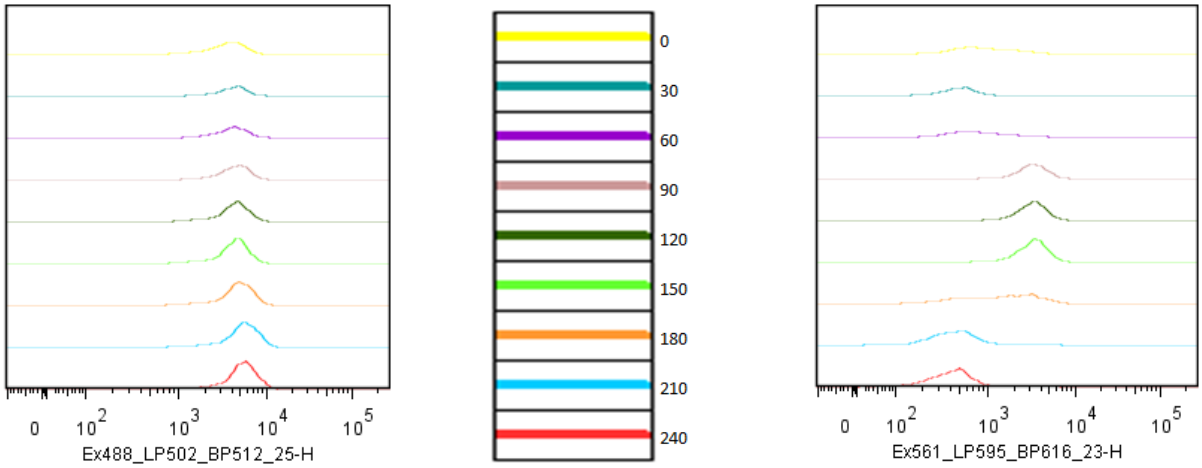

Figure 36: Time course histogram overlay of the YFP (left) and mCH (right) fluorescence intensities expressed in a wild-type Salmonella strain. The strain has been grown in competition with two other wild-type strains, expressing mCH and GFPweak, respectively (not shown). On the X axis the intensity in the correspondent channel is shown, the high of each peak visualizes the relative cell count within the measured sample (Y max. is set to 300). The color code reflects the time-points in minutes. Bacterial populations corresponding to the same time point are identical on the right and the left graphs. Right-hand: growing relative count of cells with YFP in the first two hours of growth (visualized in the Ex488_LP502_BP512_25-H channel). Left-hand: discontinuous intensity of the mCH signal, showing the shift of the population from a mCH negative (time-points 30 and 60 min) to a mCH positive (time-points 90 – 150 min), back to a mCH negative state (time-points 180 – 240 min) (visualized in the Ex561_LP595_BP616_23-H channel).

Optimization of the neither of the luciferase assay in MES-ch nor of the competitive assay could be achieved in frame of this project, but the *in vitro* growth rates of all deletion mutants in LB low salt are evaluated to a significant extent.

5.2.2 Cell morphology and control of fluorescence induction

In 2011 it was published, that a tRME deletion mutant (*S.* Typhimurium *ΔgidA*) forms filaments [85]. A severe cell shape alteration like this can disturb the reliability of growth rate measurements and can influence the virulence significantly. To evaluate if filamentation or other anomalous growth types have an influence in the characterized *ΔtRME* strains, their morphology was monitored in different growth phases in MES-ch and in the late stationary phase in LB low salt using phase contrast wide-field microscopy.

The observed cell size alterations, ranging from small cells to filaments with the optical mass of approximately five bacteria, were only transient without any obvious correlation to the growth phase (Table 9). The microscopy pictures are in Appendix G.

Medium	**MES-ch**	**MES-ch**	**MES-ch**	**LB low salt**
Growth phase	**exponential**	**stationary**	**late stationary**	**late stationary**
ΔyfhQ	ND	small	ND	ND
ΔspoU	ND	5 fold longer	normal	ND
ΔmnmA	twice as long	twice as long	ND	twice as long

Table 9: Summary of the observed cell morphologies. Only the ΔtRME mutants for which an abnormal morphology was observed are shown. For each condition and strain only a singel experiment was conducted.

Severe cell aberrations seem to occur only when the bacteria grow very fast, for example during exponential growth in very rich medium (NZY medium supplemented with 0.2% glucose in [85]). *Salmonella* grows with a generation time of 6 hours in the typhoid fever model, and the filaments formation implying problems in cell division only upon fast growth, thus abnormal cell morphology is less likely to be the primary factor influencing the virulence in *ΔtRME* strains.

To define the correlation between the aberrations and the respective growth phase, parallel evaluation of the bacterial growth and the cells size in frame of a time course with microscopy is necessary. But a detailed study about the sizes of the different tRME lacking mutants would have gone beyond the frame of this project.

Fluorescence microscopy was mainly used to make detection of the bacteria more efficient. But also the induction of fluorescence protein expression in 19 hour MES-ch culture was evaluated. Most bacteria within the samples expressed the correct fluorescence proteins in detectable amounts, although variation within a culture is high. Examples of the recorded pictures are shown in Appendix G.

5.3 Virulence of *Salmonella* lacking tRNA modifying enzymes

As a central criterion for evaluation of tRMEs as potential drug targets, the propagation of *ΔtRME* strains in the mouse model of typhoid fever infection has been characterized.

Modern *in vivo* experiments use broadly the competitive index (CI) as measurement unit for virulence attenuation, because it allows usage of a lower amount of animals and reduces problems in comparison due to host-to-host variations. In this test equal numbers of the wild-type and mutant strains are combined in the inoculum and the mixed pool of bacteria recovered from the infected organs can then be defined e.g. by different fluorescence markers [126, 127]. Mathematically the CI is defined as the ratio between the mutant strain and the wild-type in the output divided by the ratio of the two strains in the input. CIs lower than 1 indicate a competitive disadvantage of mutant relative to wild-type [128]. A drawback of this method, which should be considered in experiment design, is that some mutations leading to avirulence of the affected strain might be complemented in *trans* by the presence of the wild-type in the same tissue.

For most of the tested *ΔtRME* mutants a more severe phenotype was observed *in vivo* than *in vitro* (LB low salt), due to limited nutrient availability and the pressure caused by the host's immune system (Figure 37).

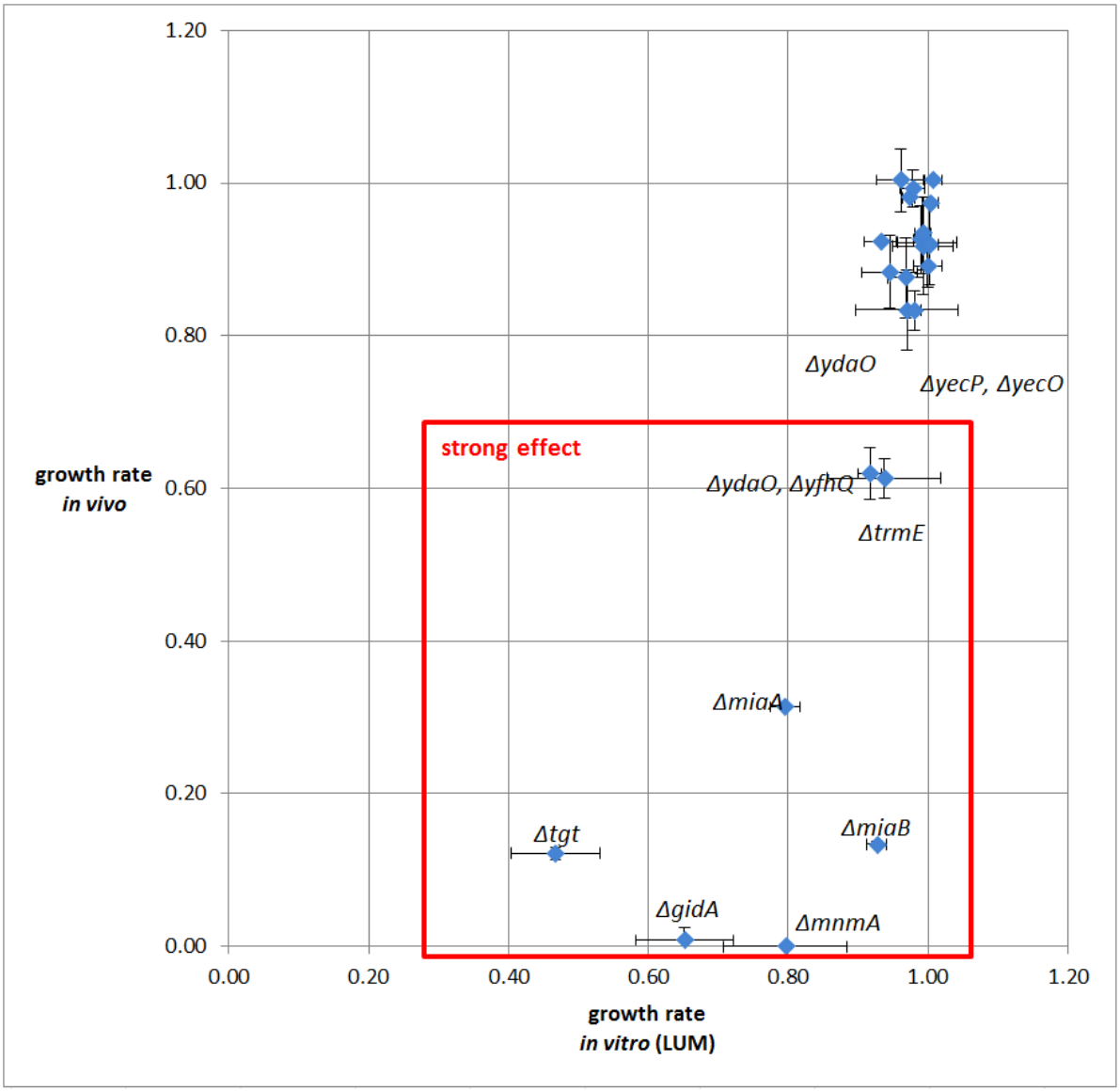

Figure 37: Comparison of the in vitro growth rates (LB low salt, luciferase assay) and the growth rates in the mouse in vivo growth rates (calculated from the CI). Strains with severe effects are labeled and highlighted with the red box.

All evaluated growth rates (their averages and their standard deviations) for growth in LB low salt are listed in Table 10, all growth rates for growth in MES-ch are listed in Table 11, and the growth rates based on the CI of mice infections are listed in Table 12.

Deleted gene	ybbB	yibK	ydaO	yfhQ	ydaO yfhQ	ydaO yecO	spoU	yecO	yecP	yecP yecO	miaA	miaB	miaE
Method	OD												
Average	1,04	ND	0,99	1,03	ND	ND	0,97	1,06	1,08	ND	0,87	0,97	1,01
Stdev	0,00	ND	0,00	0,00	ND	ND	0,00	0,00	0,00	ND	0,00	0,00	0,00
Replicas	1	0	1	1	0	0	1	1	1	0	1	1	1
Method	CFU												
Average	1,01	ND	1,04	0,99	ND	ND	0,99	0,88	1,34	ND	1,06	1,24	0,94
Stdev	0,00	ND	0,00	0,00	ND	ND	0,00	0,00	0,00	ND	0,00	0,00	0,00
Replicas	1	0	1	1	0	0	1	1	1	0	1	1	1
Method	LUM												
Average	0,99	0,96	0,97	0,95	0,94	0,97	0,96	0,99	1,00	0,98	0,80	0,93	1,01
Stdev	0,04	0,03	0,07	0,04	0,08	0,03	0,04	0,01	0,04	0,01	0,02	0,01	0,01
Replicas	6	15	6	6	18	18	6	6	6	18	11	11	6

Deleted gene	miaE mnmC	trmE	gidA	mnmC	mnmA	ygcF	ybaX	queF	tgt	queA	queA_p	queA queA_p	yjeS
Method	OD												
Average	ND	0,79	0,79	ND	0,53	0,94	0,88	0,98	0,46	1,04	1,06	ND	0,98
Stdev	ND	0,00	0,00	ND	0,05	0,00	0,00	0,00	0,01	0,00	0,00	ND	0,00
Replicas	0	1	1	0	2	1	1	1	2	1	1	0	1
Method	CFU												
Average	ND	0,85	0,99	ND	ND	0,94	0,81	0,96	ND	1,02	0,99	ND	1,06
Stdev	ND	0,00	0,00	ND	ND	0,00	0,00	0,00	ND	0,00	0,00	ND	0,00
Replicas	0	1	1	0	0	1	1	1	0	1	1	0	1
Method	LUM												
Average	0,93	0,92	0,65	0,99	0,80	0,97	0,90	1,00	0,47	0,98	1,00	1,00	1,00
Stdev	0,02	0,02	0,07	0,01	0,09	0,01	0,02	0,01	0,06	0,02	0,01	0,02	0,01
Replicas	11	7	25	6	21	6	6	6	25	6	6	18	6

Table 10: Relative growth rates of all deletion strains. The cultures were grown in LB low salt. The used methods (OD, CFU, and LUM) are indicated, the averages and standard deviations, and the amount of replicas, which were successfully conducted for the respective deletion strain with each method in this medium. ND stands for not determined.

Deleted gene	ybbB	yibK	ydaO	yfhQ	ydaO yfhQ	ydaO yecO	spoU	yecO	yecP	yecP yecO	miaA	miaB	miaE
Method	OD												
Average	0,93	0,95	1,02	1,10	ND	ND	0,97	0,95	1,08	ND	1,04	1,02	0,93
Stdev	0,00	0,03	0,00	0,00	ND	ND	0,00	0,00	0,00	ND	0,14	0,02	0,00
Replicas	1	2	1	1	0	0	1	1	1	0	2	2	1
Method	CFU												
Average	0,94	ND	0,91	0,86	ND	ND	1,27	0,76	0,96	ND	1,28	0,98	0,90
Stdev	0,00	ND	0,00	0,00	ND	ND	0,00	0,00	0,00	ND	0,29	0,06	0,00
Replicas	1	0	1	1	0	0	1	1	1	0	2	2	1
Method	LUM												
Average	0,89	ND	1,01	1,03	0,89	0,96	1,04	1,04	0,63	0,89	ND	ND	1,14
Stdev	0,07	ND	0,11	0,19	0,09	0,12	0,17	0,18	0,06	0,10	ND	ND	0,09
Replicas	6	0	5	8	7	6	8	8	6	5	0	0	8

Deleted gene	miaE mnmC	trmE	gidA	mnmC	mnmA	ygcF	ybaX	queF	tgt	queA	queA_p	queA queA_p	yjeS
Method	OD												
Average	ND	1,18	1,09	1,26	ND	1,09	1,11	1,02	ND	1,13	1,28	0,93	1,05
Stdev	ND	0,10	0,08	0,02	ND	0,00	0,05	0,00	ND	0,00	0,00	0,05	0,17
Replicas	0	4	3	2	0	1	2	1	0	1	1	2	3
Method	CFU												
Average	ND	1,06	1,01	ND	ND	1,00	0,96	0,76	ND	0,99	1,15	ND	0,85
Stdev	ND	0,09	0,00	ND	ND	0,00	0,00	0,00	ND	0,00	0,00	ND	0,00
Replicas	0	2	1	0	0	1	2	1	0	1	1	0	1
Method	LUM												
Average	ND	0,77	ND	0,83	ND	0,94	0,95	1,02	ND	0,97	0,99	0,85	1,04
Stdev	ND	0,08	ND	0,14	ND	0,15	0,26	0,17	ND	0,07	0,06	0,06	0,04
Replicas	0	6	0	13	0	9	11	18	0	6	5	2	4

Table 11: Relative growth rates of all deletion strains. The cultures were grown in MES-ch and MES-ch 5x (only for luciferase assay). The used methods (OD, CFU, and LUM) are indicated, the averages and standard deviations, and the amount of replicas, which were successfully conducted for the respective deletion strain with each method in this medium. ND stands for not determined.

Deleted gene	ybbB	yibK	ydaO	yfhQ	ydaO yfhQ	ydaO yecO	spoU	yecO	yecP	yecP yecO	miaA	miaB	miaE
Method	*in vivo*												
Average	0,92	1,00	0,83	0,88	0,61	0,88	ND	0,93	0,92	0,83	0,31	0,13	1,00
Stdev	0,06	0,04	0,05	0,05	0,03	0,05	ND	0,04	0,00	0,03	0,00	0,00	0,00
Replicas	3	2	3	3	3	3	0	2	2	3	2	2	2

Deleted gene	miaE mnmC	trmE	gidA	mnmC	mnmA	ygcF	ybaX	queF	tgt	queA	queA_p	queA queA_p	yjeS
Method	*in vivo*												
Average	0,92	0,62	0,01	0,93	0,00	0,98	ND	ND	0,12	0,99	0,97	0,89	0,92
Stdev	0,00	0,03	0,02	0,05	0,00	0,00	ND	ND	0,01	0,02	0,00	0,03	0,05
Replicas	1	2	2	3	3	1	0	0	3	2	2	3	3

Table 12: Relative growth rates of all deletion strains. The experiments were conducted via infection of BALB/c mice. Calculation of the relative growth rate is based on the relative cell count before and after infection. The averages and standard deviations are indicated, and the amount of replicas, which were successfully conducted for the respective deletion strain. ND stands for not determined.

Analysis of individual *ΔtRME* phenotypes shows that deletion of *tgt* causes a severe phenotype *in vitro* (in rich and minimal medium) and *in vivo*. Tgt is conducting a major change of the anticodon, the exchange of guanine for the much bigger queuine. The influence of queuosine modifications on translational is not yet fully understood. However, queuosine modifications are known to prevent aminoacylation with wrong amino acids therefore reduce miscoding errors [51, 52]. This can have an impact on the functionality of the produced proteins. Further lack of Q modifications is shown to increase the rate of frameshifting [57-59]. In 1982 a study on *Δtgt E.coli* was published, showing that the bacteria do only suffer from a disadvantage in unsuitable conditions, like in the stationary phase. These results are contradictory to ours, which might be due to species differences between *E.coli* and *S.* Typhimurium. For example control the virulence genes expression in *Salmonella* is very sensible regulated, because they are only needed in specific conditions and their production lowers bacterial growth, as lot of energy and resources are needed [129]. tRME deletions are suspected to cause pleiotropic effects, thus the expression inhibition of virulence genes might be decreased, causing slower growth of the bacteria. According to unpublished lab data expression of transcriptional regulator (PhoP), which is known to be connected to virulence [32], is indeed upregulated 4 fold in the *Δtgt* mutant and 2.2 fold in the *ΔmnmA* mutant, giving a hint that virulence gene regulation might be affected by the lacking tRMEs. Further evaluation of the virulence genes expression is needed to elaborate this hypothesis.

Based on the observations in *Shigella*, Tgt was chosen to be targeted in a screen for inhibitors, as its substrate recognition site is different from the human ortholog, although the human and the prokaryotic Tgt are highly homologous [130, 131].

Abolishment of queuine production should impose the same effect on the growth rate as loss of the modification due to deletion of Tgt. However deletion of the enzymes, which contribute to queuine synthesis before it is attached to the tRNA (non tRMEs) did not influence *Salmonella* growth rates *in vitro* severely (Figure 38). Presence of queuine in LB low salt medium cannot be excluded, as the medium contains Yeast extract, however no growth defect has been observed in the synthetic medium MES-ch, for which the absence of queuine can be guaranteed. The significance of our MES-ch data low, but none of deletion mutants shows a severe growth defect. As no analogues of YgcF, YbaX, and QueF could be found with blastp analysis, it is unlikely that other enzymes are capable to balance their deletion out. It is possible that an analogical metabolite that can take over the function of queuine. Finally, the Tgt enzyme might have an additional function which is not related to tRNA modification.

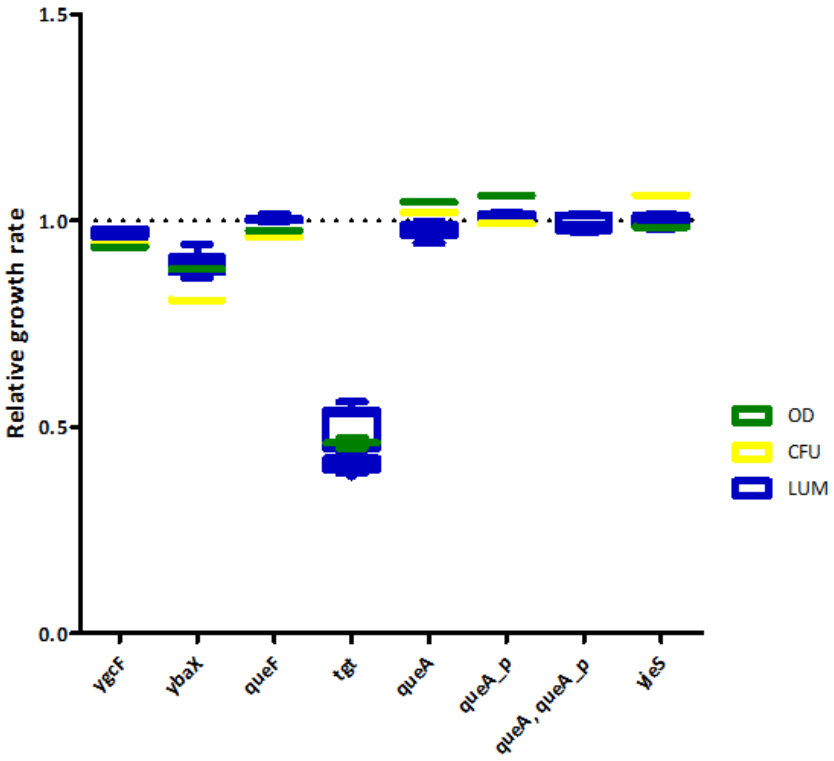

Figure 38: Growth rates of the strains lacking enzymes of the queuine synthesis pathway (ΔygcF, ΔybaX, ΔqueF), the tRME incorporating queuine into tRNA (Δtgt), and the downstream queuosine modifying enzymes (ΔqueA, ΔqueA_p, ΔqueA + ΔqueA_p, ΔyjeS), respectively.

TrmE and GidA are in the literature suggested to work in concert to create the (c)nm^{5}U modification. This would also suggest that deletion of *trmE* causes the same phenotype as deletion of *gidA*. Our data shows that the *gidA* deletion causes a much severe growth rate reduction than deletion of *trmE*. The essential 50S ribosomal subunit stability factor EngA shows similarities to TrmE and might be capable to execute the function of TrmE. Both enzymes are GTPases, but TrmE is described to exhibit untypically high GTPase hydrolysis rate and a low affinity for GTP and GDP [83]. It needs to be determined, if EngA can balance the deletion of *trmE* to some extent out. The severe growth rate reduction of the *mnmA* lacking mutant can arise from the importance of the thiol group for the recognition of tRNA by aminoacyl-synthetases, as it is shown for $tRNA^{Glu}_{mnm5s2UUC}$ and $tRNA^{Lys}_{mnm5s2UUU}$. But also an influence on frameshifting is shown [57-59].

Although the xmo^{5}U34 modification is described to be of crucial importance to enable $tRNA^{Thr}_{cmo5UGU}$, $tRNA^{Leu}_{cmo5UAG}$, $tRNA^{Ser}_{cmo5UGA}$, $tRNA^{Val}_{cmo5UAC}$, $tRNA^{Ala}_{cmo5UGC}$ and $tRNA^{Pro}_{cmo5UGG}$ to wobble to all codons within their family codon boxes, only the double deletion strain showed a moderate phenotype *in vivo*. Wild-type *Salmonella* encodes for Ala and Val two tRNAs each (U34 and G34) and for Thr, Leu, Ser, Pro three tRNAs each (U34, G34 and C34). None of the tRNA genes was deleted in the mutants within this project, thus the effect of lacking modifications could be widely balanced by the other tRNAs within the given tRNA repertoire. Further other S-

adenosylmethionine-dependent methyltransferases are known, which might serve as analogues of the deleted enzymes YecO and YecP (Table 13).

	E value	Query coverage	Max. identity
UbiE (for YecO)	0.009	71%	20%
UbiG (for YecP)	0.0008	38%	27%

Table 13: Most promising blastp results for YecO and YecP.

The *miaA* deletion mutant showed a moderate growth rate reduction of 20% in LB low salt, and severe fitness costs *in vivo*. Deletion of *miaB* on the other hand showed in *vitro* hardly any effect on the growth rate (in the range of natural variation), but a severe growth rate reduction down to 10% of the wild-type during infection. For the *miaE* deletion mutant no growth rate reduction could be observed. The *in vitro* results correspond to published data [99, 100], and our *in vivo* data are also supported by previous findings that *miaA* and *miaB* deletion mutants are more sensible to less optimal growth conditions [101]. The fact that the *miaB* deletion strains showed less virulence than the *miaA* strain might be due to an additional unknown function of *miaB*. Data on frameshifting in *ΔmiaA* and *ΔmiaB* support the importance of these two enzymes for translational accuracy [57-59].

Further we have observed that the double deletion *ΔydaO ΔyfhQ* strain has significant growth reduction *in vivo* and *in vitro*, although deletion of the single enzyme had no significant effect. This supports the theory that inhibition of two tRMEs working on different positions on the tRNA and thus depletion of two modifications causes a more severe effect than inhibition of only single enzymes.

It was planed to restore the gene deletions causing the most promising phenotypes (*ΔgidA, ΔmiaA, ΔmiaB, Δtgt, ΔtrmE,* and *ΔtrmU*), but unfortunatelly this part of the project could not be finished in the given time frame.

5.4 Frameshifting in Salmonella lacking tRNA modifying enzymes

There have been extensive studies published demonstrating the role of particular tRMEs in frameshifting control, but it is necessary to prove that our observed phenotypes of the *ΔtRME* strains are correlated to the extent of frameshifting in each strain. Therefore a frameshifting reporter has been designed to measure frameshifting in *Salmonella* in culture and in the mouse typhoid fever model.

The codon-specific reporter system consists of a series of plasmids; each of them encodes two fluorescent proteins with green and red emission positioned in tandem. A linker joins the fluorescence proteins, which is designed to puts them out of the reading frame of each other. The first protein (GFP) is expressed constitutively, whereas the second protein (mCH) is only efficiently translated upon -1 frameshifting, which results in a translational fusion of the two fluorescence proteins. The green-to-red fluorescence ratio thus reflects -1 frameshifting frequency. The reporters differ in linker sequences which carry a codon-specific frameshifting site.

In the frames of this project the core reporter plasmid pACH5-1 has been optimized via insertion of a linker sequence, giving rise to plasmid pACH10 (Figure 39). In the next step pACH10 has been used to create a set of codon-specific reporter plasmids.

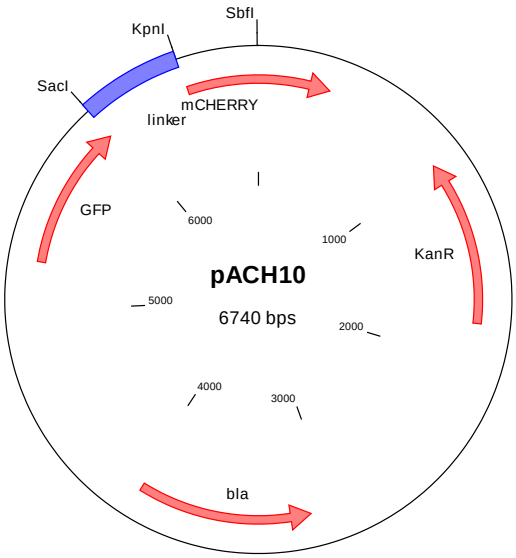

Figure 39: Map of pACH10, the linker sequence masked by the restriction sites of SacI and KpnI is indicated in purple. Genes encoding GFP, mCh, the ampicillin and the kanamycin resistance cassettes are marked in red.

The linker sequences are ligated with pACH10 using the restriction sites of SacI and KpnI on the plasmid and the pre-phosphorylated ends of the linker sequences, which are designed to fit to the overhangs on the double-digested plasmid. The encoding region of GFP ends shortly before the beginning of the linker sequence (Figure 40).

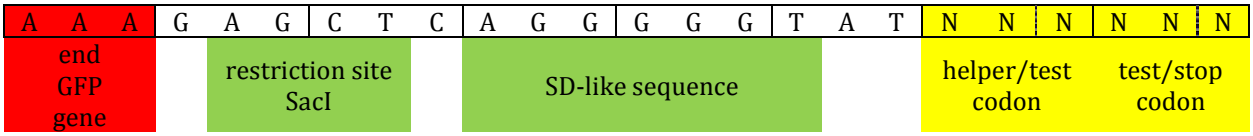

Figure 40: Scheme of translation of A and P site linkers (5' of the unique linker sequence) inserted into pACH10. The end of the GFP sequence lacking the stop codon is shown. The linker sequence itself starts at the restriction site of SacI. The dashed lines indicate the new reading frame in case of frameshifting.

Linkers to study the rate of frameshifting due the A site effects of undermodified tRNA start with at the 5' end with an in-frame SD-like sequence (AGGGGGTAT), followed by a helper codon and the test codon (Figure 41). SD-like sequences are known to cause premature release of the tRNA on the E site [47] and thereby higher the probability of frameshifting. The helper codon is designed to be bound by a tRNA which easily shifts to the test codon. The helper codon ends with the same nucleotide as the test codon starts with, or at least one to which the anticodon can easily wobble. Essentially the helper codon is not allowed to be modified by the tested enzyme. Further the helper codon consists of three identical nucleotides, if possible.

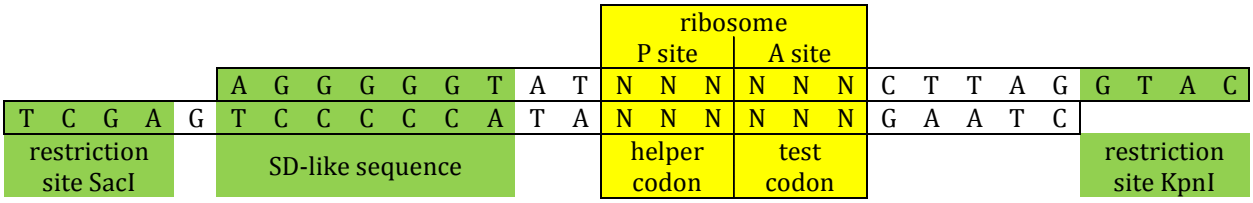

Figure 41: Scheme of linker design for A site linkers. The restriction sites of SacI and KpnI are used for ligation of the linker sequence with pACH10. The SD-like sequence and the helper codon trigger frameshifting at the test codon.

If no frameshift takes place translation will be terminated 9 codons after the test codon, at a stop codon (TAA) within the mCH sequence (Figure 42).

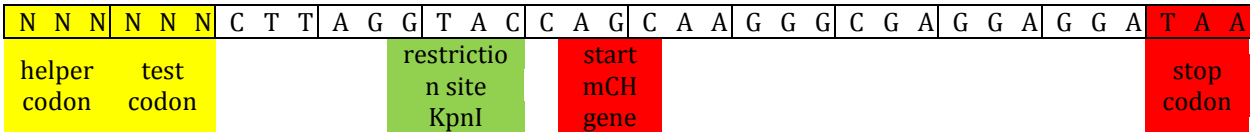

Figure 42: Scheme of translation of an A site linker (3' of the unique linker sequence) inserted into pACH10. In case of no frameshift translation proceeds in frame and is stopped at a stop codon within the mCH sequence, 9 codons after the test codon.

If a -1 frameshift occurs a functional mCH will be translated (Figure 43).

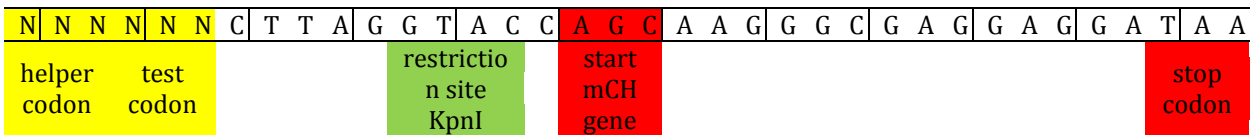

Figure 43: Scheme of translation of an A site linker (3' of the unique linker sequence) inserted into pACH10. In case of a -1 frameshift a functional mCH is added to the previously translated GFP and the stop codon is not recognized.

Linkers to study the rate of frameshifting due the P site effect also start with the SD-like sequence, followed by a test codon and an in-frame stop codon (TAA). For each pathway test codons were chosen, for which theoretically the decoding accuracy relies on the presence of the tRNA modification normally incorporated by the deleted tRME (Figure 44).

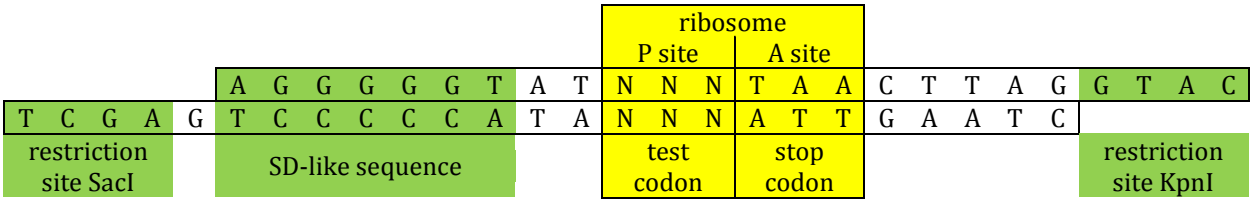

Figure 44: Linker design for P site linkers. In case of no frameshift translation is stopped immediately at the stop codon which follows the test codon.

In frame of this project a small part of the frameshift reporter plasmid library, meaning four plasmids designed to monitor the P site effect and three to monitor the A site effect of lacking xnm^{5}U34-type modifications, was used. Their sequences and predicted effects are listed in Table 14.

Name	helper codon	test codon	predicted effect
pACH10-A1	CCC	AAG	frameshift
pACH10-A3	CCC	CAA	negative control
pACH10-A4	CCC	CAG	frameshift
pACH10-P2	-	AAG	see pACH10-A1
pACH10-P3	-	AAA	negative control
pACH10-P4	-	CAA	see pACH10-A3
pACH10-P5	-	CAG	see pACH10-A4

Table 14: Within this project used frameshift reporter plasmids, their unique sequences and the predicted effects of tRME deletions.

First the strains *ΔtrmE* and *ΔmnmC* were chosen to be tested for their frameshift proneness. Therefore each frameshift reporter plasmids was introduced into the wild-type and in both deletion strains. The deletion strains were then grown in parallel with the wild-type strain and with replicas in MES-ch in the chemostat or in flasks.

The advantage of the chemostat is that separate bacterial cultures can be kept in the same growth phase independent of the initial growth rate of an individual bacterial strain. This is achieved via limitation of bacterial growth rates to an arbitrary chosen one via continuous dilution of the cultures with fresh medium controlled by high–precision pumps [132]. Maintaining the exponential growth phase and harmonizing all *ΔtRME* mutants is of crucial importance for the experiment, as the rate of frameshifts varies between different growth phases. The chemostat allows adjustment of the bacterial growth rate in each reactor, by adjusting the relative amount of media exchange. This dilution rate depends on the area of the influx tubing, the pumping speed of the influx pump, and the culture volume within the reactor. Calculation of the generation time in hours (G) can be done with the formula $G = (\ln 2 \times V) / (S \times \vartheta)$, whereas V stands for the culture volume in ml, S for the area of the influx tubing in cm^2, and ϑ for the linear velocity of the liquid in the tubing.

In this project it was desired to keep the cultures for five generations in the exponential phase with a generation time of 6 hours (*in vivo*-like doubling time). As technical problems with the chemostat emerged, the bacteria were grown in flasks. A major drawback of this method is that the *ΔtRME* strains have very diverse growth rates and it is technically challenging to harmonize them.

To evaluate if maturation of mCH influences the results, a trial was done in which the samples were 1) measured directly; 2) placed on ice for 1,5 hours (to inhibit growth and allow maturation); 3) incubated with Cam for 1,5 hours (to stop translation and allow maturation); 4) incubated with Cam and placed on ice for 1,5 hours. This intermediate steps did not improve the quality of the results.

Some frameshift reporter plasmids produced a very weakly fluorescing GFP (pACH10-A3 and pACH10-P3) (Figure 45). These differences can by explained with different effects of 3' ends produced by the linkers, which might induce degradation of the protein. Further basic questions about the experiment design emerged, as the mCH signal of some frameshift reporter plasmids reached only the same intensity as bacterial autofluorescence. Interestingly this effect was stronger in the *ΔtrmE* mutant than in the wild-type.

Further control experiments on differential stability of the reporter proteins are needed to make the reporter tool applicable for frameshifting measurements.

SL1344 pACH5-1 (control)

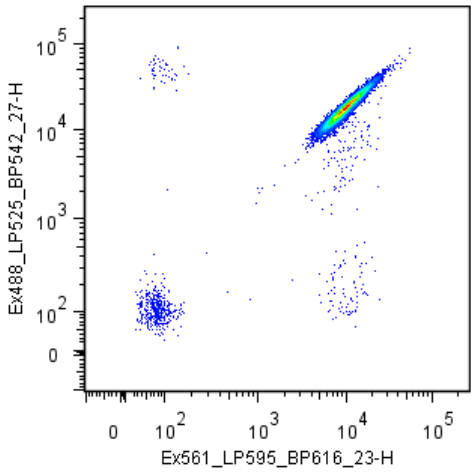

SL1344 pACH10-A1

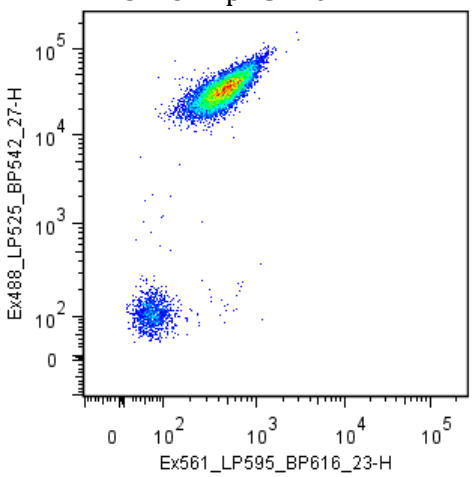

SL1344 pACH10-A3

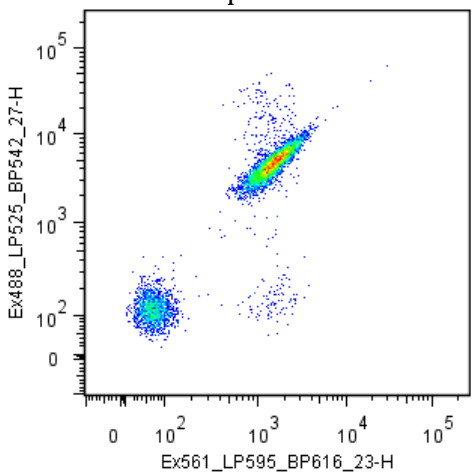

SL1344 pACH10-A4

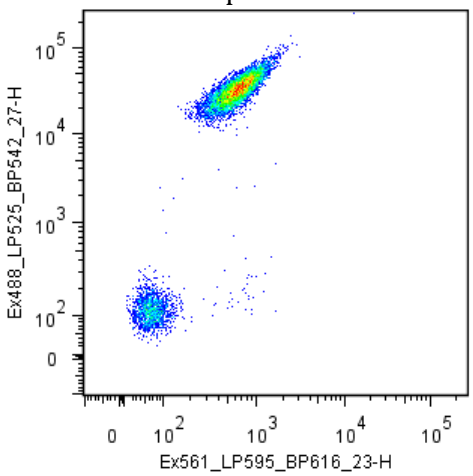

SL1344 pACH10-P2

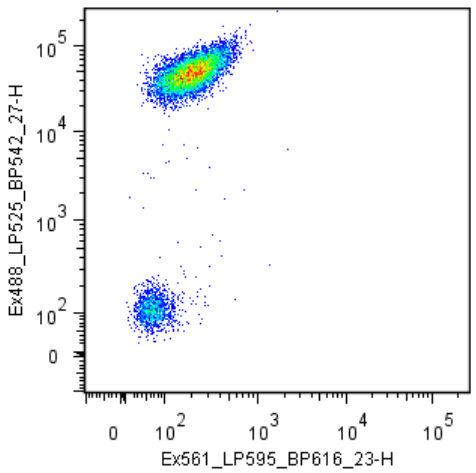

SL1344 pACH10-P3

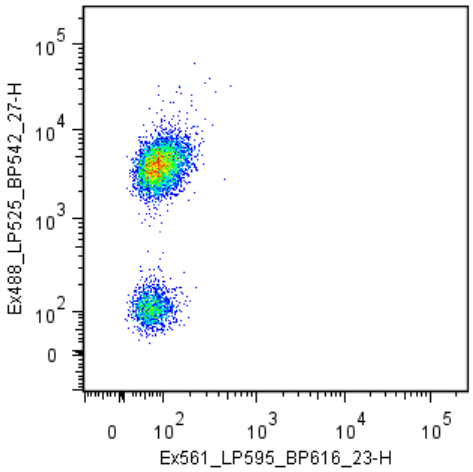

SL1344 pACH10-P4

SL1344 pACH10-P5

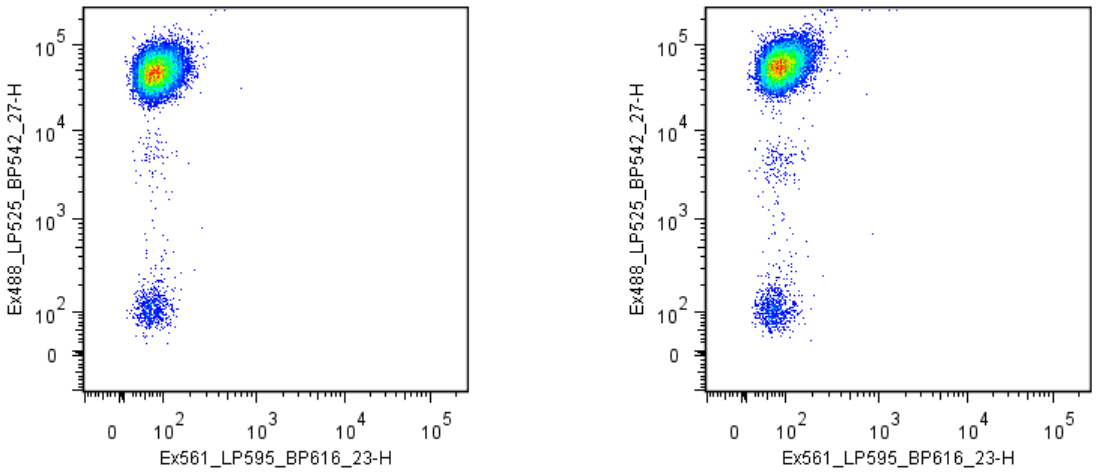

Figure 45: FACS data of wild-type strains carrying the frameshift reporter plasmids grown for 7 hours in MES-ch. Cells are shown in the channels Ex488_LP525_BP542_27-H and Ex561_LP595_BP616_23-H. Signals weaker than 10^2 are considered to arise due to autofluorescence. Cell debris was previously removed by gating the upper population emerging when the FSC-H and SSC-H channels are ploted against each other. Data was processed using FlowJo.

6 Conclusion

In frame of this project:

- 21 single tRME deletion strains and 5 double tRME deletion strains of *Salmonella* Typhimurium have been created;
- *ΔgidA*, *ΔtrmE*, *ΔmiaA*, *ΔmiaB*, and *Δtgt* strains demonstrated a growth rate reduction of 40-99% in the mouse model of typhoid fever, which corresponds to significant virulence loss;
- the *ΔmnmA* strain was cleared from the liver and the spleen within three days of post-infection in the mouse model of typhoid fever, demonstrating complete avirulence;
- the double deletion strain *ΔydaO ΔyfhQ* showed a growth rate reduction of 40% in the mouse model of typhoid fever and a growth rate reduction of 5% *in vitro*, although single deletion strains had no significant decrease in their fitness;
- among the tRME deletion strains with virulence loss *ΔmiaB* and *ΔtrmE* did not show significant growth reduction in rich growth medium, implying that specific mechanisms related to *Salmonella* pathogenicity have been affected by the tRME abolishment.

In order to infer whether the growth reduction and virulence loss effects indeed derived from the impediment of mistranslation control in the certain tRME deletion strains, further experiments with frameshifting and misreading reporters would be necessary.

Nevertheless, tRNA modifying enzymes have a potential to serve as drug targets, which have hardly been considered before. Some of them are not critical in rich nutrition conditions, thus they offer the advantage that their inhibition would not affect the general microbial flora, decreasing side-effects and slowing down the development of bacterial resistance against an inhibiting drug. If the listed tRMEs are suitable targets in terms of the possibilities to inhibit their function needs to be determined, conveniently detailed structural data of many tRNA modifying enzymes are already available.

Beside the demonstrated potential of tRME as drug targets, tRME deletion strains could be used as novel vaccines, as it was suggested for *Streptococcus pyogenes ΔgidA* and *ΔmnmE* strains [133]. The deletion strains are avirulent due to hindered translation, but still show a nearly normal expression profile and thus present the same antigens to the immune system as the virulent strains do.

7 Materials and methods

7.1 Media

Chemicals are obtained from Sigma, if not indicated otherwise.

Liquid cultures in rich medium are done in Luria Bertani low salt medium (LB, Tryptone 10 g/l, Yeast Extract 5 g/l, NaCl 5 g/l). Further minimal medium MES-ch (and its variations MES-ch 5x and MES-ch gly) is used to mimic the growth conditions within macrophages (components see Table 15). LA low salt solid medium (LB low salt+ Agar 15 g/l) are used for plating of bacteria cultures. For phage transduction LB broth is used to prepare the donor strain (LB low salt supplemented with 0.2 % glucose (Roth), 0.2 g/l $MgSO_4$ x $7H_2O$, 9.92 g/l K_2HPO_4, 35 g/l Na_2HPO_4 x $2H_2O$, 1 g/l NH_4Cl and 1.82 g/l citric acid (all chemical from Merck)). To execute phage transduction in the recipient strain LB low salt medium with 10 mM $CaCl_2$ and 20 mM $MgSO_4$ and LB low salt medium with 3.8 g/l EGTA are used. EBU plates for selection of phage-free colonies consist of 10 g/l Tryptone, 5 g/l Yeast Extract, 5 g/l NaCL. 15 g/l Agar, 1 % Evans-Blue-Solution, 1 % Fluorescein-Solution, 12,5 % K_2HPO_4-Solution , and 20 % Glucose-Solution.

Component	Final concentration		
	MES-ch	**MES-ch 5x**	**MES-ch gly**
MES (pH 3.0)	100 mM	100 mM	100 mM
KCl	5 mM	5 mM	5 mM
NH4Cl	15 mM	15 mM	15 mM
K2SO4	0.5 mM	0.5 mM	0.5 mM
KH2PO4	1 mM	1 mM	1 mM
MgSO4	8 mM	8 mM	8 mM
Casamino acids	0.02%	0.02%	0.02%
Glycerol	0.02%	**0.1%**	**0.4%**
***N*-Acetyl-D-glucosamin**	0.0042%	**0.021%**	0.0042%
Glucose	0.003%	**0.015%**	0.003%
D-(+)-Glucosamine hydrochloride	0.0018%	**0.009%**	0.0018%
pH 5.0			

Table 15: Ingredients of MES-ch, MES-ch 5x, and MES-ch gly. Differences between the media are written in bold.

Antibiotics are used in the following concentrations: 90 streptomycin µg/ml 50 µg/ml kanamycin, 100 µg/ml ampicillin, 170 µg/ml chloramphenicol.

7.2 Strains and plasmids

The mutants created in this project base on the *Salmonella enterica* serovar Typhimurium strain SL1344 [134]. SL1344 is auxotrophic for histidine and carries a streptomycin resistance cassette. SBM224 (SL1344 *ΔgalK ΔhisG Δres Δ4495 Δ4526* + pKD46) is used for electroporation. To create deletion strains, which express fluorescence proteins when induced, gene deletions are transduced into SBM319 (SL1344 GFPs@sifB + mCherry@virK), SBM321 (YFPs@sifB +

mCherry@virK), and SBM322 (CFP@sifB + mCherry@virK). Further diverse strains created by members of the Bumann group are used for transduction of gene deletions, transformation of plasmids, and/or phenotype observations. If not indicated otherwise, strains are grown in MES-ch containing Str shacking at 37°C. LB low salt over-night cultures of all created strains are separated from the medium using centrifugation (2 min at +14 rpm), solved in ddH_2O containing 7% DMSO, and stored at -80°C.

The temperature-sensitive plasmid pKD46, which encodes the arabinose-induced λ Red recombination system and an ampicillin resistance cassette (permissive temperature 28°C, restrictive temperature 42°C) is carried by the strain SBM224. To remove the antibiotic cassette, which was inserted in order to create gene deletion mutants, the plasmid pCP20 is required. This is a temperature-sensitive plasmid, which carries the FLP recombinase and an ampicillin resistance cassette (permissive temperature 28°C, restrictive temperature 42°C). To enable the bacteria of light generation for the luciferase assay the plasmid pCSλ Amp (kindly provided by Nicole Freed, University of Basel) is used. It carries a SC101* ori, a luxCDABE operon under control of a synthetic λ promotor and an Amp^R marker. The operon lux CDABE causes expression of the bacterial luciferase (genes *luxA* and *luxB*), and of the necessary multienzyme complex (*luxC*, *luxD* and *luxE*) [135, 136]. The plasmid pACH5-1 was created by Dr. Anna Chirkova. Further plasmids for the frameshift reporter assay were created, based on pACH5-1. All plasmid maps are shown in Appendix C.

7.3 Genetic manipulations

7.3.1 Generation of knock-out Salmonella strains

Salmonella Typhimurium deletion strains are created by replacing whole genes of the strain SL1344 *ΔgalK ΔhisG Δres Δ4495 Δ4526* + pKD46 with an antibiotic resistance cassette using the FLP recombination system following the protocol described in [137]. The purification of the PCR products for downstream applications is operated with the Promega Wizard® Plus SV Minipreps DNA Purification System (according to its protocol). Gene deletion mutants are verified via PCR. PCR products are visualized using gel electrophorese, therefore 1 or 2% agarose (depending on the product size and desired accuracy) is heated up in 1xTBE buffer [113]. When the gel is lukewarm GR Safe DNA stain (2 µl/50ml gel, obtained by InnoVita) is added. If necessary the PCR products are digested with AluI (Fermentas, used according to its protocol). To allow size determination 100 bp or 1 Kb ladders (Fermentas) are used.For visualization of the DNA a transilluminator emitting blue light (Invitrogen) is used with an orange filter.

Gene deletions are transduced into SL1344, color strains or cured deletion strains with p22 phages. Phages are prepared following the protocol described in [118] and stored in presence of 4% chloroform. An over-night culture of the recipient strain is mixed 1:1 with LB low salt 10 mM $CaCl_2$ 20 mM $MgSO_4$ and 1, 5, and 20 µl of the phages, respectively. After maximal 15 minutes, infection is stopped by addition of LB low salt 10 mM EGTA. This mixture is incubated for 1h, spun down, most of the supernatant (except 100-200 µl) is removed, bacteria are resolved in the remaining medium, and plated out on LB low salt plates containing the selecting antibiotic. Then

the colonies are picked and struck out on EBU plates. Gene deletion and absence of p22 phages are verified via PCR.

To remove antibiotic cassettes first the plasmid pCP20 is introduced via electroporation into the respective strain. Therefore a day-culture is grown to the exponential growth phase in LB low salt (OD_{600} 0.6-0.9), and washed four times with sterile, ice-cold ddH_2O (spin cells down, remove supernatant, resolve in sterile, ice-cold ddH_2O) to gain electro-competence. For every electroporation approximately 15 ml of culture are recommended, which are concentrated during/after washing to 50 µl. The amount of plasmid necessary for successful electroporation depends on its concentration. In case of highly concentrated plasmids with the organisms methylation-pattern 1 µl can be sufficient. Electroporation is performed with pre-cooled electroporation cuvettes (BioRad) in a MicroPulser electroporator (BioRad). After electroporation cells are grown for 1 hour in LB low salt without any antibiotics at 28°C. The cultures are then spun down, most of the supernatant (except 100-200 µl) is removed, bacteria are resolved and plated out on LB low salt plates containing Str and Amp, and grown on 28°C over-night or longer if necessary. A few colonies of each plate are used to set up day-cultures in LB low salt containing only Str. After 2 hours on 28°C they are shifted to 42°C. After 3-4 hours growth on 42°C the cultures are spun down, most of the supernatant (except 100-200 µl) is removed, bacteria are resolved and plated out onto LB low salt plates containing only Str. Verification of the desired resistance cassette loss is done first via replica plating (taking up the colonies on a sterile piece of tissue and placing the colonies in the same orientation on another plate using a stamp) on LB low salt plates containing the antibiotic for which the resistance is desired to be lost, then via PCR with the control primers used for creation of the gene deletion mutant.

7.3.2 Plasmid cloning

Based on pACH5-1, pACH10 is created via insertion of a 802 bp linker sequence at the restriction sites of SacI and SbfI. The sequence consists of 1) a 469 nt piece of the plasmid with the restriction site of SacI and a fusion overhang and 2) the first 355 nt of mCH (also ATC instead of ATG) with the fitting fusion overhang toward 1) and a SbfI restriction site. The used primers are: 1) f_K_sacI_Ile8 and r_K_Ile8; 2) f_M_Ile8 and r_M_Ile8 (Table 16). Both sequences are fused and multiplied (3 PCR cycles without primers, then 25 cycles with f_K_sacI_Ile8 and r_M_Ile8). The sequence and pACH5-1 are first digested with SacI afterwards with SbfI (both NEB, used according to its protocols) and ligated with T4 DNA ligase (Fermentas, used according to its protocol). The arising plasmid, named pACH10, is electroporated into *E.coli*, purified with Promega Wizard® Plus SV Minipreps DNA Purification System (according to its protocol), verified by the length of the PCR product with the primers fACH3_CFP and mama_ile8_c (pACH10 1460 bp, pACH5-1 1059 bp), and by sequencing executed by Microsynth AG Barcode Economy Service.

Primer name		Sequence	
mama_ile8_c	5'	AGGACAGCTTCAAGTAGTCG	3'
fACH3_CFP	5'	TGATAGAGGATCCTCTAGATTTAAGAAGG	3'
f_K_sacI_Ile8	5'	CGCCTGAGCTCGAGACGAAATACGCGATCGCTG	3'
r_K_Ile8	5'	CGATGTTATCCTCCTCGCCCTTGCTGGTACCAACGTCTTGCTCGAGGCCGCG	3'

f_M_Ile8	5'	AAGGGCGAGGAGGATAAC**ATC**GCCATCATCAAGGAGTTCATGC	3'
r_M_Ile8	5'	CGCCGTCCTGCAGGGAGGAG	3'

Table 16: Sequences of the primers used for plasmid cloning.

The linkers were ordered from Sigma-Aldrich in form of phosphorylated primers. To prepare the linkers for insertion 2 µM of each (forward and reverse primer) were mixed and heated up onto 92°C for 2 minutes.

To insert the linker sequences, the mother plasmid pACH10 first digested with SacI afterwards with KpnI (both NEB, used according to its protocols). The double digested sequence is purified via an 2% agarose gel by its size and separated from the gel with Machery-Nagel NucleoSpin® Gel and PCR Clean-up (according to its protocol) ligated 1h at 16°C with the linkers using T4 DNA ligase (Fermentas used according to its protocol), purified with Promega Wizard® Plus SV Minipreps DNA Purification System (according to its protocol) and electroporated into *E.coli* DH5α. Positive clones are selected via their ampicillin resistance and successful ligation is verified by the length of the PCR product using the primers mama_ile8_c and fACH3_CFP (no insert 1460 bp, insert 1052 bp). Further minipreps of the plasmids are sequenced executed by Microsynth AG Barcode Economy Service. Correct plasmids are then electroplated into SL1344. The plasmids are further purified from *Salmonella* Typhimurium using Promega PureYield™ Plasmid Midiprep System (according to its protocol).

7.4 *In vitro* growth rate measurements

To evaluate growth curves with OD_{600} and/or CFU measurements, LB low salt or MES-ch day-cultures containing Str are inoculated with over-night cultures of the strains of interest (grown in presence of all possible antibiotics) to an calculated OD_{600} of 0.05 and grown shacking at 37°C. Until the cultures reached the stationary growth phase (approximately 4 hours), OD_{600} values are measured every 30 minutes. During the first hours of the stationary growth phase the procedure is repeated every hour and finally 24 hours after introduction of the culture. In parallel aliquots to plate out are taken. The aliquots are diluted in PBS (obtained by Gibco), plated out on LB low salt Str plates, and incubated at 37°C over-night. The next day, the colonies are counted. The dilution should be in a range that accurate counting of the colonies is possible, but the result is still significant (Table 17).

OD_{600}	dilution
< 0.05	10^{-4}
0.05 – 0.5	10^{-5}
0.5 – 1.5	10^{-6}
> 1.5	10^{-7}

Table 17: Used dilution ranges for CFU measurements in dependence of the OD_{600} values.

The doubling time is calculated as the reciprocal value of the slope from the logarithmic values (base 2) of the growth curves during exponential growth phase. In detail, this is done by manual estimation of the exponential growth phase, calculation of the logarithmic values in EXCEL with the command =LOG(number;2), calculation of the slope with the command =SLOPE(known_y's;known_x's), and the reciprocal value with =1/number. To allow comparison

between experiments the growth rate is calculated by normalization of all mutant doubling times to the doubling time of wild-type in the same experiment.

To execute the luciferase assay over-night cultures of strains with the plasmid pCSα Amp are grown presence of all possible antibiotics. A 96-well plate with black walls (Corning® 96 Well Flat Clear Bottom Black Polystyrene TC-Treated Microplates) is filled with 190 µl LB low salt or MES-ch medium with Str and Amp in each well. The over-night cultures are washed, if the type of growth medium is changed, and transferred into the plate to a final dilution of 5000. The development of the luminescence signal (490 nm) is monitored for 8-16 hours using plate readers with the program Gen5 1.05 and 2.0, respectively (Synergy 2 Multi-Mode Microplate Reader and Synergy H4 Hybrid Multi-Mode Microplate Reader both BioTek). The settings for the plate reader are chosen as follows: 37°C, cycles of every 2 minutes: measure OD_{600}, measure LUM, shake 30'. To calculate the doubling time from the gained data set scripts, written by members of the Bumann group, are used with Strawberry Perl 5 and RStudio. First the way the values are listened in the obtained .txt file is changed using "file_converter.pl" in command promp. This script changes the formatting in the .txt file of which the complete name is written in the file "file name.txt", located in D:\format_files. The file produced by this command has the name LUM_formatted.txt. Then the script "Growth rate program for Lum.R" is called in RStudio using "source ("D:/Growth rate calculations/Growth rate program for Lum.R"). Then the doubling time can be calculated using "gr.rates<-growth.plots (dir="D:/format_files", growth.file="LUM_formatted.txt", growth.pdf="LUM_growth.pdf", rates.out="LUM_results.txt", win=40, min.rsq=0.95)". The term win stands for the count of data points through which the line (with which the doubling time is calculated) must reach, with at least the R^2 value chosen with the term min.rsq (indicated in the commands with green). All terms written in blue must be adapted to the name and exact position of the used files and scripts. The terms in red can be varied as desired.

To execute a growth competition assay *in vitro*, MES-ch over-night cultures of fluorescent *Salmonella* Typhimurium strains grown in presence of all possible antibiotics are mixed evenly, and inoculated into fresh MES-ch containing Str to an OD_{600} of 0.05. During the first 4 hours of growth samples are taken every 30 minutes and their fluorescence emission is measured via FACS. To estimate the growth rate of a deletion strain compared to the wild-type, the change in cell count of its population over time in comparison to the wild-types population cell count change is calculated.

7.5 Wide-field microscopy (fluorescence and phase contrast)

2% agarose (solved in PBS) is heated up and polymerized in a BIORAD SDS PAGE apparatus to a 2 mm thick layer, which is cut into small pieces of approximately 5 x 5 mm and placed on slides. Then 2 µl bacterial cultures are placed onto the agarose gel and covered with a coverslip. To guarantee the maintenance of the coverslip, it is additionally fixed with a few drops of nail polish in its corners.

To visualize the phenotypes of the bacteria a IX71 Microscope (Olympus) is used in combination with a CoolSNAP HQ2 camera (Princeton Instruments), a 300W Xenon Light Source to excite the fluorescent proteins, a 100x Plan Semi-Apochromat UPLFL 100XO3PH objective with oil

immersion and 1.3 NA (Olympus), GFP filterset (Chroma, excitation at 470/40 nm, emission 525/50 nm), mCherry filterset (Chroma, excitation at 572/35 nm, emission 632/60 nm), CFP filterset (Chroma, excitation at 438/24 nm, emission 470/24 nm), YFP filterset (Chroma, excitation at 513/17 nm, emission 559/38 nm), and dichroic mirrors for GFP/mCherry or YFP/CFP. For acquisition the Deltavision's Softworx 5.5 software is used.

Detailed settings are listed in Table 18. Due to differences in the alignment for Köhler illumination the needed exposure times and filter settings differ among experiments.

	exposure time (sec)	EX filter	EM filter	ND filter
Phase contrast	0.3	blank	blank	32%
	0.4	blank	blank	50%
	0.25	blank	blank	50%
CFP	3	CFP	CFP	100%
mCh	1	mCh	mCh	100%
YFP	3	YFP	YFP	100%
GFP	0.4	GFP	GFP	100%
	0.3	GFP	GFP	100%

Table 18: Used microscope settings.

After acquisition the DV files created by Softworx were changed to 16-bit JGP files and scale bars were inserted using ImageJ.

7.6 Competitive index determination in BALB/c mice

All animal related procedures were carried out in the lab by the personal certified for animal experimentation according to the European and Swiss legislation. BALB/c mice were infected intravenously with 500-8000 CFU *Salmonella* Typhimurium. The strains were expressing at least one fluorescent protein (GFP, CFP, GFPweak, mCH, YFP + mCH, GFP + mCH, or CFP + mCH). At day 4 of infection mice were sacrificed, spleen and liver retrieved followed by homogenization and flow cytometry analysis.

To estimate the growth rate of a mutant compared to the wild-type, the CI value is inverted and the log2 is calculated. This value is subtracted from the theoretical amount of divisions during infection X and divided by X. As *Salmonella* divides *in vivo* every 6 hours, in case of an infection time of 4 days X is 16.

7.7 Frameshift reporter assay

The chemostat system was set with 24 reactor tubes for 16 ml max culture capacity (Duran). Reactor tubes are held in a water bath. Through the rubber seal of each reactor four needles are punctured: one for the influx of fresh medium, one for the efflux of culture, one for the influx of sterile air, and one to place the inoculum in the sterile system. The whole system is connected via tubings (Ismatec). The efflux tubings have a diameter of 2.79 mm, the diameter of the influx tubings can be varied (0.63, 0.76, 0.89, 1.02, 1.3, 1.52, or 2.79 mm). Influx and efflux of liquids are driven by pumps (Ismatec tubing pump IPC-N 24 and IP 24). The efflux pump is switched on much stronger than the influx pump, causing removal of all liquid over the chosen threshold (high of the needle) and occurrence of a vacuum, which drives the passive influx of air. Mixing of

the samples within the reactors is performed by the continuous influx of air and a small magnetic steering bar in each reactor, driven by two magnetic stirrers placed under the water bath.

For inoculation of the chemostat, concentrates of over-night cultures grown in presence of all possible antibiotics are used. The chemostat cultures are inoculated to a theoretical OD_{600} of 0.05 in 10 ml MES-ch, grown for 4 hours at 37°C to reach a sufficient density with only the efflux pump turned on, and incubated with medium exchange at a flow rate of 1.155 ml/h at 37°C. Then the whole culture of each reactor is mixed, the OD_{600} is measured and aliquots are measured via FACS.

Instead of the mini-chemostat system also flasks can be used. The 20 ml cultures are also inoculated to an OD_{600} of 0.05 with over-night cultures grown for 16 h. Aliquots of the day culture are measured after 4 and 7 hours of growth via FACS. To simulate a 16 hours time-point the over-night cultures are measured too. To allow maturation of the fluorescence proteins, cell proliferation can be stopped before measurement with 170 µg/ml CAM.

The proneness of a *ΔtRME* strain to frameshift on a specific test codon relative to the wild-type is evaluated by the following calculation: the auto-fluorescence using the median intensity of green and red fluorescence, respectively, from a culture of the tested strain without frameshift reporter plasmid is subtracted; the ratio of red to green fluorescence within the sample is calculated; the average of the ratios from the control samples are taken; every value of the same deletion strain is normalized to this average; the average of every replica group is taken, and put into perspective of the wild-type average for the respective frameshift reporter.

8 References

1. Coates, A., et al., *The future challenges facing the development of new antimicrobial drugs.* Nat Rev Drug Discov, 2002. 1(11): p. 895-910.
2. Powers, J.H., *Antimicrobial drug development--the past, the present, and the future.* Clin Microbiol Infect, 2004. 10 Suppl 4: p. 23-31.
3. Singh, S.B. and J.F. Barrett, *Empirical antibacterial drug discovery--foundation in natural products.* Biochem Pharmacol, 2006. 71(7): p. 1006-15.
4. Coates, A.R., G. Halls, and Y. Hu, *Novel classes of antibiotics or more of the same?* Br J Pharmacol, 2011. 163(1): p. 184-94.
5. Levy, S.B. and B. Marshall, *Antibacterial resistance worldwide: causes, challenges and responses.* Nat Med, 2004. 10(12 Suppl): p. S122-9.
6. Silver, L.L. and K.A. Bostian, *Discovery and development of new antibiotics: the problem of antibiotic resistance.* Antimicrob Agents Chemother, 1993. 37(3): p. 377-83.
7. Tenover, F.C., *Mechanisms of antimicrobial resistance in bacteria.* Am J Infect Control, 2006. 34(5 Suppl 1): p. S3-10; discussion S64-73.
8. Bax, R.P., et al., *Antibiotic resistance--what can we do?* Nat Med, 1998. 4(5): p. 545-6.
9. WHO. 2012; Available from: www.who.int/world-health-day/2011.
10. Fernandes, P., *Antibacterial discovery and development--the failure of success?* Nat Biotechnol, 2006. 24(12): p. 1497-503.
11. Lange, R.P., et al., *The targets of currently used antibacterial agents: lessons for drug discovery.* Curr Pharm Des, 2007. 13(30): p. 3140-54.
12. Devasahayam, G., W.M. Scheld, and P.S. Hoffman, *Newer antibacterial drugs for a new century.* Expert Opin Investig Drugs, 2010. 19(2): p. 215-34.
13. Hughes, D., *Exploiting genomics, genetics and chemistry to combat antibiotic resistance.* Nat Rev Genet, 2003. 4(6): p. 432-41.
14. Knowles, D.J., *New strategies for antibacterial drug design.* Trends Microbiol, 1997. 5(10): p. 379-83.
15. Gwynn, M.N., et al., *Challenges of antibacterial discovery revisited.* Ann N Y Acad Sci, 2010. 1213: p. 5-19.
16. Wimberly, B.T., *The use of ribosomal crystal structures in antibiotic drug design.* Curr Opin Investig Drugs, 2009. 10(8): p. 750-65.
17. Klebe, G., *Recent developments in structure-based drug design.* J Mol Med (Berl), 2000. 78(5): p. 269-81.
18. Blondelle, S.E., E. Perez-Paya, and R.A. Houghten, *Synthetic combinatorial libraries: novel discovery strategy for identification of antimicrobial agents.* Antimicrob Agents Chemother, 1996. 40(5): p. 1067-71.
19. Giammanco, G.M., et al., *Persistent endemicity of Salmonella bongori 48:z(35):--in Southern Italy: molecular characterization of human, animal, and environmental isolates.* J Clin Microbiol, 2002. 40(9): p. 3502-5.
20. Groisman, E.A. and H. Ochman, *How Salmonella became a pathogen.* Trends Microbiol, 1997. 5(9): p. 343-9.
21. Hensel, M., *Salmonella pathogenicity island 2.* Mol Microbiol, 2000. 36(5): p. 1015-23.
22. Coburn, B., G.A. Grassl, and B.B. Finlay, *Salmonella, the host and disease: a brief review.* Immunology and cell biology, 2007. 85(2): p. 112-8.
23. Sampson, L.L., et al., *Translation initiation controls the relative rates of expression of the bacteriophage lambda late genes.* Proc Natl Acad Sci U S A, 1988. 85(15): p. 5439-43.

24. Pang, T., et al., *Typhoid fever--important issues still remain.* Trends in microbiology, 1998. 6(4): p. 131-3.
25. Wang, X. and M.F. Slavik, *Rapid detection of Salmonella in chicken washes by immunomagnetic separation and flow cytometry.* Journal of food protection, 1999. 62(7): p. 717-23.
26. Haraga, A., M.B. Ohlson, and S.I. Miller, *Salmonellae interplay with host cells.* Nature reviews. Microbiology, 2008. 6(1): p. 53-66.
27. Garcia-del Portillo, F., et al., *Salmonella induces the formation of filamentous structures containing lysosomal membrane glycoproteins in epithelial cells.* Proceedings of the National Academy of Sciences of the United States of America, 1993. 90(22): p. 10544-8.
28. McGhie, E.J., et al., *Salmonella takes control: effector-driven manipulation of the host.* Current opinion in microbiology, 2009. 12(1): p. 117-24.
29. Jostins, L., et al., *Host-microbe interactions have shaped the genetic architecture of inflammatory bowel disease.* Nature, 2012. 491(7422): p. 119-24.
30. Bhan, M.K., R. Bahl, and S. Bhatnagar, *Typhoid and paratyphoid fever.* Lancet, 2005. 366(9487): p. 749-62.
31. Thompson, J.A., S. Helaine, and D.W. Holden, *The Salmonella-Mouse Interaction: A Versatile Model to Study Bacterial Infection*, in *Bacterial Virulence. Basic Principles, Models and Global Approaches*, P. Sansonetti, Editor. 2010, Wiley-VCH Verlag Weinheim.
32. van Velkinburgh, J.C. and J.S. Gunn, *PhoP-PhoQ-regulated loci are required for enhanced bile resistance in Salmonella spp.* Infection and immunity, 1999. 67(4): p. 1614-22.
33. Porwollik, S., et al., *Characterization of Salmonella enterica subspecies I genovars by use of microarrays.* Journal of bacteriology, 2004. 186(17): p. 5883-98.
34. McClelland, M., et al., *Complete genome sequence of Salmonella enterica serovar Typhimurium LT2.* Nature, 2001. 413(6858): p. 852-6.
35. Parkhill, J., et al., *Complete genome sequence of a multiple drug resistant Salmonella enterica serovar Typhi CT18.* Nature, 2001. 413(6858): p. 848-52.
36. Watson, J.D., *Molecular biology of the gene*. 5th ed. 2003, San Francisco: Pearson/Benjamin Cummings. xxvix, 732 p.
37. Zaher, H.S. and R. Green, *Fidelity at the molecular level: lessons from protein synthesis.* Cell, 2009. 136(4): p. 746-62.
38. Madigan, M.T., J.M. Martinko, and J. Parker, *Brock biology of microorganisms*. 9th ed. 2000, Upper Saddle River, NJ: Prentice Hall. xix, 991, 53 p.
39. Agris, P.F., *Bringing order to translation: the contributions of transfer RNA anticodon-domain modifications.* EMBO reports, 2008. 9(7): p. 629-35.
40. Zaher, H.S. and R. Green, *Quality control by the ribosome following peptide bond formation.* Nature, 2009. 457(7226): p. 161-6.
41. Atkins, J.F. and G.R. Bjork, *A gripping tale of ribosomal frameshifting: extragenic suppressors of frameshift mutations spotlight P-site realignment.* Microbiology and molecular biology reviews : MMBR, 2009. 73(1): p. 178-210.
42. Huang, Y., et al., *Selection for minimization of translational frameshifting errors as a factor in the evolution of codon usage.* Nucleic acids research, 2009. 37(20): p. 6799-810.
43. Kurland, C.G., *Translational accuracy and the fitness of bacteria.* Annual review of genetics, 1992. 26: p. 29-50.
44. Drummond, D.A. and C.O. Wilke, *The evolutionary consequences of erroneous protein synthesis.* Nature reviews. Genetics, 2009. 10(10): p. 715-24.
45. Kohanski, M.A., et al., *Mistranslation of membrane proteins and two-component system activation trigger antibiotic-mediated cell death.* Cell, 2008. 135(4): p. 679-90.

46. Itzkovitz, S. and U. Alon, *The genetic code is nearly optimal for allowing additional information within protein-coding sequences.* Genome research, 2007. 17(4): p. 405-12.
47. Marquez, V., et al., *Maintaining the ribosomal reading frame: the influence of the E site during translational regulation of release factor 2.* Cell, 2004. 118(1): p. 45-55.
48. Goto-Ito, S., et al., *Tertiary structure checkpoint at anticodon loop modification in tRNA functional maturation.* Nature structural & molecular biology, 2009. 16(10): p. 1109-15.
49. Grosjean, H., et al., *Enzymatic formation of modified nucleosides in tRNA: dependence on tRNA architecture.* Journal of molecular biology, 1996. 255(1): p. 67-85.
50. Grosjean, H., V. de Crecy-Lagard, and C. Marck, *Deciphering synonymous codons in the three domains of life: co-evolution with specific tRNA modification enzymes.* FEBS letters, 2010. 584(2): p. 252-64.
51. Rould, M.A., J.J. Perona, and T.A. Steitz, *Structural basis of anticodon loop recognition by glutaminyl-tRNA synthetase.* Nature, 1991. 352(6332): p. 213-8.
52. Cusack, S., A. Yaremchuk, and M. Tukalo, *The crystal structures of T. thermophilus lysyl-tRNA synthetase complexed with E. coli tRNA(Lys) and a T. thermophilus tRNA(Lys) transcript: anticodon recognition and conformational changes upon binding of a lysyl-adenylate analogue.* The EMBO journal, 1996. 15(22): p. 6321-34.
53. Wang, X., Q. Yan, and M.X. Guan, *Deletion of the MTO2 gene related to tRNA modification causes a failure in mitochondrial RNA metabolism in the yeast Saccharomyces cerevisiae.* FEBS letters, 2007. 581(22): p. 4228-34.
54. Nakanishi, K., et al., *Structural basis for translational fidelity ensured by transfer RNA lysidine synthetase.* Nature, 2009. 461(7267): p. 1144-8.
55. Christian, T., et al., *Control of catalytic cycle by a pair of analogous tRNA modification enzymes.* Journal of molecular biology, 2010. 400(2): p. 204-17.
56. Murphy, F.V.t., et al., *The role of modifications in codon discrimination by tRNA(Lys)UUU.* Nature structural & molecular biology, 2004. 11(12): p. 1186-91.
57. Urbonavicius, J., *Transfer RNA modifications that alter +1 frameshifting in general fail to affect -1 frameshifting.* RNA, 2003. 9(6): p. 760-768.
58. Urbonavicius, J., et al., *Improvement of reading frame maintenance is a common function for several tRNA modifications.* The EMBO journal, 2001. 20(17): p. 4863-73.
59. Li, J., et al., *Three modified nucleosides present in the anticodon stem and loop influence the in vivo aa-tRNA selection in a tRNA-dependent manner.* J Mol Biol, 1997. 271(2): p. 209-21.
60. Björk, G.R. and T.G. Hagervall, *Transfer RNA Modification*, in *Escherichia Coli and Samonella. Cellular and Molecular Biology*, B.S. Curtiss, et al., Editors. 2005, ASM Press: Washington DC.
61. Urbonavicius, J., J.M. Durand, and G.R. Bjork, *Three modifications in the D and T arms of tRNA influence translation in Escherichia coli and expression of virulence genes in Shigella flexneri.* Journal of bacteriology, 2002. 184(19): p. 5348-57.
62. Vinayak, M. and C. Pathak, *Queuosine modification of tRNA: its divergent role in cellular machinery.* Bioscience reports, 2010. 30(2): p. 135-48.
63. Bregeon, D., et al., *Translational misreading: a tRNA modification counteracts a +2 ribosomal frameshift.* Genes & development, 2001. 15(17): p. 2295-306.
64. Licznar, P., et al., *Programmed translational -1 frameshifting on hexanucleotide motifs and the wobble properties of tRNAs.* The EMBO journal, 2003. 22(18): p. 4770-8.
65. Durand, J.M., et al., *The modified nucleoside 2-methylthio-N6-isopentenyladenosine in tRNA of Shigella flexneri is required for expression of virulence genes.* Journal of bacteriology, 1997. 179(18): p. 5777-82.

66. Durand, J.M., et al., *vacC, a virulence-associated chromosomal locus of Shigella flexneri, is homologous to tgt, a gene encoding tRNA-guanine transglycosylase (Tgt) of Escherichia coli K-12.* Journal of bacteriology, 1994. 176(15): p. 4627-34.
67. Durant, P.C. and D.R. Davis, *The effect of pseudouridine and pH on the structure and dynamics of the anticodon stem-loop of tRNA(Lys,3).* Nucleic acids symposium series, 1997(36): p. 56-7.
68. Kinscherf, T.G. and D.K. Willis, *Global regulation by gidA in Pseudomonas syringae.* Journal of bacteriology, 2002. 184(8): p. 2281-6.
69. Sage, A.E., A.I. Vasil, and M.L. Vasil, *Molecular characterization of mutants affected in the osmoprotectant-dependent induction of phospholipase C in Pseudomonas aeruginosa PAO1.* Molecular microbiology, 1997. 23(1): p. 43-56.
70. Gray, J., J. Wang, and S.B. Gelvin, *Mutation of the miaA gene of Agrobacterium tumefaciens results in reduced vir gene expression.* Journal of bacteriology, 1992. 174(4): p. 1086-98.
71. Miles, Z.D., et al., *Discovery of epoxyqueuosine (oQ) reductase reveals parallels between halorespiration and tRNA modification.* Proceedings of the National Academy of Sciences of the United States of America, 2011. 108(18): p. 7368-72.
72. Blaise, M., et al., *Crystal structure of glutamyl-queuosine tRNAAsp synthetase complexed with L-glutamate: structural elements mediating tRNA-independent activation of glutamate and glutamylation of tRNAAsp anticodon.* J Mol Biol, 2008. 381(5): p. 1224-37.
73. Noguchi, S., et al., *Isolation and characterization of an Escherichia coli mutant lacking tRNA-guanine transglycosylase. Function and biosynthesis of queuosine in tRNA.* The Journal of biological chemistry, 1982. 257(11): p. 6544-50.
74. Meier, F., et al., *Queuosine modification of the wobble base in tRNAHis influences 'in vivo' decoding properties.* The EMBO journal, 1985. 4(3): p. 823-7.
75. Beier, H., et al., *UAG readthrough during TMV RNA translation: isolation and sequence of two tRNAs with suppressor activity from tobacco plants.* The EMBO journal, 1984. 3(2): p. 351-6.
76. Hagervall, T.G., et al., *Role of tRNA modification in translational fidelity.* Biochim Biophys Acta, 1990. 1050(1-3): p. 263-6.
77. Johnston, H.M., et al., *Model for regulation of the histidine operon of Salmonella.* Proc Natl Acad Sci U S A, 1980. 77(1): p. 508-12.
78. Morris, R.C., K.G. Brown, and M.S. Elliott, *The effect of queuosine on tRNA structure and function.* J Biomol Struct Dyn, 1999. 16(4): p. 757-74.
79. Salazar, J.C., et al., *A truncated aminoacyl-tRNA synthetase modifies RNA.* Proc Natl Acad Sci U S A, 2004. 101(20): p. 7536-41.
80. Perret, V., et al., *Relaxation of a transfer RNA specificity by removal of modified nucleotides.* Nature, 1990. 344(6268): p. 787-9.
81. Sylvers, L.A., et al., *A 2-thiouridine derivative in tRNAGlu is a positive determinant for aminoacylation by Escherichia coli glutamyl-tRNA synthetase.* Biochemistry, 1993. 32(15): p. 3836-41.
82. Pearson, D. and T. Carell, *Assay of both activities of the bifunctional tRNA-modifying enzyme MnmC reveals a kinetic basis for selective full modification of cmnm5s2U to mnm5s2U.* Nucleic acids research, 2011. 39(11): p. 4818-26.
83. Armengod, M.E., et al., *Enzymology of tRNA modification in the bacterial MnmEG pathway.* Biochimie, 2012.
84. Numata, T., et al., *Snapshots of tRNA sulphuration via an adenylated intermediate.* Nature, 2006. 442(7101): p. 419-24.
85. Shippy, D.C., et al., *Biological and virulence characteristics of Salmonella enterica serovar Typhimurium following deletion of glucose-inhibited division (gidA) gene.* Microbial pathogenesis, 2011. 50(6): p. 303-13.

86. Nasvall, S.J., P. Chen, and G.R. Bjork, *The modified wobble nucleoside uridine-5-oxyacetic acid in tRNAPro(cmo5UGG) promotes reading of all four proline codons in vivo.* RNA, 2004. 10(10): p. 1662-73.
87. Nasvall, S.J., P. Chen, and G.R. Bjork, *The wobble hypothesis revisited: uridine-5-oxyacetic acid is critical for reading of G-ending codons.* RNA, 2007. 13(12): p. 2151-64.
88. Modomics. 2012; Available from: http://modomics.genesilico.pl/.
89. Samuelsson, T., et al., *Aberrations of the classic codon reading scheme during protein synthesis in vitro.* The Journal of biological chemistry, 1980. 255(10): p. 4583-8.
90. Takai, K., et al., *A single uridine modification at the wobble position of an artificial tRNA enhances wobbling in an Escherichia coli cell-free translation system.* FEBS letters, 1999. 447(1): p. 1-4.
91. Phelps, S.S., et al., *Modified nucleotides in tRNA(Lys) and tRNA(Val) are important for translocation.* Journal of molecular biology, 2004. 338(3): p. 439-44.
92. Sorensen, M.A., et al., *Over expression of a tRNA(Leu) isoacceptor changes charging pattern of leucine tRNAs and reveals new codon reading.* Journal of molecular biology, 2005. 354(1): p. 16-24.
93. Gabriel, K., J. Schneider, and W.H. McClain, *Functional evidence for indirect recognition of G.U in tRNA(Ala) by alanyl-tRNA synthetase.* Science, 1996. 271(5246): p. 195-7.
94. Kothe, U. and M.V. Rodnina, *Codon reading by tRNAAla with modified uridine in the wobble position.* Molecular cell, 2007. 25(1): p. 167-74.
95. Weixlbaumer, A., et al., *Mechanism for expanding the decoding capacity of transfer RNAs by modification of uridines.* Nature structural & molecular biology, 2007. 14(6): p. 498-502.
96. Mathevon, C., et al., *tRNA-modifying MiaE protein from Salmonella typhimurium is a nonheme diiron monooxygenase.* Proceedings of the National Academy of Sciences of the United States of America, 2007. 104(33): p. 13295-300.
97. Jenner, L.B., et al., *Structural aspects of messenger RNA reading frame maintenance by the ribosome.* Nature structural & molecular biology, 2010. 17(5): p. 555-60.
98. Demeshkina, N., et al., *Interactions of the ribosome with mRNA and tRNA.* Current opinion in structural biology, 2010. 20(3): p. 325-32.
99. Ericson, J.U. and G.R. Bjork, *Pleiotropic effects induced by modification deficiency next to the anticodon of tRNA from Salmonella typhimurium LT2.* Journal of bacteriology, 1986. 166(3): p. 1013-21.
100. Diaz, I., S. Pedersen, and C.G. Kurland, *Effects of miaA on translation and growth rates.* Molecular & general genetics : MGG, 1987. 208(3): p. 373-6.
101. Esberg, B. and G.R. Bjork, *The methylthio group (ms2) of N6-(4-hydroxyisopentenyl)-2-methylthioadenosine (ms2io6A) present next to the anticodon contributes to the decoding efficiency of the tRNA.* Journal of bacteriology, 1995. 177(8): p. 1967-75.
102. Persson, B.C. and G.R. Bjork, *Isolation of the gene (miaE) encoding the hydroxylase involved in the synthesis of 2-methylthio-cis-ribozeatin in tRNA of Salmonella typhimurium and characterization of mutants.* Journal of bacteriology, 1993. 175(24): p. 7776-85.
103. Persson, B.C., et al., *The ms2io6A37 modification of tRNA in Salmonella typhimurium regulates growth on citric acid cycle intermediates.* Journal of bacteriology, 1998. 180(12): p. 3144-51.
104. Diaz, I. and M. Ehrenberg, *ms2i6A deficiency enhances proofreading in translation.* J Mol Biol, 1991. 222(4): p. 1161-71.
105. Gregory, S.T., K.R. Lieberman, and A.E. Dahlberg, *Mutations in the peptidyl transferase region of E. coli 23S rRNA affecting translational accuracy.* Nucleic acids research, 1994. 22(3): p. 279-84.

106. Bjornsson, A. and L.A. Isaksson, *UGA codon context which spans three codons. Reversal by ms2i6A37 in tRNA, mutation in rpsD(S4) or streptomycin.* J Mol Biol, 1993. 232(4): p. 1017-29.
107. Bouadloun, F., et al., *Influence of modification next to the anticodon in tRNA on codon context sensitivity of translational suppression and accuracy.* Journal of bacteriology, 1986. 166(3): p. 1022-7.
108. Wolfe, M.D., et al., *Functional diversity of the rhodanese homology domain: the Escherichia coli ybbB gene encodes a selenophosphate-dependent tRNA 2-selenouridine synthase.* The Journal of biological chemistry, 2004. 279(3): p. 1801-9.
109. Wittwer, A.J. and W.M. Ching, *Selenium-containing tRNA(Glu) and tRNA(Lys) from Escherichia coli: purification, codon specificity and translational activity.* BioFactors, 1989. 2(1): p. 27-34.
110. Dumelin, C.E., et al., *Discovery and biological characterization of geranylated RNA in bacteria.* Nature chemical biology, 2012.
111. Benitez-Paez, A., et al., *YibK is the 2'-O-methyltransferase TrmL that modifies the wobble nucleotide in Escherichia coli tRNA(Leu) isoacceptors.* RNA, 2010. 16(11): p. 2131-43.
112. Baumann, U., W. Fischer, and M. Sprinzl, *Analysis of modification-dependent structural alterations in the anticodon loop of Escherichia coli tRNAArg and their effects on the translation of MS2 RNA.* Eur J Biochem, 1985. 152(3): p. 645-9.
113. Jager, G., et al., *The conserved Cys-X1-X2-Cys motif present in the TtcA protein is required for the thiolation of cytidine in position 32 of tRNA from Salmonella enterica serovar Typhimurium.* Journal of bacteriology, 2004. 186(3): p. 750-7.
114. Purta, E., et al., *The yfhQ gene of Escherichia coli encodes a tRNA:Cm32/Um32 methyltransferase.* BMC molecular biology, 2006. 7: p. 23.
115. Ladner, J.E., et al., *Structure of yeast phenylalanine transfer RNA at 2.5 A resolution.* Proceedings of the National Academy of Sciences of the United States of America, 1975. 72(11): p. 4414-8.
116. Quigley, G.J., et al., *Hydrogen bonding in yeast phenylalanine transfer RNA.* Proceedings of the National Academy of Sciences of the United States of America, 1975. 72(12): p. 4866-70.
117. Casjens, S. and M. Hayden, *Analysis in vivo of the bacteriophage P22 headful nuclease.* J Mol Biol, 1988. 199(3): p. 467-74.
118. Thierauf, A., G. Perez, and A.S. Maloy, *Generalized transduction.* Methods in molecular biology, 2009. 501: p. 267-86.
119. Cox, M.M., *The FLP protein of the yeast 2-microns plasmid: expression of a eukaryotic genetic recombination system in Escherichia coli.* Proceedings of the National Academy of Sciences of the United States of America, 1983. 80(14): p. 4223-7.
120. Zhu, X.D. and P.D. Sadowski, *Cleavage-dependent ligation by the FLP recombinase. Characterization of a mutant FLP protein with an alteration in a catalytic amino acid.* The Journal of biological chemistry, 1995. 270(39): p. 23044-54.
121. Rollenhagen, C., et al., *Antigen selection based on expression levels during infection facilitates vaccine development for an intracellular pathogen.* Proc Natl Acad Sci U S A, 2004. 101(23): p. 8739-44.
122. Tu, S.C. and H.I. Mager, *Biochemistry of bacterial bioluminescence.* Photochem Photobiol, 1995. 62(4): p. 615-24.
123. Wilson, T. and J.W. Hastings, *Bioluminescence.* Annu Rev Cell Dev Biol, 1998. 14: p. 197-230.
124. Merzlyak, E.M., et al., *Bright monomeric red fluorescent protein with an extended fluorescence lifetime.* Nat Methods, 2007. 4(7): p. 555-7.
125. Rollenhagen, C. and D. Bumann, *Salmonella enterica highly expressed genes are disease specific.* Infect Immun, 2006. 74(3): p. 1649-60.

126. Jungblut, P.R. and D. Bumann, *Immunoproteome of Helicobacter pylori.* Methods Enzymol, 2002. 358: p. 307-16.
127. Sabarth, N., et al., *Identification of surface proteins of Helicobacter pylori by selective biotinylation, affinity purification, and two-dimensional gel electrophoresis.* J Biol Chem, 2002. 277(31): p. 27896-902.
128. Freter, R. and P.C. O'Brien, *Role of chemotaxis in the association of motile bacteria with intestinal mucosa.* Infection and immunity, 1981. 34(1): p. 222-33.
129. Hebrard, M., et al., *The challenge of relating gene expression to the virulence of Salmonella enterica serovar Typhimurium.* Curr Opin Biotechnol, 2011. 22(2): p. 200-10.
130. Stengl, B., et al., *Crystal structures of tRNA-guanine transglycosylase (TGT) in complex with novel and potent inhibitors unravel pronounced induced-fit adaptations and suggest dimer formation upon substrate binding.* Journal of molecular biology, 2007. 370(3): p. 492-511.
131. Ritschel, T., et al., *How to replace the residual solvation shell of polar active site residues to achieve nanomolar inhibition of tRNA-guanine transglycosylase.* ChemMedChem, 2009. 4(12): p. 2012-23.
132. Nanchen, A., A. Schicker, and U. Sauer, *Nonlinear dependency of intracellular fluxes on growth rate in miniaturized continuous cultures of Escherichia coli.* Applied and environmental microbiology, 2006. 72(2): p. 1164-72.
133. Cho, K.H. and M.G. Caparon, *tRNA modification by GidA/MnmE is necessary for Streptococcus pyogenes virulence: a new strategy to make live attenuated strains.* Infect Immun, 2008. 76(7): p. 3176-86.
134. Bouadloun, F., et al., *Influence of modification next to the anticodon in tRNA on codon context sensitivity of translational suppression and accuracy.* J Bacteriol, 1986. 166(3): p. 1022-7.
135. Kishony, R. and S. Leibler, *Environmental stresses can alleviate the average deleterious effect of mutations.* Journal of biology, 2003. 2(2): p. 14.
136. Rocco, C.J. and J.C. Escalante-Semerena, *In Salmonella enterica, 2-methylcitrate blocks gluconeogenesis.* Journal of bacteriology, 2010. 192(3): p. 771-8.
137. Datsenko, K.A. and B.L. Wanner, *One-step inactivation of chromosomal genes in Escherichia coli K-12 using PCR products.* Proceedings of the National Academy of Sciences of the United States of America, 2000. 97(12): p. 6640-5.

Appendices

A Abbreviations

Abbreviation	Full name
Amp	ampicillin
ATP	adenosine triphosphate
blastp	Basic Local Alignment Search Tool (conduced on amino acid level)
CI	competitive index
Cam	chloramphenicol
CFP	cyan fluorescent protein (excitation and emission maxima at 445 nm and 470 nm respectively)
CFU	colony forming unit
Cm	2′-O-methylcytidine
cmnm^{5}ges^{2}U	5-carboxymethylaminomethyl-2-geranylthiouridine
cmnm^{5}s^{2}U	5-carboxymethylaminomethyl-2-thiouridine
cmnm^{5}se^{2}U	5-carboxymethylaminomethyl-2-selenouridine
cmnm^{5}U	5-carboxymethylaminomethyluridine
cmnm^{5}Um	5-carboxymethylaminomethyl-2′-O-methyluridine
cmo^{5}U	uridine 5-oxyacetic acid
E. coli	*Escherechia coli*
EBU	Evans Blue-Uranine
EDTA	ethylenediaminetetraacetic acid
FRT	flippase recognition target sites
galQ	galactosyl-queuosine
GFP	green fluorescent protein (excitation and emission maxima at 488nm and 505nm respectively)
gluQ	glutamyl-queuosine
i^{6}A	N6-isopentenyladenosine
io^{6}A	N6-(cis-hydroxyisopentenyl)adenosine
Kan	Kanamycin
LB	Luria Bertani broth
LP502	Longpass filter, transmit wavelength that are longer then 502nm
LUM	luciferase assay
mCh	red fluorescent protein mCherry (excitation and emission maxima at 587 nm and 610 nm respectively)
mcmo^{5}U	uridine 5-oxyacetic acid methyl ester
MES	2-(*N*-morpholino)ethanesulfonic acid
mnm^{5}s^{2}U	5-methylaminomethyl-2-thiouridine
mnm^{5}se^{2}U	5-methylaminomethyl-2-selenouridine
mnm^{5}U	5-methylaminomethyluridine
ms^{2}i^{6}A	2-methylthio-N6-isopentenyladenosine
ms^{2}io^{6}A	2-methylthio-N6-(cis-hydroxyisopentenyl) adenosine
nm^{5}U	5-aminomethyluridine
OD600	Optical density measured at 600nm

oQ	epoxyqueuosine
PBS	phosphate buffered saline
PCR	polymerase chain reaction
preQ0	7-cyano-7-deazaguanosine
preQ1	7-aminomethyl-7-deazaguanosine
Q	queuosine
R	purine (adenine or guanine)
s^2C	2-thiocytidine
Sec	selenocysteine
Str	Streptomycin
t^6A	N6-threonylcarbamoyladenosine
Y	pyrimidine (thymine, cytosine or uracil)
YFP	yellow fluorescent protein (excitation and emission maxima at 488nm and 525nm respectively)
ΔtRME	Salmonella strain lacking single or multiple tRNA modifying enzyme

B PCR

The PCR mixture and cycler settings are shown in Table I and II, respectively. All used primers (obtained from Sigma-Aldrich) are listed separately.

12.5 µl PCR mixture	
5x buffer	2.50
25 mM $MgCL_2$	1.00
2 mM dNTPs	1.25
GoTaq Flexi DNA polymerase	0.10
H_2O	4.90
10 mM primer forward	0.38
10 mM primer reverse	0.38
DNA-template (in 7% DMSO)	2.00

Table I: PCR mixture for a 12.5 µl mixture, chemicals obtained from Promega.

Time	Temperature in °C	Number of cycles
3'	94	
30''	94	9
30'	65	
2'	72	
30''	94	25
30''	56	

2'	72
5'	72
∞	8

Table II: Used cycler settings.

C Plasmids

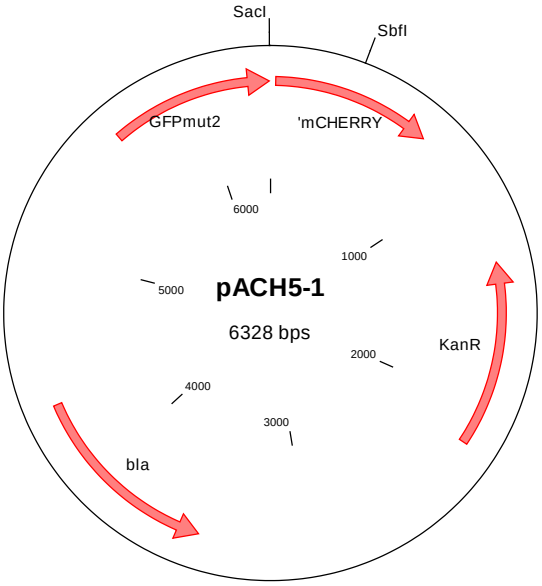

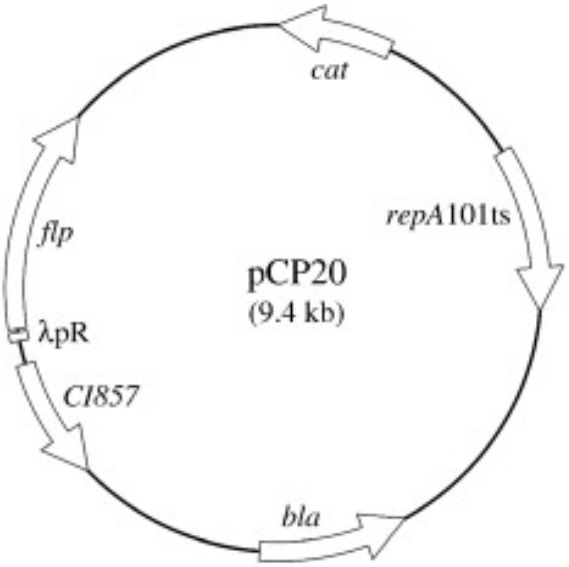

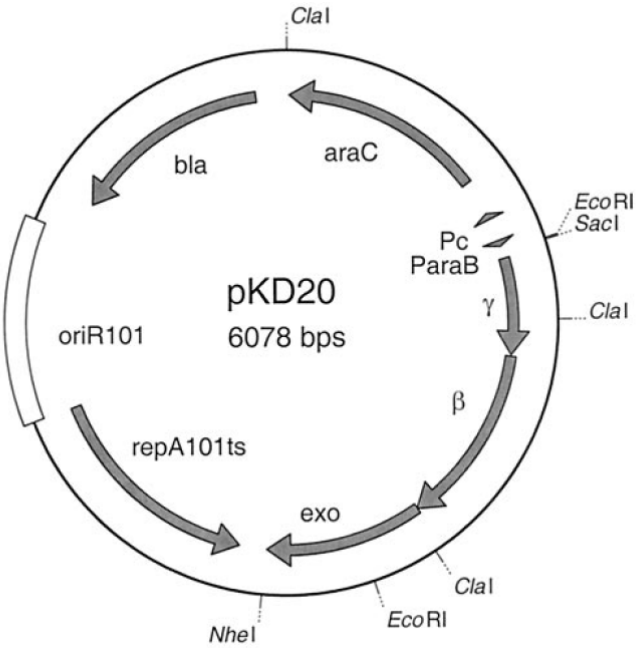

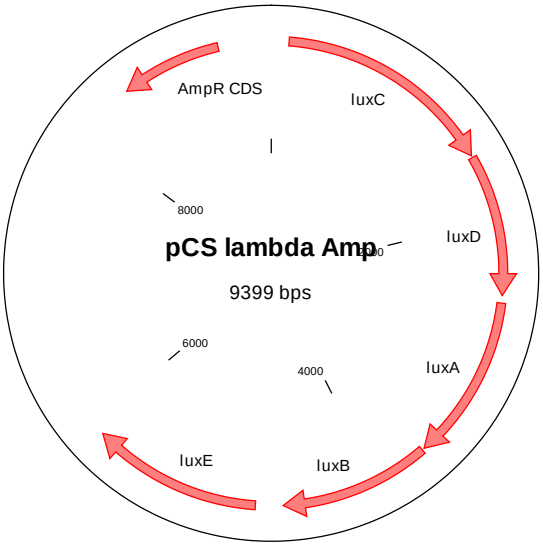

D Resistance cassettes

Kanamycin resistance cassette

Primer binding sites are highlighted in yellow. FRT sites are highlighted in blue.

GTGTAGGCTGGAGCTGCTTCGAAGTTCCTATACTTTCTAGAGAATAGGAACTTCGGAATAGGAACTTCAAGATCCCCTTATTAGAAGAACTCGTCAAGAAGGCGATAGAAGGCGATGCGCTGCGAATCGGGAGCGGCGATACC
GTAAAGCACGAGGAAGCGGTCAGCCCATTCGCCGCCAAGCTCTTCAGCAATATCACGGGTAGCCAACGCTATGTCCTGATAGCGGTCCGCCACACCCAGCCGGCCACAGTCGATGAATCCAGAAAAGCGGCCATTTTCCACCAT
GATATTCGGCAAGCAGGCATCGCCATGGGTCACGACGAGATCCTCGCCGTCGGGCATGCGCGCCTTGAGCCTGGCGAACAGTTCGGCTGGCGCGAGCCCCTGATGCTCTTCGTCCAGATCATCCTGATCGACAAGACCGGCTTC
CATCCGAGTACGTGCTCGCTCGATGCGATGTTTCGCTTGGTGGTCGAATGGGCAGGTAGCCGGATCAAGCGTATGCAGCCGCCGCATTGCATCAGCCATGATGGATACTTTCTCGGCAGGAGCAAGGTGAGATGACAGGAGAT
CCTGCCCCGGCACTTCGCCCAATAGCAGCCAGTCCCTTCCCGCTTCAGTGACAACGTCGAGCACAGCTGCGCAAGGAACGCCCGTCGTGGCCAGCCACGATAGCCGCGCTGCCTCGTCCTGCAGTTCATTCAGGGCACCGGACAG
GTCGGTCTTGACAAAAAGAACCGGGCGCCCCTGCGCTGACAGCCGGAACACGGCGGCATCAGAGCAGCCGATTGTCTGTTGTGCCCAGTCATAGCCGAATAGCCTCTCCACCCAAGCGGCCGGAGAACCTGCGTGCAATCCATC
TTGTTCAATCATGCGAAACGATCCTCATCCTGTCTCTTGATCAGATCTTGATCCCCTGCGCCATCAGATCCTTGGCGGCAAGAAAGCCATCCAGTTTACTTTGCAGGGCTTCCCAACCTTACCAGAGGGCGCCCCAGCTGGCAATTC
CGGTTCGCTTGCTGTCCATAAAACCGCCCAGTCTAGCTATCGCCATGTAAGCCCACTGCAAGCTACCTGCTTTCTCTTTGCGCTTGCGTTTTCCCTTGTCCAGATAGCCCAGTAGCTGACATTCATCCGGGGTCAGCACCGTTTCTGC
GGACTGGCTTTCTACGTGTTCCGCTTCCTTTAGCAGCCCTTGCGCCCTGAGTGCTTGCGGCAGCGTGAGCTTCAAAAGCGCTCTGAAGTTCCTATACTTTCTAGAGAATAGGAACTTCGAACTGCAGGTCGACGGATCCCCGGAAT

Chloramphenicol resistance cassette

Primer binding sites are highlighted in yellow. FRT sites are highlighted in blue.

GTGTAGGCTGGAGCTGCTTCGAAGTTCCTATACTTTCTAGAGAATAGGAACTTCGGAATAGGAACTTCATTTAAATGGCGCGCCTTACGCCCCGCCCTGCCACTCATCGCAGTACTGTTGTATTCATTAAGCATCTGCCGACATGG
AAGCCATCACAAACGGCATGATGAACCTGAATCGCCAGCGGCATCAGCACCTTGTCGCCTTGCGTATAATATTTGCCCATGGTGAAAACGGGGGCGAAGAAGTTGTCCATATTGGCCACGTTTAAATCAAAACTGGTGAAACTCA
CCCAGGGATTGGCTGAGACGAAAAACATATTCTCAATAAACCCTTTAGGGAAATAGGCCAGGTTTTCACCGTAACACGCCACATCTTGCGAATATATGTGTAGAAACTGCCGGAAATCGTCGTGGTATTCACTCCAGAGCGATGA
AAACGTTTCAGTTTGCTCATGGAAAACGGTGTAACAAGGGTGAACACTATCCCATATCACCAGCTCACCGTCTTTCATTGCCATACGTAATTCCGGATGAGCATTCATCAGGCGGGCAAGAATGTGAATAAAGGCCGGATAAAAC
TTGTGCTTATTTTTCTTTACGGTCTTTAAAAAGGCCGTAATATCCAGCTGAACGGTCTGGTTATAGGTACATTGAGCAACTGACTGAAATGCCTCAAAATGTTCTTTACGATGCCATTGGGATATATCAACGGTGGTATATCCAGTG
ATTTTTTTCTCCATTTTAGCTTCCTTAGCTCCTGAAAATCTCGACAACTCAAAAAATACGCCCGGTAGTGATCTTATTTCATTATGGTGAAAGTTGGAACCTCTTACGTGCCGATCAACGTCTCATTTTCGCCAAAAGTTGGCCCAGG
GCTTCCCGGTATCAACAGGGACACCAGGATTTATTTATTCTGCGAAGTGATCTTCCGTCACAGGTAGGCGCGCCGAAGTTCCTATACTTTCTAGAGAATAGGAACTTCGGAATAGGAACTAAGGAGGATATTCATATG

E List of all used mutants

Nr.	gene names	STM Nr.	used strain	genotype	fluorescence	plasmid	comments	resistence
SMI01	trmE	STM3843	SBM224	trmE::kanR ΔgalK His+ Δ0357 Δ4495 Δ4526			EP PCR	Str, Kan
SMI02	mnmC	STM2379	SBM224	mnmC::kanR ΔgalK His+ Δ0357 Δ4495 Δ4526			EP PCR	Str, Kan
SMI03	queF	STM2968	SBM224	queF::kanR ΔgalK His+ Δ0357 Δ4495 Δ4526			EP PCR	Str, Kan
SMI04	yjeS	STM4355	SBM224	yjeS::kanR ΔgalK His+ Δ0357 Δ4495 Δ4526			EP PCR	Str, Kan

SMI05	ybaX	STM0455	SBM224	ybaX::kanR ΔgalK His+ Δ0357 Δ4495 Δ4526			EP PCR	Str, Kan
SMI06	ygcF	STM2951	SBM224	ygcF::kanR ΔgalK His+ Δ0357 Δ4495 Δ4526			EP PCR	Str, Kan
SMI13	trmE	STM3843	SL1334	trmE::kanR			p22	Str, Kan
SMI14	mnmC	STM2379	SL1334	mnmC::kanR			p22	Str, Kan
SMI15	queF	STM2968	SL1334	queF::kanR			p22	Str, Kan
SMI16	yjeS	STM4355	SL1334	yjeS::kanR			p22	Str, Kan
SMI17	ybaX	STM0455	SL1334	ybaX::kanR			p22	Str, Kan
SMI18	ygcF	STM2951	SL1334	ygcF::kanR			p22	Str, Kan
SMI19	ygcF	STM2951	SBM319	ygcF::kanR	**GFPs**@sifB + **mCherry@virK**		p22	Str, Kan
SMI20	mnmC	STM2379	SBM319	mnmC::kanR	**GFPs**@sifB + **mCherry@virK**		p22	Str, Kan
SMI21	ybaX	STM0455	SBM319	ybaX::kanR	**GFPs**@sifB + **mCherry@virK**		p22	Str, Kan
SMI22	trmE	STM3843	SBM321	trmE::kanR	**YFPs**@sifB + **mCherry@virK**		p22	Str, Kan
SMI23	yjeS	STM4355	SBM321	yjeS::kanR	**YFPs**@sifB + **mCherry@virK**		p22	Str, Kan
SMI25	queA, queA_p	STM0404, STM1548	SACH49	queA::kanR ΔqueA_p	**GFPs**@sifB + **mCherry@virK**		p22	Str, Kan
SMI26	yecP, yecO	STM1906, STM1905	SACH45	yecP::kanR ΔyecO	**CFP**@sifB + **mCherry@virK**		p22	Str, Kan
SMI27	ydaO, yecO	STM1654, STM1905	SACH45	ydaO::kanR ΔyecO	**CFP**@sifB + **mCherry@virK**		p22	Str, Kan
SMI28	ydaO, yfhQ	STM1654, STM2545	SACH46	ydaO::kanR ΔyfhQ	**YFPs**@sifB + **mCherry@virK**		p22	Str, Kan
SMI29			SL1334	SL1344		**pCSλ** AMP	EP pCSλ AMP	Str, Amp
SMI30	trmE	STM3843	SMI13	trmE::kanR		**pCSλ** AMP	EP pCSλ AMP	Str, Kan, Amp
SMI31	queF	STM2968	SMI15	queF::kanR		**pCSλ** AMP	EP pCSλ AMP	Str, Kan, Amp
SMI32	yjeS	STM4355	SMI16	yjeS::kanR		**pCSλ** AMP	EP pCSλ	Str, Kan,

							AMP	Amp
SMI33	ybaX	STM0455	SMI17	ybaX::kanR		**pCSλ** AMP	EP pCSλ AMP	Str, Kan, Amp
SMI34	ygcF	STM2951	SMI18	ygcF::kanR		**pCSλ** AMP	EP pCSλ AMP	Str, Kan, Amp
SMI35	queF	STM2968	SBM321	queF::kanR			p22	Str, Kan
SMI36	queA	STM0404	SACH27	queA::kanR	**GFPs**@sifB + **mCherry@virK**	**pCSλ** AMP	EP pCSλ AMP	Str, Kan, Amp
SMI37	ybbB	STM0513	SACH28	ybbB::kanR	**GFPs**@sifB + **mCherry@virK**	**pCSλ** AMP	EP pCSλ AMP	Str, Kan, Amp
SMI38	ydaO	STM1654	SACH29	ydaO::kanR	**CFP**@sifB + **mCherry@virK**	**pCSλ** AMP	EP pCSλ AMP	Str, Kan, Amp
SMI39	yecO	STM1905	SACH30	yecO::kanR	**CFP**@sifB + **mCherry@virK**	**pCSλ** AMP	EP pCSλ AMP	Str, Kan, Amp
SMI40	yfhQ	STM2545	SACH31	yfhQ::kanR	**YFPs**@sifB + **mCherry@virK**	**pCSλ** AMP	EP pCSλ AMP	Str, Kan, Amp
SMI41	spoU	STM3743	SACH32	spoU::kanR	**YFPs**@sifB + **mCherry@virK**	**pCSλ** AMP	EP pCSλ AMP	Str, Kan, Amp
SMI42	miaE	STM4471	SACH33	miaE::kanR	**YFPs**@sifB + **mCherry@virK**	**pCSλ** AMP	EP pCSλ AMP	Str, Kan, Amp
SMI43	queA_p	STM1548	SACH34	queA_p::kanR	**GFPs**@sifB + **mCherry@virK**	**pCSλ** AMP	EP pCSλ AMP	Str, Kan, Amp
SMI44	yecP	STM1906	SACH50	yecP::kanR	**CFP**@sifB + **mCherry@virK**	**pCSλ** AMP	EP pCSλ AMP	Str, Kan, Amp
SMI45	queA, queA_p	STM0404, STM1548	SMI25	queA::kanR ΔqueA_p	**GFPs**@sifB + **mCherry@virK**	**pCSλ** AMP	EP pCSλ AMP	Str, Kan, Amp
SMI46	yecP, yecO	STM1906, STM1905	SMI26	yecP::kanR ΔyecO	**CFP**@sifB + **mCherry@virK**	**pCSλ** AMP	EP pCSλ AMP	Str, Kan, Amp
SMI47	ydaO, yecO	STM1654, STM1905	SMI27	ydaO::kanR ΔyecO	**CFP**@sifB + **mCherry@virK**	**pCSλ** AMP	EP pCSλ AMP	Str, Kan, Amp
SMI48	ydaO, yfhQ	STM1654, STM2545	SMI28	ydaO::kanR ΔyfhQ	**YFPs**@sifB + **mCherry@virK**	**pCSλ** AMP	EP pCSλ AMP	Str, Kan, Amp
SMI49			SBM319	SL1344	**GFPs**@sifB + **mCherry@virK**	**pCSλ** AMP	EP pCSλ AMP	Str, Amp
SMI50			SBM321	SL1344	**YFPs**@sifB +	**pCSλ** AMP	EP pCSλ	Str, Amp

					mCherry@virK		AMP	
SMI51			SBM322	SL1344	**CFP**@sifB + **mCherry@virK**	**pCSλ** AMP	EP pCSλ AMP	Str, Amp
SMI52	mnmC	STM2379	SMI14	mnmC::kanR		**pCSλ** AMP	EP pCSλ AMP	Str, Kan, Amp
SMI53	ygcF	STM2951	SMI19	ygcF::kanR	**GFPs**@sifB + **mCherry@virK**	**pCSλ** AMP	EP pCSλ AMP	Str, Kan, Amp
SMI54	mnmC	STM2379	SMI20	mnmC::kanR	**GFPs**@sifB + **mCherry@virK**	**pCSλ** AMP	EP pCSλ AMP	Str, Kan, Amp
SMI55	ybaX	STM0455	SMI21	ybaX::kanR	**GFPs**@sifB + **mCherry@virK**	**pCSλ** AMP	EP pCSλ AMP	Str, Kan, Amp
SMI56	trmE	STM3843	SMI22	trmE::kanR	**YFPs**@sifB + **mCherry@virK**	**pCSλ** AMP	EP pCSλ AMP	Str, Kan, Amp
SMI57	yjeS	STM4355	SMI23	yjeS::kanR	**YFPs**@sifB + **mCherry@virK**	**pCSλ** AMP	EP pCSλ AMP	Str, Kan, Amp
SMI58	queF	STM2968	SMI35	queF::kanR	**YFPs**@sifB + **mCherry@virK**	**pCSλ** AMP	EP pCSλ AMP	Str, Kan, Amp
SMI59	htpG	STM0487	SBM224	htpG::kanR ΔgalK His+ Δ0357 Δ4495 Δ4526			EP PCR	Str, Kan
SMI60	clpA	STM0945	SBM224	clpA::kanR ΔgalK His+ Δ0357 Δ4495 Δ4526			EP PCR	Str, Kan
SMI61	clpB	STM2660	SBM224	clpB::kanR ΔgalK His+ Δ0357 Δ4495 Δ4526			EP PCR	Str, Kan
SMI62	ibpB	STM3808	SBM224	IbpB::kanR ΔgalK His+ Δ0357 Δ4495 Δ4526			EP PCR	Str, Kan
SMI63	IbpA	STM3809	SBM224	IbpA::kanR ΔgalK His+ Δ0357 Δ4495 Δ4526			EP PCR	Str, Kan
SMI64	hslU	STM4091	SBM224	hslU::kanR ΔgalK His+ Δ0357 Δ4495 Δ4526			EP PCR	Str, Kan
SMI65	yibK	STM3695	SBM224	yibK::kanR ΔgalK His+ Δ0357 Δ4495 Δ4527			EP PCR	Str, Kan
SMI66	yadB	STM0185	SBM224	yadB::kanR ΔgalK His+ Δ0357 Δ4495 Δ4527			EP PCR	Str, Kan
SMI67	IpbA, IpbB	STM3808, STM3809	SBM224	(IpbA+IpbB)::kanR ΔgalK His+ Δ0357 Δ4495 Δ4528			EP PCR	Str, Kan
SMI68	miaE, mnmC	STM4471, STM2379	SACH48	mnmC::kanR ΔmiaE	**YFPs**@sifB + **mCherry@virK**		p22	Str, Kan
SMI69	htpG	STM0487	SBM319	htpG::kanR	**GFPs**@sifB + **mCherry@virK**		p22	Str, Kan
SMI70	clpA	STM0945	SBM319	clpA::kanR	**GFPs**@sifB +		p22	Str, Kan

					mCherry@virK			
SMI71	clpB	STM2660	SBM319	clpB::kanR	**GFPs**@sifB + **mCherry@virK**		p22	Str, Kan
SMI72	ibpB	STM3808	SBM321	IbpB::kanR	**YFPs**@sifB + **mCherry@virK**		p22	Str, Kan
SMI73	IbpA	STM3809	SBM321	IbpA::kanR	**YFPs**@sifB + **mCherry@virK**		p22	Str, Kan
SMI74	hslU	STM4091	SBM321	hslU::kanR	**YFPs**@sifB + **mCherry@virK**		p22	Str, Kan
SMI75	yibK	STM3695	SBM322	yibK::kanR	**CFP**@sifB + **mCherry@virK**		p22	Str, Kan
SMI76	yadB	STM0185	SBM322	yadB::kanR	**CFP**@sifB + **mCherry@virK**		p22	Str, Kan
SMI77	lpbA, IpbB	STM3808, STM3809	SBM322	(lpbA+IpbB)::kanR	**CFP**@sifB + **mCherry@virK**		p22	Str, Kan
SMI78	htpG	STM0487	SL1344	htpG::kanR			p22	Str, Kan
SMI79	clpA	STM0945	SL1344	clpA::kanR			p22	Str, Kan
SMI83	hslU	STM4091	SL1344	hslU::kanR			p22	Str, Kan
SMI84	yibK	STM3695	SL1344	yibK::kanR			p22	Str, Kan
SMI86	lpbA, IpbB	STM3808, STM3809	SL1344	(lpbA+IpbB)::kanR			p22	Str, Kan
SMI87			SL1344			pACH5-1	EP pACH5-1	Str, Kan, Amp
SMI88			SL1344			pACH10-A1	EP pACH10-A1	Str, Kan, Amp
SMI89			SL1344			pACH10-A3	EP pACH10-A3	Str, Kan, Amp
SMI90			SL1344			pACH10-A4	EP pACH10-A4	Str, Kan, Amp
SMI91			SL1344			pACH10-P2	EP pACH10-P2	Str, Kan, Amp
SMI92			SL1344			pACH10-P3	EP pACH10-P3	Str, Kan, Amp
SMI93			SL1344			pACH10-P4	EP pACH10-P4	Str, Kan, Amp
SMI94			SL1344			pACH10-P5	EP pACH10-	Str, Kan,

						P5	Amp
SMI95	mnmA	STM1234	SL1344	mnmA::kanR		p22	Str, Kan
SMI97	queA_p	STM1548	SACH35	ΔqueA_p		curing	Str
SMI98	queA, queA_p	STM0404, STM1548	SMI97	queA::kanR ΔqueA_p		p22	Str, Kan
SMI99	gidA	STM3874	SACH24	gidA::KanR	pACH5-1	EP pACH5-1	Str, Kan, Amp
SMI100	gidA	STM3874	SACH24	gidA::KanR	pACH10-A1	EP pACH10-A1	Str, Kan, Amp
SMI101	gidA	STM3874	SACH24	gidA::KanR	pACH10-A3	EP pACH10-A3	Str, Kan, Amp
SMI102	gidA	STM3874	SACH24	gidA::KanR	pACH10-A4	EP pACH10-A4	Str, Kan, Amp
SMI103	gidA	STM3874	SACH24	gidA::KanR	pACH10-P2	EP pACH10-P2	Str, Kan, Amp
SMI104	gidA	STM3874	SACH24	gidA::KanR	pACH10-P3	EP pACH10-P3	Str, Kan, Amp
SMI105	gidA	STM3874	SACH24	gidA::KanR	pACH10-P4	EP pACH10-P4	Str, Kan, Amp
SMI106	gidA	STM3874	SACH24	gidA::KanR	pACH10-P5	EP pACH10-P5	Str, Kan, Amp
SMI107	trmE	STM3843	SMI13	trmE::kanR	pACH5-1	EP pACH5-1	Str, Kan, Amp
SMI108	trmE	STM3843	SMI13	trmE::kanR	pACH10-A1	EP pACH10-A1	Str, Kan, Amp
SMI109	trmE	STM3843	SMI13	trmE::kanR	pACH10-A3	EP pACH10-A3	Str, Kan, Amp
SMI110	trmE	STM3843	SMI13	trmE::kanR	pACH10-A4	EP pACH10-A4	Str, Kan, Amp
SMI111	trmE	STM3843	SMI13	trmE::kanR	pACH10-P2	EP pACH10-P2	Str, Kan, Amp
SMI112	trmE	STM3843	SMI13	trmE::kanR	pACH10-P3	EP pACH10-P3	Str, Kan, Amp
SMI113	trmE	STM3843	SMI13	trmE::kanR	pACH10-P4	EP pACH10-P4	Str, Kan, Amp

SMI114	trmE	STM3843	SMI13	trmE::kanR		pACH10-P5	EP pACH10-P5	Str, Kan, Amp
SMI115	mnmC	STM2379	SMI14	mnmC::kanR		pACH5-1	EP pACH5-1	Str, Kan, Amp
SMI116	mnmC	STM2379	SMI14	mnmC::kanR		pACH10-A1	EP pACH10-A1	Str, Kan, Amp
SMI117	mnmC	STM2379	SMI14	mnmC::kanR		pACH10-A3	EP pACH10-A3	Str, Kan, Amp
SMI118	mnmC	STM2379	SMI14	mnmC::kanR		pACH10-A4	EP pACH10-A4	Str, Kan, Amp
SMI119	mnmC	STM2379	SMI14	mnmC::kanR		pACH10-P2	EP pACH10-P2	Str, Kan, Amp
SMI120	mnmC	STM2379	SMI14	mnmC::kanR		pACH10-P3	EP pACH10-P3	Str, Kan, Amp
SMI121	mnmC	STM2379	SMI14	mnmC::kanR		pACH10-P4	EP pACH10-P4	Str, Kan, Amp
SMI122	mnmC	STM2379	SMI14	mnmC::kanR		pACH10-P5	EP pACH10-P5	Str, Kan, Amp
SMI123	tgt	STM0405	SBM228	tgt::kanR ΔgalK His+ Δ0357 Δ4495 Δ4526		**pCSλ** AMP	EP pCSλ AMP	Str, Kan, Amp
SMI124	miaA	STM4360	SBM233	miaA::Kan		**pCSλ** AMP	EP pCSλ AMP	Str, Kan, Amp
SMI125	miaB	STM0670	SBM234	miaB::Kan		**pCSλ** AMP	EP pCSλ AMP	Str, Kan, Amp
SMI126	gidA	STM3874	SBM236	gidA::Kan		**pCSλ** AMP	EP pCSλ AMP	Str, Kan, Amp
SMI127	miaE, mnmC	STM4471, STM2379	SMI68	mnmC::kanR ΔmiaE		**pCSλ** AMP	EP pCSλ AMP	Str, Kan, Amp
SMI128	mnmA	STM1234	SMI95	mnmA::Kan		**pCSλ** AMP	EP pCSλ AMP	Str, Kan, Amp
SMI129	yibK	STM3695	SMI75	yibK::kanR	**CFP**@sifB + **mCherry@virK**	**pCSλ** AMP	EP pCSλ AMP	Str, Kan, Amp
SBM224				ΔgalK His+ Δ0357 Δ4495 Δ4526		pKD46	EP strain	Str, Amp

SBM319				SL1344	**GFPs**@sifB + **mCherry@virK**	colour strain	Str
SBM321				SL1344	**YFPs**@sifB + **mCherry@virK**	colour strain	Str
SBM322				SL1344	**CFP**@sifB + **mCherry@virK**	colour strain	Str
SBM228	tgt	STM0405	SBM224	tgt::Kan			Str, Kan
SBM229	mnmA	STM1234	SBM224	mnmA::Kan			Str, Kan
SBM233	miaA	STM4360		miaA::Kan	**CFP**@sifB		Str, Kan
SBM234	miaB	STM0670		miaB::Kan	**GFPweak2**@sifB		Str, Kan
SBM236	gidA	STM3874		gidA::Kan	**GFPs**@sifB		Str, Kan
SACH24	gidA	STM3874	SL1344	gidA::KanR		p22	
SACH27	queA	STM0404	SBM319	queA::KanR	**GFPs**@sifB + **mCherry@virK**	p22	Str, Kan
SACH28	ybbB	STM0513	SBM319	ybbB::KanR	**GFPs**@sifB + **mCherry@virK**	p22	Str, Kan
SACH29	ydaO	STM1654	SBM322	ydaO::KanR	**CFP**@sifB + **mCherry@virK**	p22	Str, Kan
SACH30	yecO	STM1905	SBM322	yecO::KanR	**CFP**@sifB + **mCherry@virK**	p22	Str, Kan
SACH31	yfhQ	STM2545	SBM321	yfhQ::KanR	**YFPs**@sifB + **mCherry@virK**	p22	Str, Kan
SACH32	spoU	STM3743	SBM321	spoU::KanR	**YFPs**@sifB + **mCherry@virK**	p22	Str, Kan
SACH33	miaE	STM4471	SBM321	miaE::KanR	**YFPs**@sifB + **mCherry@virK**	p22	Str, Kan
SACH34	queA_p	STM1548	SBM319	queA_p::KanR	**GFPs**@sifB + **mCherry@virK**	p22	Str, Kan
SACH35	queA_p	STM1548	SL1344	queA_p::KanR		p22	Str, Kan
SACH45	yecO	STM1905	SACH30	ΔyecO	**GFPs**@sifB + **mCherry@virK**	curing	Str
SACH46	yfhQ	STM2545	SACH31	ΔyfhQ	**YFPs**@sifB + **mCherry@virK**	curing	Str
SACH49	queA_p	STM1548	SACH34	ΔqueA_p	**CFP**@sifB + **mCherry@virK**	curing	Str
SACH50	yecP	STM1906	SBM322	yecP::KanR	**CFP**@sifB + **mCherry@virK**	p22	Str, Kan

SACH51	clpP	STM0448	SBM321	clpP::KanR	**YFPs**@sifB + **mCherry@virK**	p22	Str, Kan
SACH52	ydaO, clpP	STM1654, STM0448	SACH44	Δ ydaO, clpP::KanR	**CFP**@sifB + **mCherry@virK**	p22	Str, Kan
SACH53	yfhQ, clpP	SM2545, STM0448	SACH46	Δ yfhQ, clpP::KanR	**YFPs**@sifB + **mCherry@virK**	p22	Str, Kan
SDFR3				SL1344	**GFPs**@sifB		
SRU02				SL1344	**GFPweak2**@sifB		
SRU05				SL1344	**CFP**@sifB		
SNB10				SL1344	**mCherry**@sifB		

F Gene local context

from Ecocyc (12/10/12)

yecO

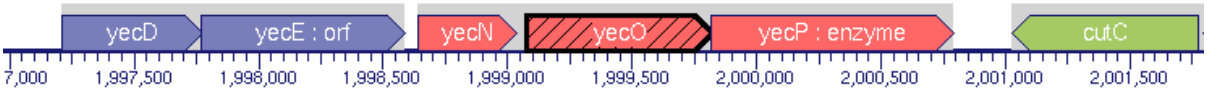

yecP

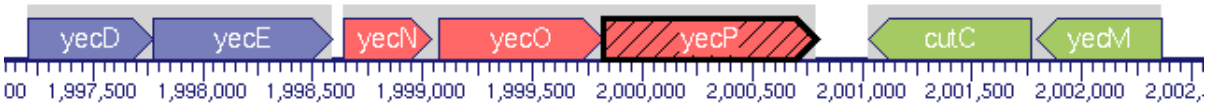

miaA

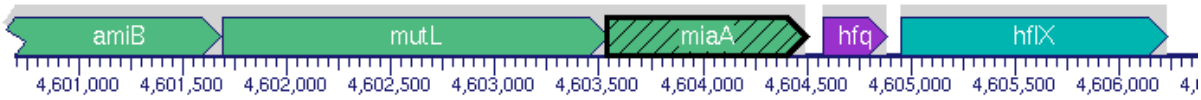

miaB

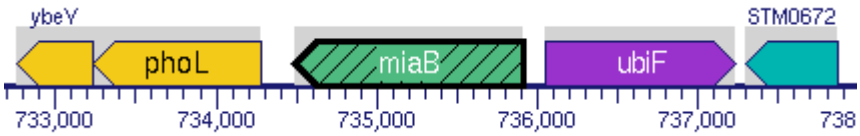

miaE

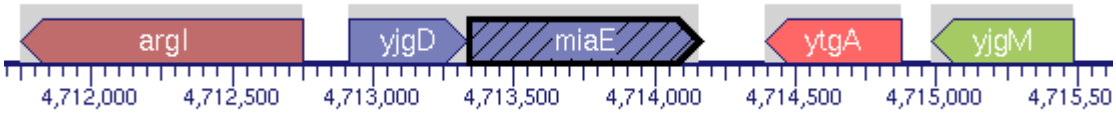

trmE

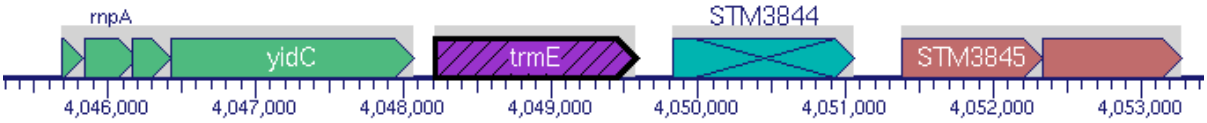

gidA

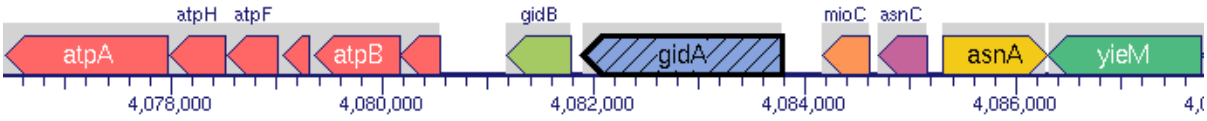

mnmC

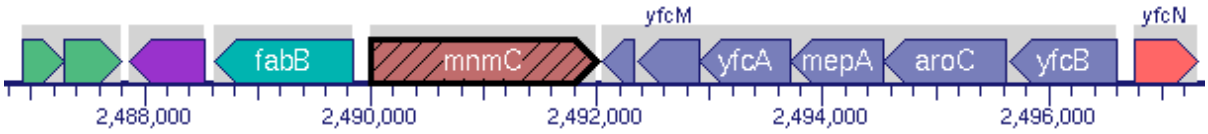

mnmA

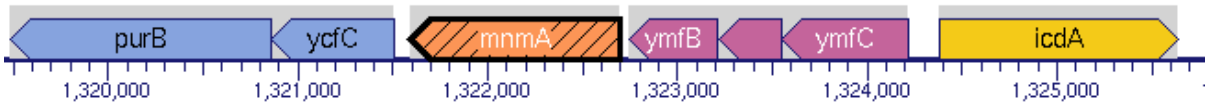

ygcF

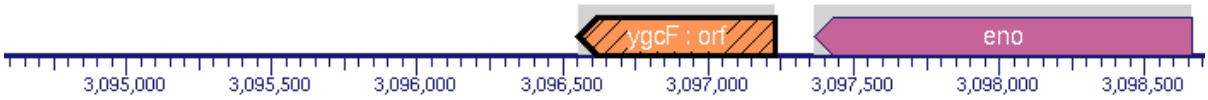

ybaX

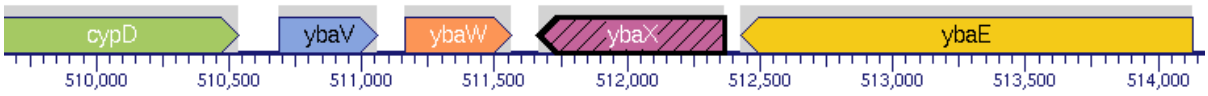

queF

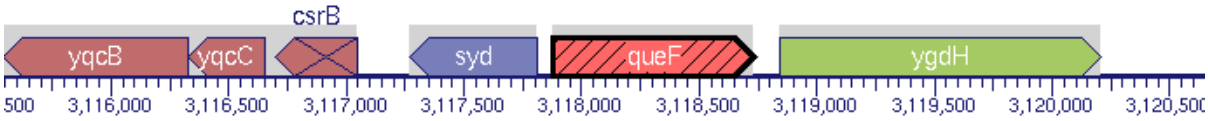

tgt

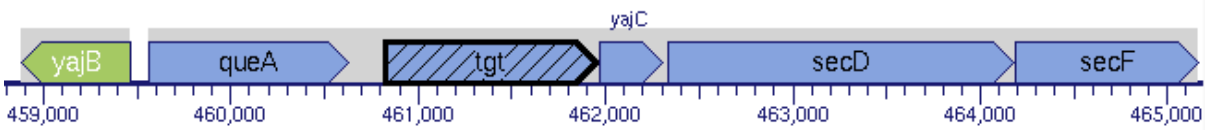

queA

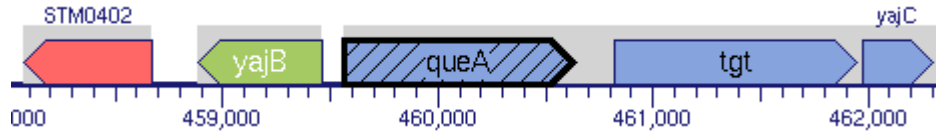

queA_p

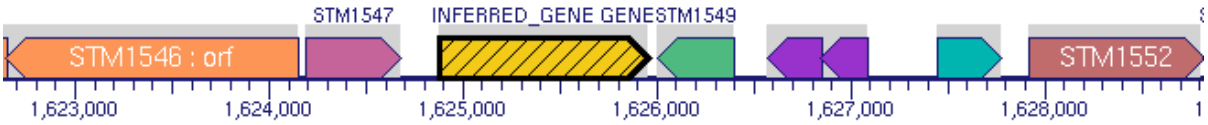

yjeS

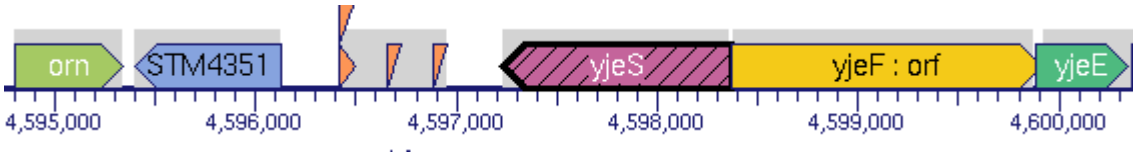

yadB

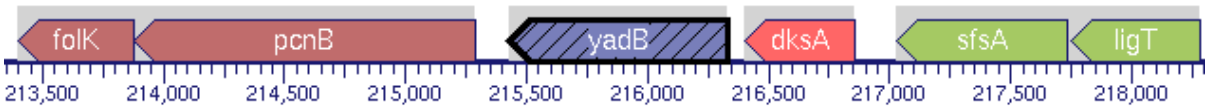

ybbB

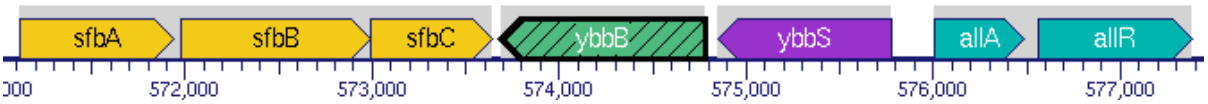

yibK

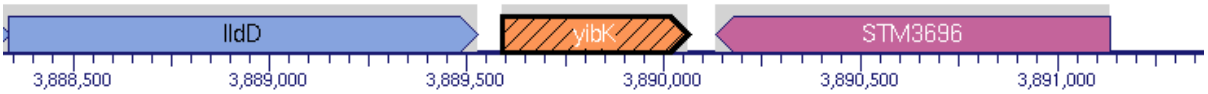

ydaO

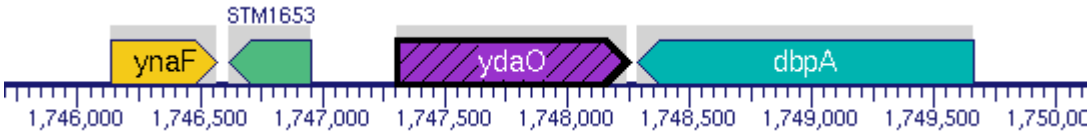

yfhQ

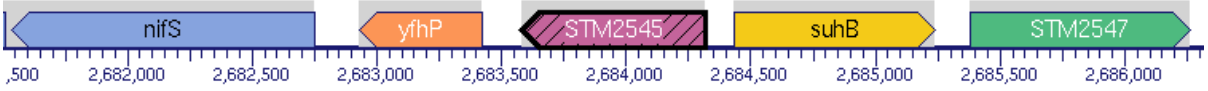

spoU

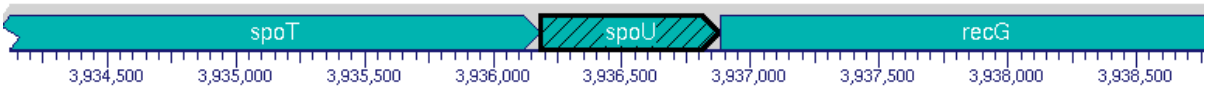

G Microscopy pictures

MES-ch (4 hours)

SL1344

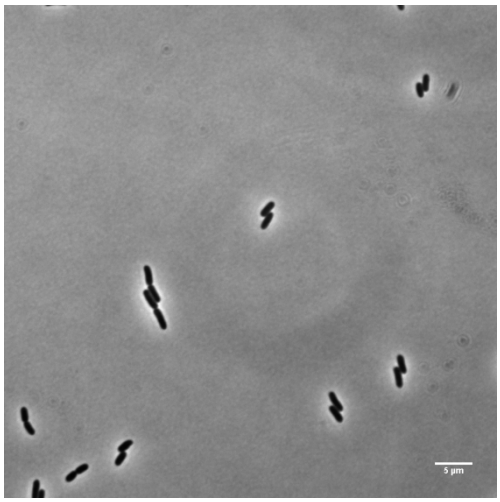

ΔyecP

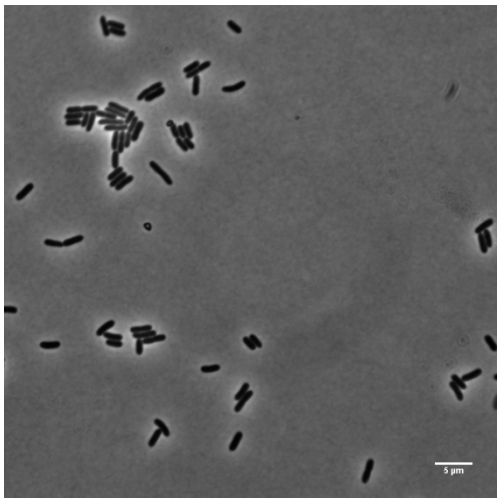

ΔmiaA

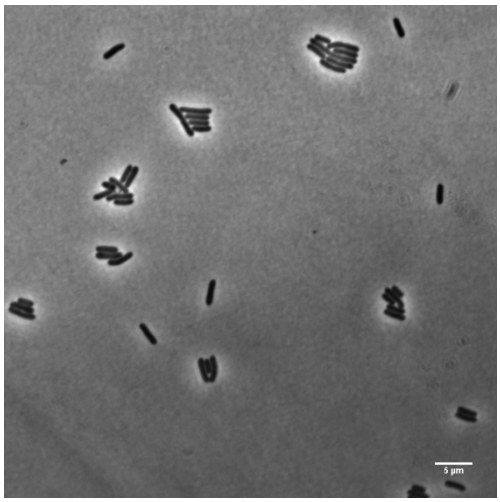

ΔmiaB

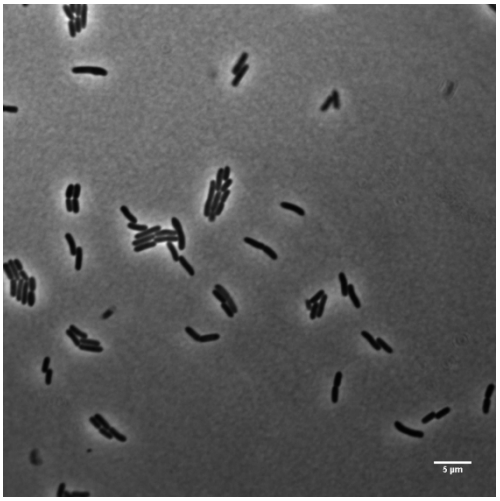

ΔtrmE

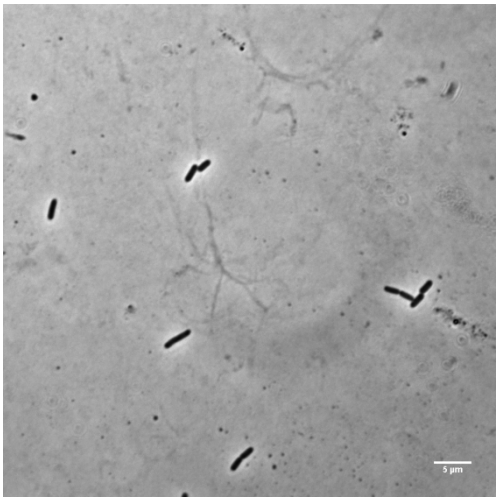

ΔgidA

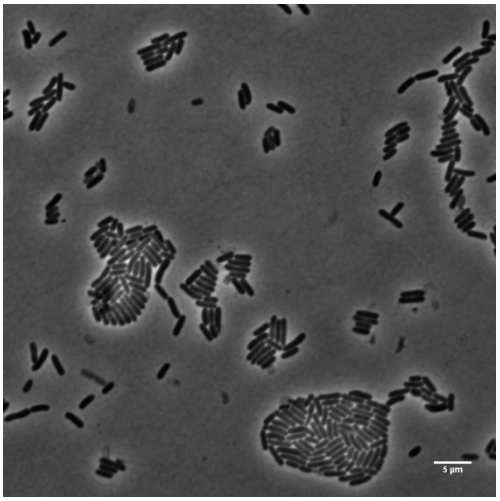

ΔmnmA

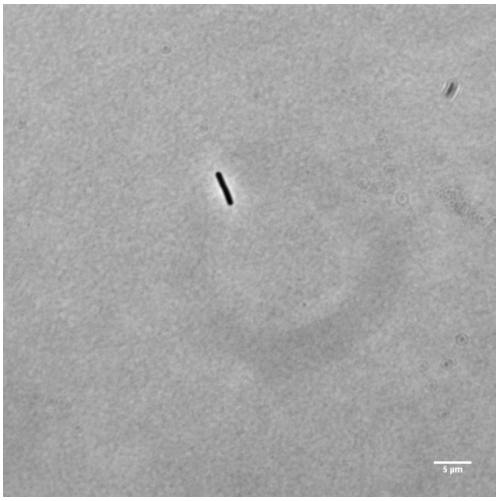

Δtgt

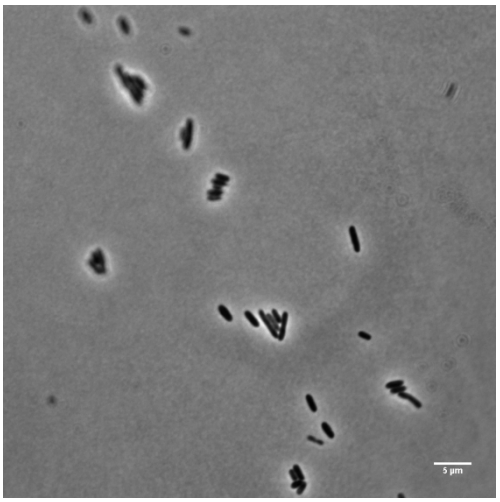

MES-ch (18 hours)

SL1344

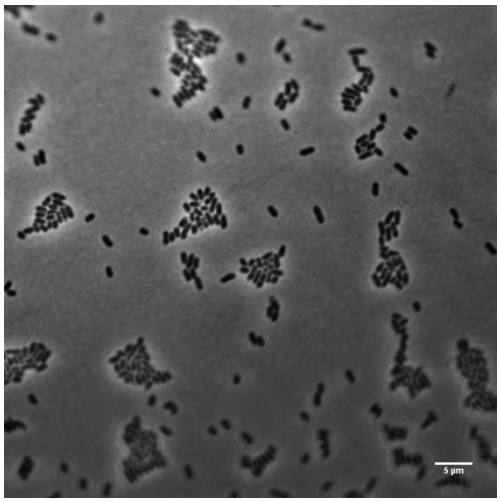

ΔyecP

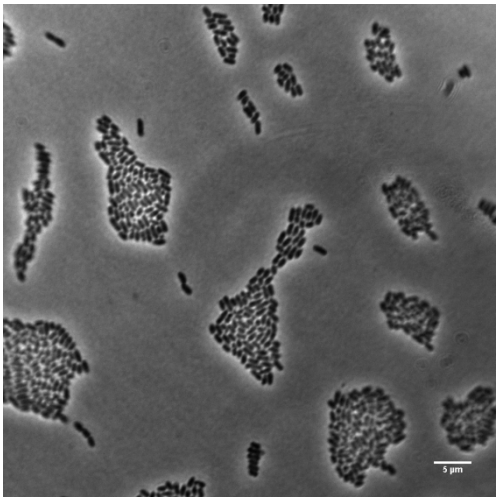

ΔtrmE

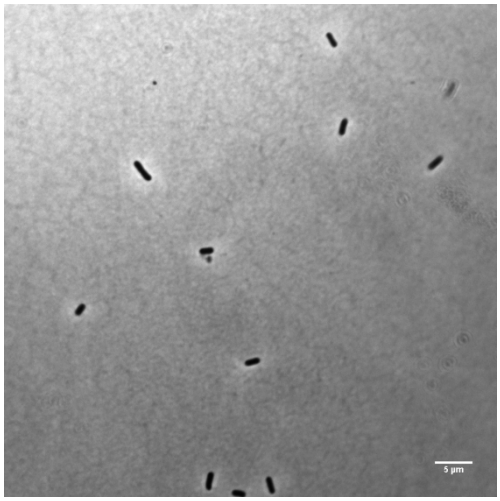

ΔgidA

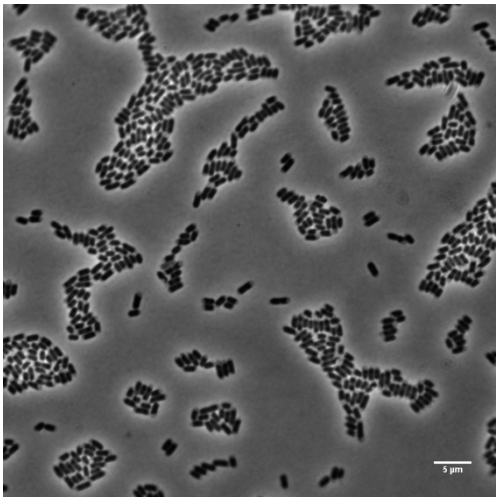

ΔmnmA

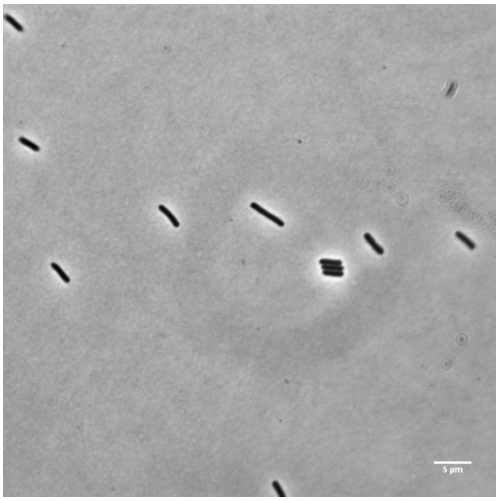

MES-ch (19 hours)

SL1344

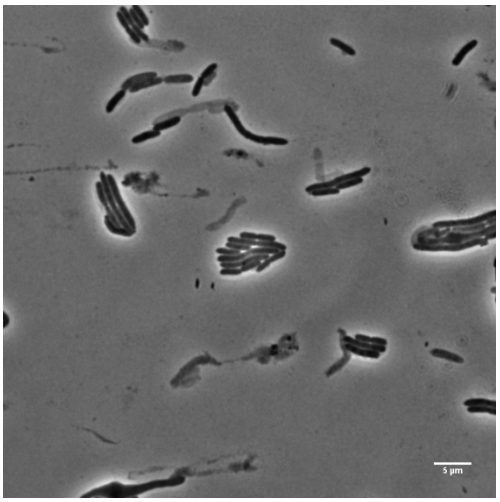

ΔybbB

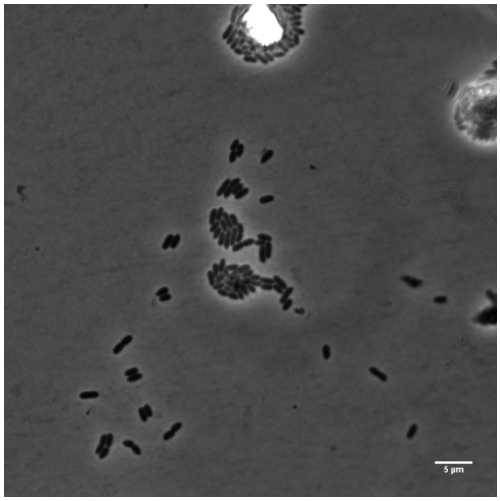

ΔydaO

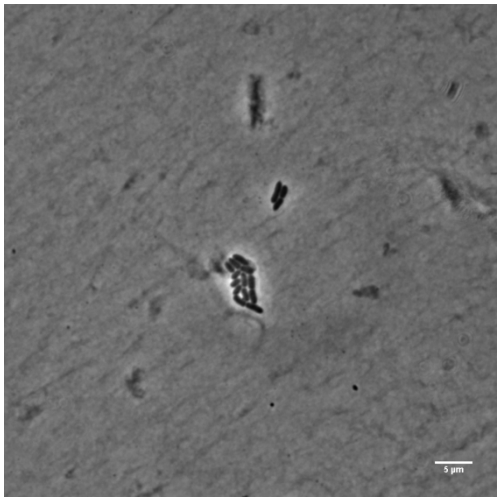

ΔyfhQ

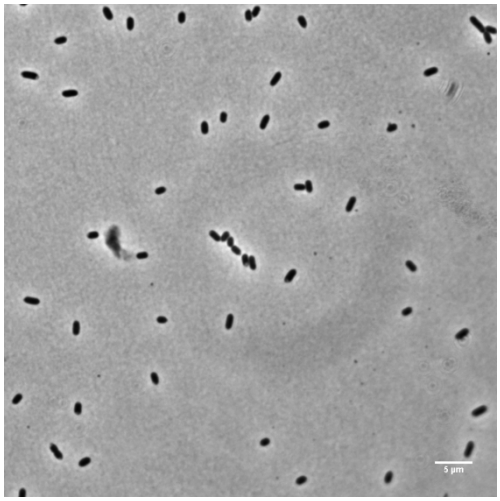

ΔydaO, yecO

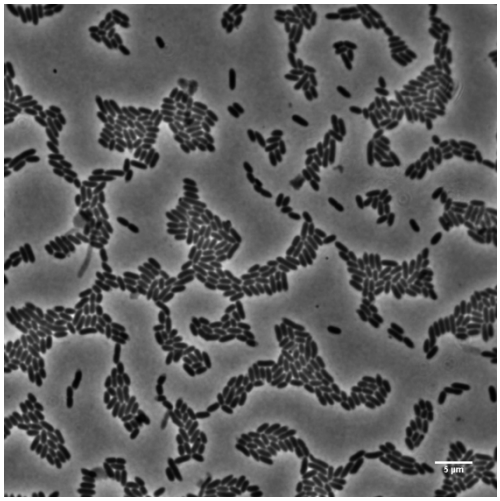

ΔspoU

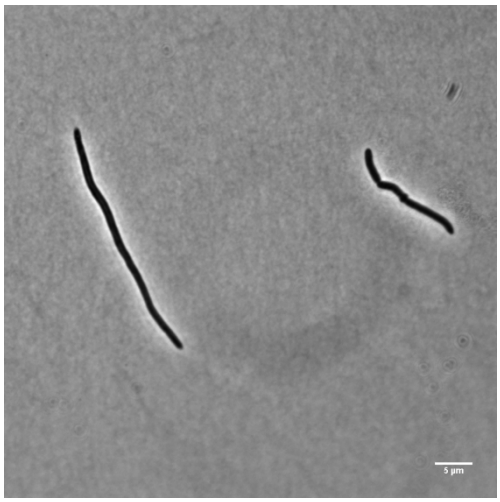

ΔyecO

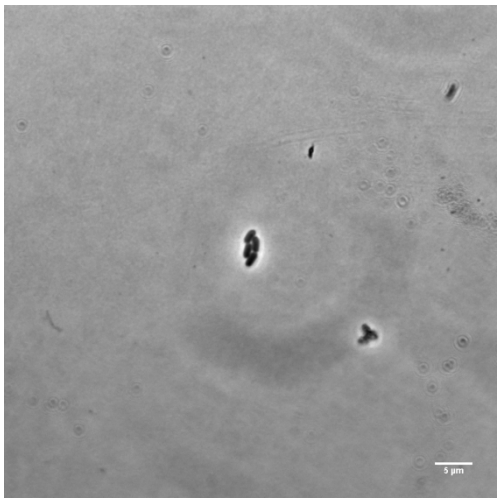

ΔyecP

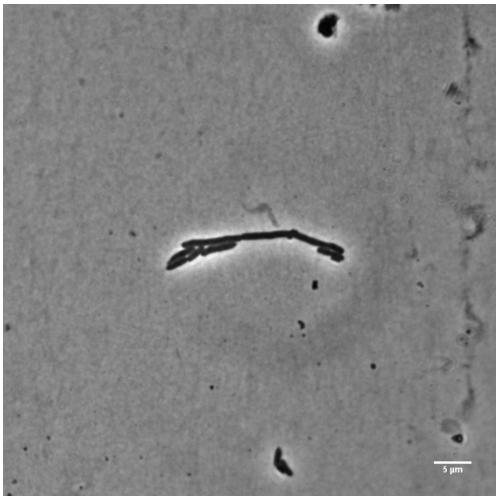

ΔyecP, yecO

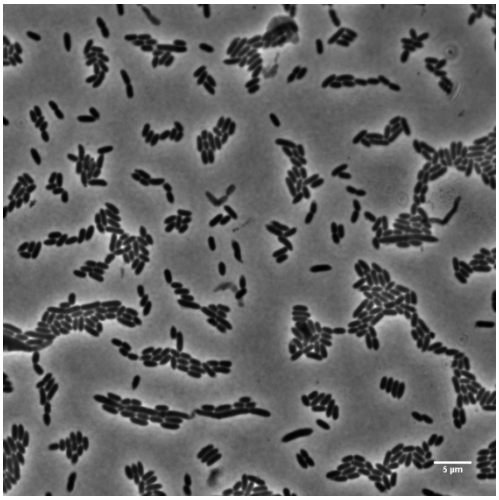

ΔmiaE

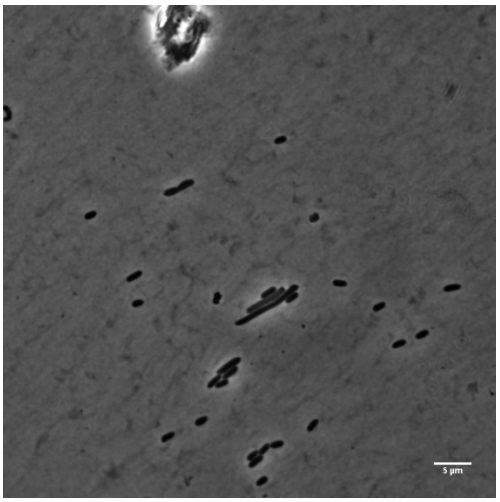

ΔqueA

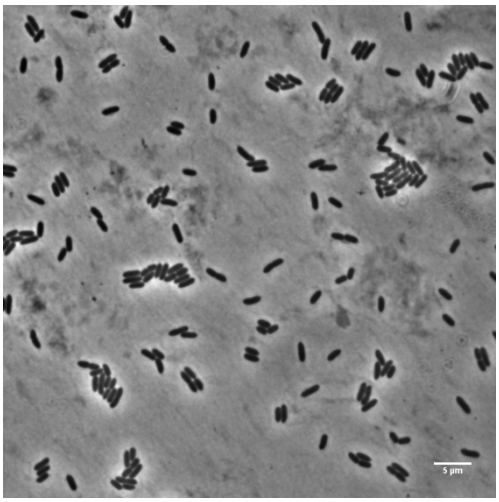

ΔqueA_p

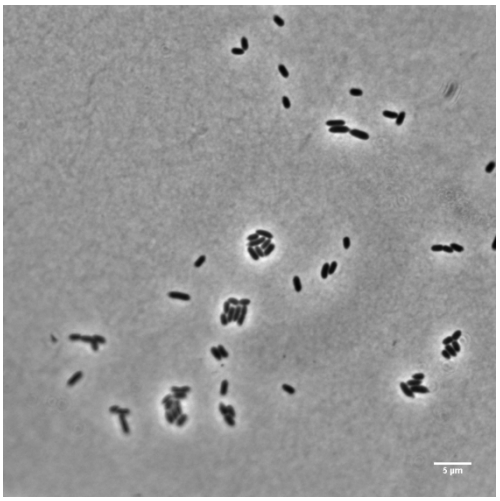

ΔqueA, queA_p

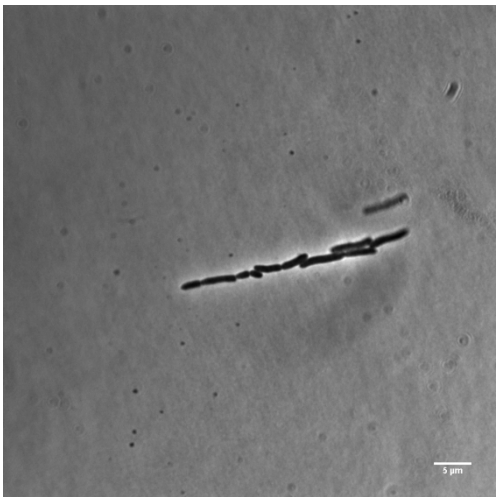

MES-ch (26 hours)

SL1344

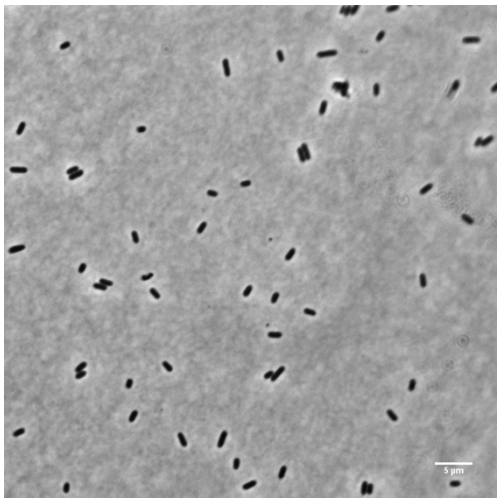

ΔydaO

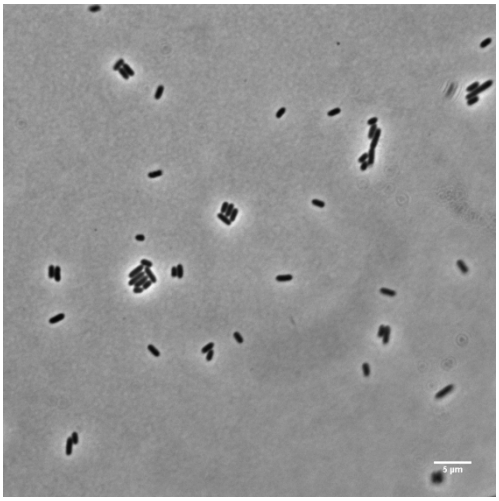

ΔydaO, yfhQ

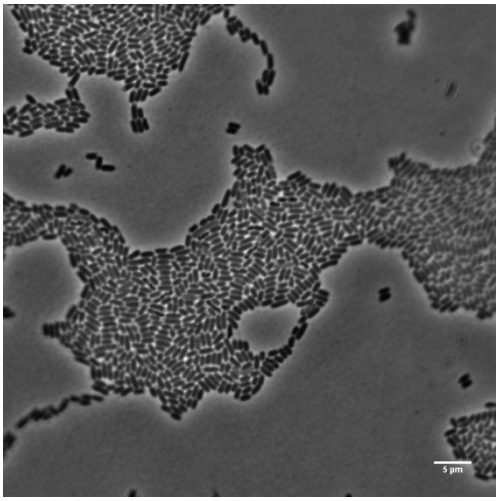

ΔspoU

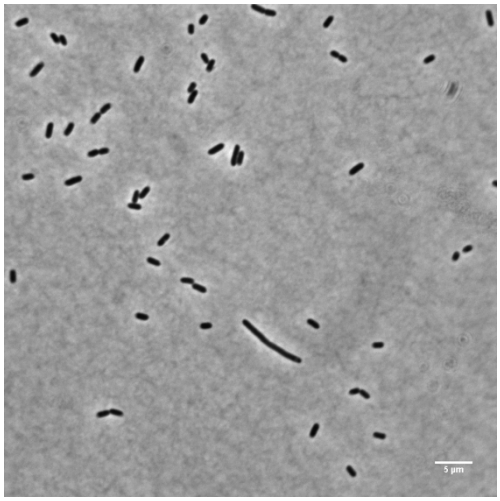

ΔyecO

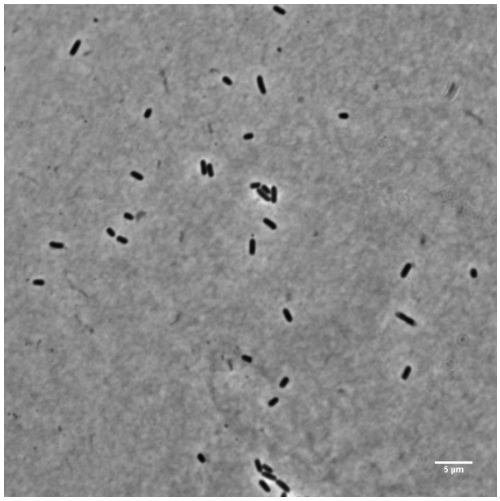

ΔyecP

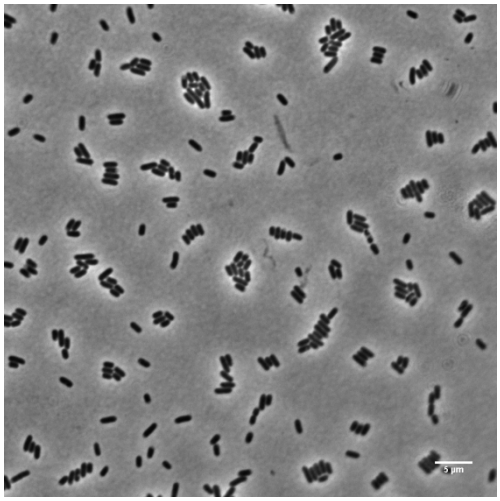

ΔmiaA

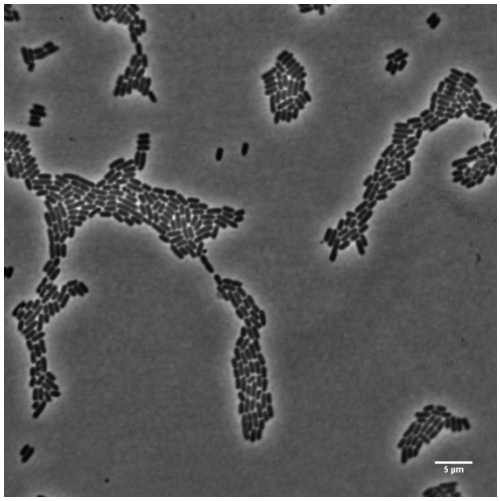

ΔmiaB

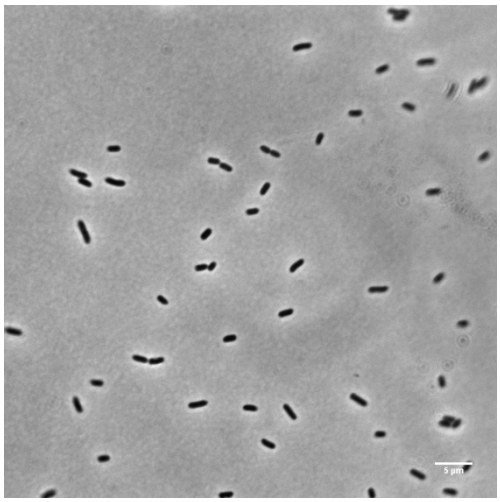

ΔtrmE

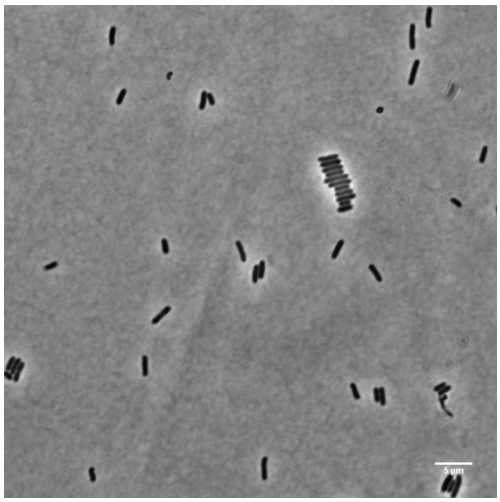

ΔmnmC

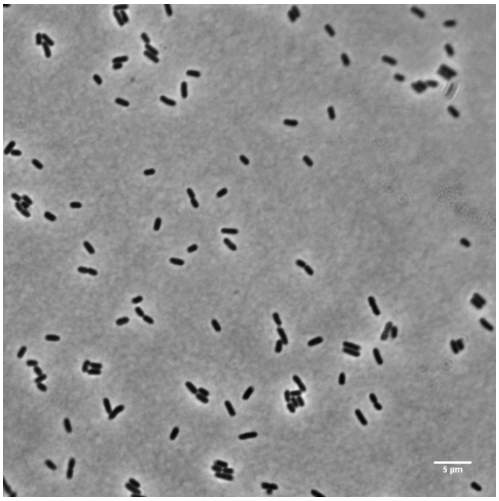

ΔygcF

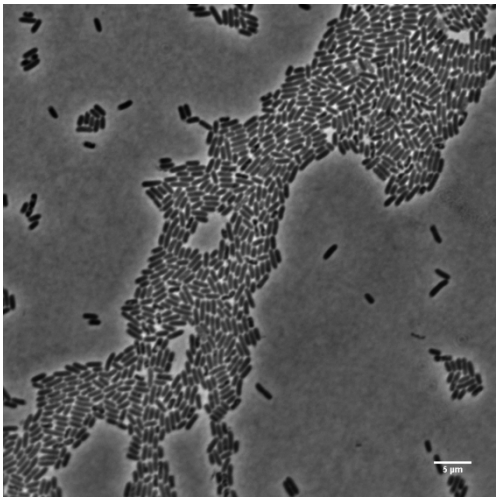

ΔybaX

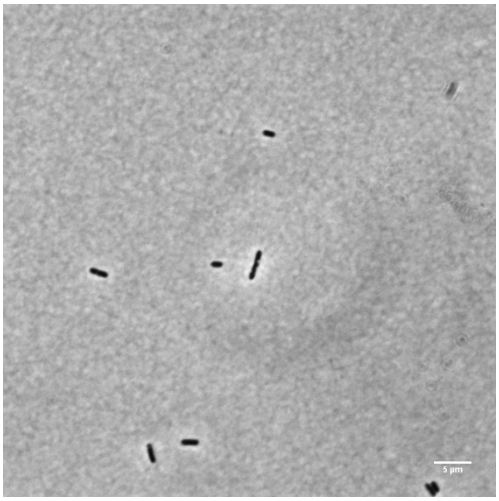

ΔqueF

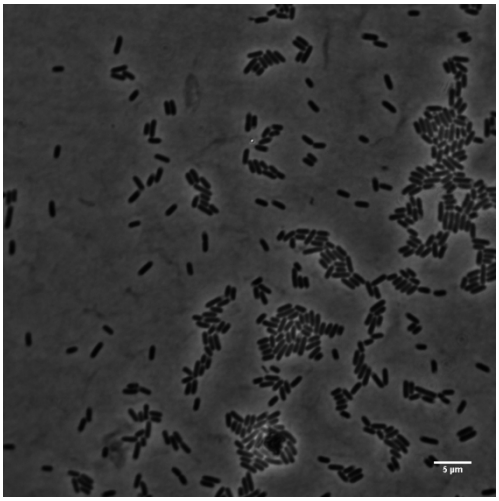

ΔqueA, queA_p

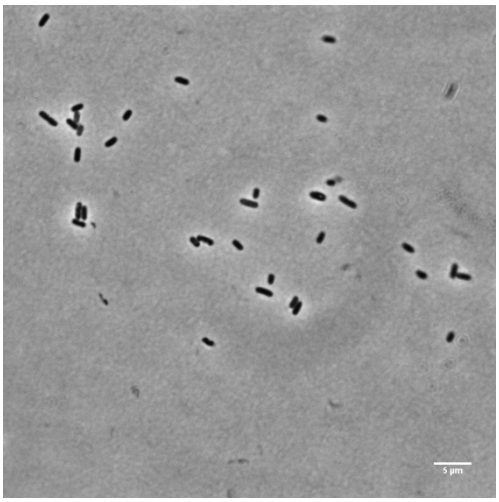

ΔyjeS

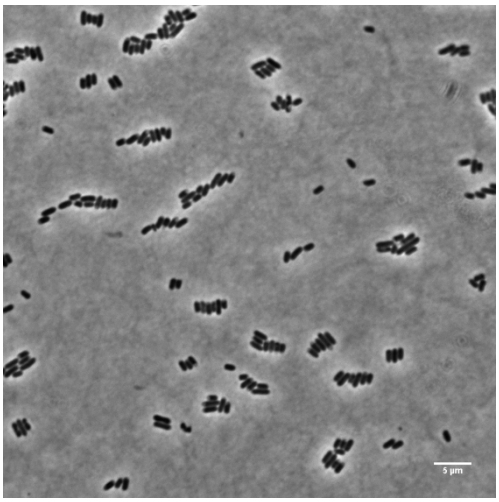

LB (21 hours)

SL1344

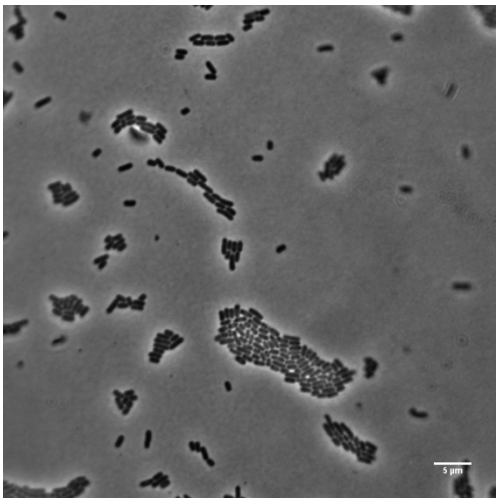

ΔyecP

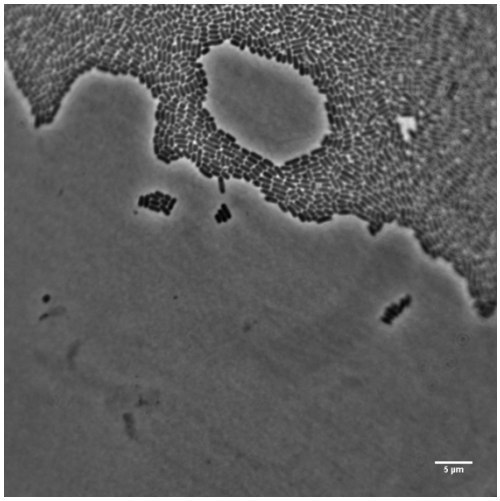

ΔmiaA

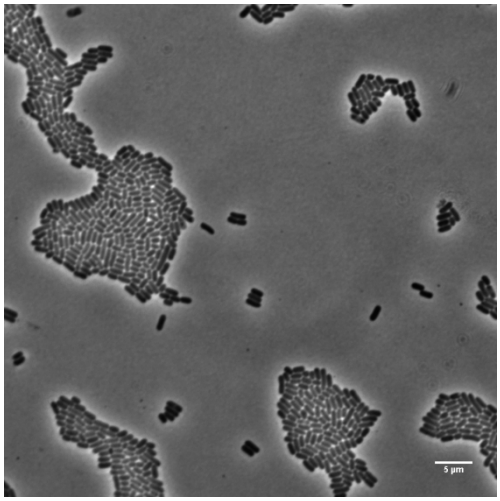

ΔtrmE

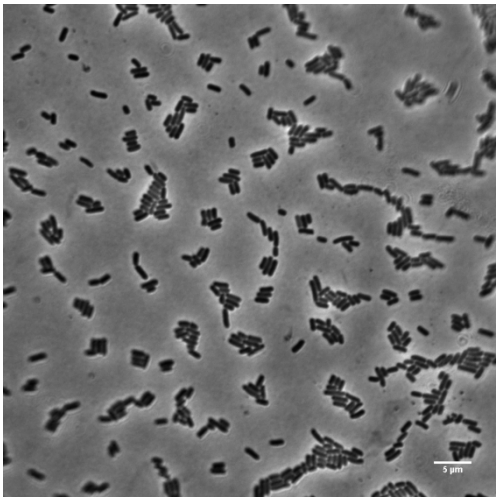

ΔgidA

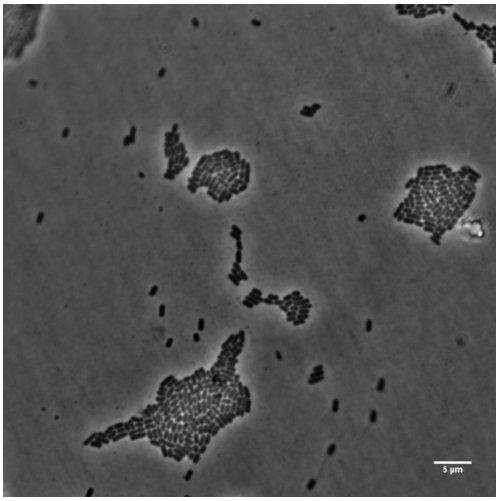

ΔmnmA

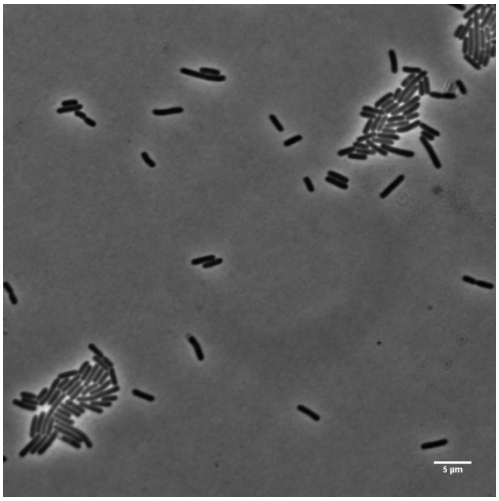

Δtgt

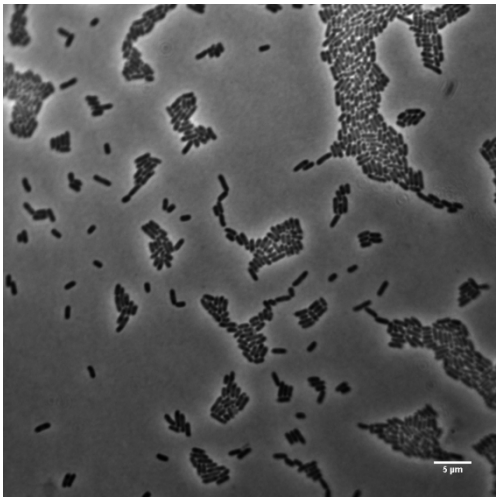

Fluorescence (examples)

phase contrast *(ΔyecP)*

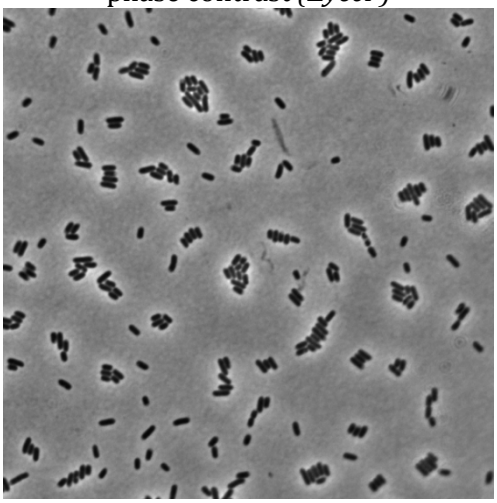

phase contrast *(ΔqueF)*

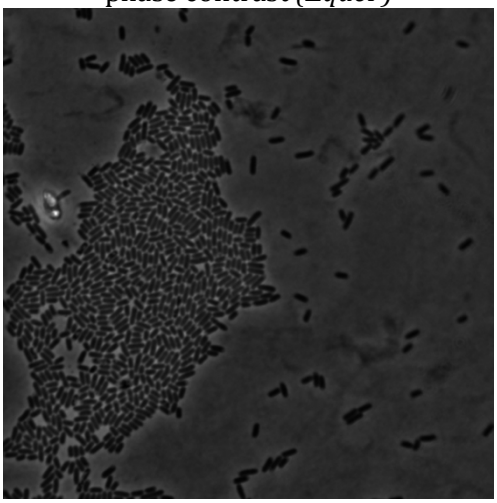

CFP *(ΔyecP)*

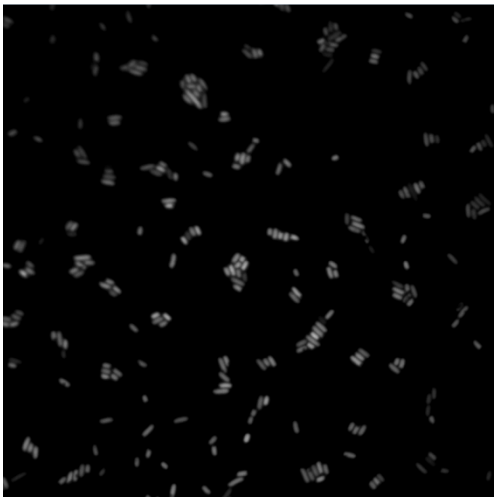

YFP *(ΔqueF)*

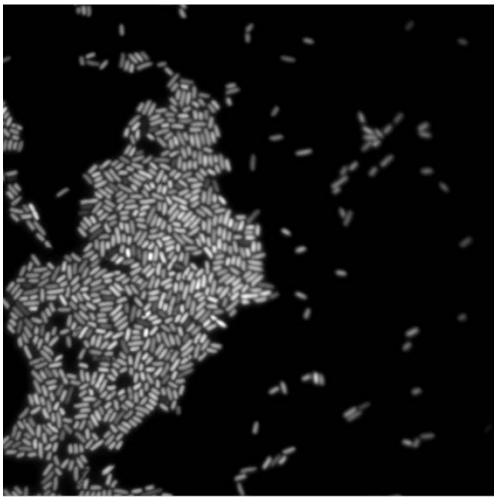

mCH *(ΔyecP)*

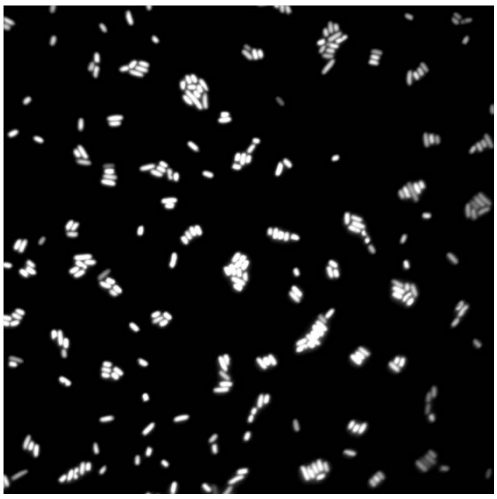

mCH *(ΔqueF)*

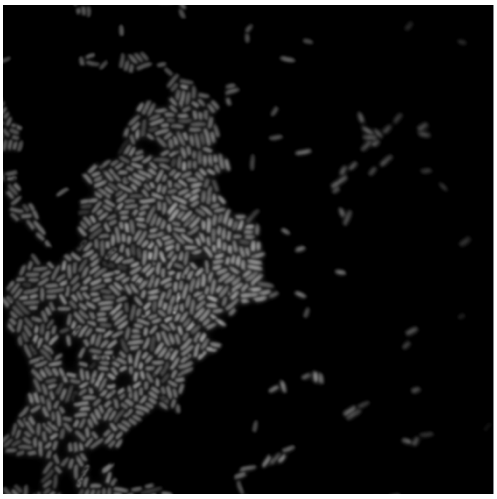

H Curriculum vitae: Melanie Christina Isele

Personal information

Date of Birth	19/08/89
Place of Birth	Dornbirn, Austria
Nationality	Austrian
Telephone	+43 650 6362280
E-Mail	melanie.isele@gmx.net

Education

01/11-12/12	Master's degree program in molecular biology with focus on molecular medicine at the University of Vienna, Austria
02-10/12	Erasmus internship at the Biozentrum, University of Basel, Switzerland
08/11-01/12	Erasmus semester at the University of Barcelona, Spain
10/07-01/11	Bachelor's degree program in biology with focus on microbiology and genetics at the University of Vienna, Austria
06/07	Secondary school leaving certificate (Matura) with natural scientific focus at the Bundesoberstufenrealgymnasium Lauterach, Austria

Experience

02-10/12	Master thesis *"Identification of drug targets for novel antimicrobials"* in the laboratory of Prof. Dr. Dirk Bumann (supervised by ao. Univ.-Prof. Dr. Gottfried Köhler and Dr. Anna Chirkova), Infection Biology, Biozentrum, University of Basel, Switzerland
09-12/11	Internship "*Preparatory work for the crystallization of Aichi- and Mengovirus polymerase*" in the laboratory of Prof. Dr. Núria Verdaguer Massana (supervised by Dr. Cristina Ferrer Orta), Department of Structural Biology, Molecular Biology Institute of Barcelona, Spanish National Research Council, Spain
04-05/11	Internship "*Development of a RT-qPCR based virus overlay blot (VOB) read-out*" in the laboratory of Prof. Dr. Dieter Blaas (supervised by Dr. Heinrich Kowalski), Institute of Medical Biochemistry, Vienna Biocenter (VBC), Medical University of Vienna, Austria

08-09/10	Bachelor thesis "*Purification of the fusion protein VP1-2xP5*" in the laboratory of Prof. Rudolf Valenta, MD (supervised by Dr. Margarete Focke-Tejkl), Christian Doppler Laboratory for Allergy Research, Division of Immunopathology, Medical University of Vienna, Austria

Skills and Qualifications

Software	Microsoft Office 2010, GraphPad Prism 6, Adobe Photoshop CS5 Extended, ImageJ, Softworx 5.5, Clone Manager 7, R Studio, FlowJo 10, BD FACS Diva Software
Instruments	BD LSRFortessa cell analyzer, IX71 Microscope (DeltaVision wide-field microscope), Mini-chemostat system, Synergy Microplate Reader, ÄKTA protein purification systems, standard laboratory equipment
Languages	German (mother tongue) English (excellent knowledge) Spanish (elementary knowledge)

Personal interests

Sports (swimming, jogging, inline skating, volleyball, cycling, sailing)
Photography
Traveling